HMAC LAYER ADHESION THROUGH TACK COAT

Final Report

SPR 782

Oregon Department of Transportation

HMAC LAYER ADHESION THROUGH TACK COAT

Final Report

SPR 782

By

Erdem Coleri, PhD
David Covey, Aiman Mahmoud, James Batti, and Natasha Anisimova

School of Civil and Construction Engineering
Oregon State University
101 Kearney Hall
Corvallis, OR 97331

for

Oregon Department of Transportation
Research Section
555 13th Street NE, Suite 1
Salem OR 97301

and

Federal Highway Administration
1200 New Jersey Avenue SE
Washington, DC 20590

February 2017

Technical Report Documentation Page

1. Report No. FHWA-OR-RD-17-05	2. Government Accession No.	3. Recipient's Catalog No.
4. Title and Subtitle HMAC Layer Adhesion Through Tack Coat		5. Report Date February 2017 6. Performing Organization Code
7. Author(s) Erdem Coleri, PhD.; David Covey; Aiman Mahmoud; James Batti; Natasha Anisimova		8. Performing Organization Report No. SPR 782
9. Performing Organization Name and Address School of Civil and Construction Engineering Oregon State University 101 Kearney Hall Corvallis, OR 97331		10. Work Unit No. (TRAIS) 11. Contract or Grant No.
12. Sponsoring Agency Name and Address Oregon Dept. of Transportation Research Section and Federal Highway Admin. 555 13th Street NE, Suite 1 1200 New Jersey Avenue SE Salem, OR 97301 Washington, DC 20590		13. Type of Report and Period Covered Final Report 14. Sponsoring Agency Code

15. Supplementary Notes

16. Abstract

Tack coats are the asphaltic emulsions applied between pavement lifts to provide adequate bond between the two surfaces. The adhesive bond between the two layers helps the pavement system to behave as a monolithic structure and improves the structural integrity. The absence, inadequacy or failure of this bond result in a significant reduction in the shear strength resistance of the pavement structure and make the system more vulnerable to many distress types, such as cracking, rutting, and potholes. In general, decisions on tack coat types and application rates are based on experience, judgment, and convenience. For this reason, unacceptable bond performance and tack coat related premature failures are inevitable due to the lack of quality-control and quality-assurance (QC/QA) procedures.

This research study presents a comprehensive field investigation consisting of field and laboratory testing, 3D finite element modeling, field coring, and construction sampling of tack coats used in Oregon. Within the study, two new tack coat materials from two companies were, for the first time, evaluated for their performance. Recommendations for the most efficient application rates along with interlayer shear strength (ISS) prediction equations based on rheological properties were developed. In this study, tools and methods (a wheel tracking device and a smart phone app) to reduce tracking were also developed. Results of the evaluation will provide valuable information about correlations between rheological tests and interlayer shear strength, as well as the effects of texture, traffic loads, and application rate on interlayer shear strength.

In this study, the Oregon Field Torque Tester (OFTT) and the wireless Oregon Field Tack Coat Tester (OFTCT) were also developed to evaluate the long-term post-construction tack coat performance of pavement sections. It was determined that OFTT and OFTCT can be successfully utilized in the field to improve tack coat bond strengths.

17. Key Words Tack coat, emulsions, bond strength, shear, tension.		18. Distribution Statement Copies available from NTIS, and online at http://www.oregon.gov/ODOT/TD/TP_RES/	
19. Security Classification (of this report)-- Unclassified	20. Security Classification (of this page)--Unclassified	21. No. of Pages 150	22. Price

Technical Report Form DOT F 1700.7 (8-72) Reproduction of completed page authorized Printed on recycled paper

SI* (MODERN METRIC) CONVERSION FACTORS

APPROXIMATE CONVERSIONS TO SI UNITS

Symbol	When You Know	Multiply By	To Find	Symbol
		LENGTH		
in	inches	25.4	millimeters	mm
ft	feet	0.305	meters	m
yd	yards	0.914	meters	m
mi	miles	1.61	kilometers	km
		AREA		
in^2	square inches	645.2	millimeters squared	mm^2
ft^2	square feet	0.093	meters squared	m^2
yd^2	square yards	0.836	meters squared	m^2
ac	acres	0.405	hectares	ha
mi^2	square miles	2.59	kilometers squared	km^2
		VOLUME		
fl oz	fluid ounces	29.57	milliliters	ml
gal	gallons	3.785	liters	L
ft^3	cubic feet	0.028	meters cubed	m^3
yd^3	cubic yards	0.765	meters cubed	m^3
NOTE: Volumes greater than 1000 L shall be shown in m^3.				
		MASS		
oz	ounces	28.35	grams	g
lb	pounds	0.454	kilograms	kg
T	short tons (2000 lb)	0.907	megagrams	Mg
		TEMPERATURE (exact)		
°F	Fahrenheit	(F-32)/1.8	Celsius	°C

APPROXIMATE CONVERSIONS FROM SI UNITS

Symbol	When You Know	Multiply By	To Find	Symbol
		LENGTH		
mm	millimeters	0.039	inches	in
m	meters	3.28	feet	ft
m	meters	1.09	yards	yd
km	kilometers	0.621	miles	mi
		AREA		
mm^2	millimeters squared	0.0016	square inches	in^2
m^2	meters squared	10.764	square feet	ft^2
m^2	meters squared	1.196	square yards	yd^2
ha	hectares	2.47	acres	ac
km^2	kilometers squared	0.386	square miles	mi^2
		VOLUME		
ml	milliliters	0.034	fluid ounces	fl oz
L	liters	0.264	gallons	gal
m^3	meters cubed	35.315	cubic feet	ft^3
m^3	meters cubed	1.308	cubic yards	yd^3
		MASS		
g	grams	0.035	ounces	oz
kg	kilograms	2.205	pounds	lb
Mg	megagrams	1.102	short tons (2000 lb)	T
		TEMPERATURE (exact)		
°C	Celsius	1.8C+32	Fahrenheit	°F

*SI is the symbol for the International System of Measurement

ACKNOWLEDGEMENTS

The authors would like to thank the Oregon Department of Transportation (ODOT) for providing funding for this research. The authors thank the members of the ODOT Project Technical Advisory Committee and ODOT research for their advice and assistance in the preparation of this report. In particular, Norris Shippen, Larry Ilg, Chris Harris, Anthony Boesen, Keven Heitschmidt, and Troy Tindall participated on the TAC. The authors would like to thank Greyson Termini of OSU for building the frames for the OFTT and OFTCT devices developed in this study. Authors would also like to thank Shashwath Sreedhar, Blaine Wruck, Mostafa Estaji, Sogol Haddadi, Yuqi Zhang Jeffery Knowles, Matt Haynes, and Dylan Kreiger for their help with field testing. Special thanks to ODOT coring crew members and Wayne Brown at the Materials lab for all their help. Authors would also like to thank Ron Depue and David Davies for their help with field testing.

DISCLAIMER

TABLE OF CONTENTS

LIST OF TABLES

LIST OF FIGURES

1.0 INTRODUCTION

1.1 TACK COAT BOND STRENGTH AND TRACKING

Tack coats are the asphalt cements applied between pavement lifts to provide adequate bond between the two surfaces. The adhesive bond between the two layers helps the pavement system to behave as a monolithic structure and improves the structural integrity. The absence, inadequacy or failure of this bond result in a significant reduction in the shear strength resistance of the pavement structure and make the system more vulnerable to many distress types, such as cracking, rutting, and potholes. In general, decisions on tack coat types and application rates are based on experience, judgment, and convenience *(Mohammad et al. 2012)*. For this reason, unacceptable bond performance and tack coat related premature failures are inevitable due to the lack of quality-control and quality-assurance (QC/QA) procedures.

Hachiya and Sato *(Hachiya and Sato 1997)* showed that high tension and shear forces created by truck loads can break the bond between the two layers when the applied stresses exceed the shear and tensile strength of the tack coat. When the bond between the two layers is broken, two layers start to act as independent layers. This change in the pavement structure shifts the critical strain location from the bottom of the asphalt structure to the debonded location *(Mohammad et al. 2012)*.

Several computer models have been developed to investigate the impacts of different variables (such as temperature, layer thicknesses, stiffness, loads, etc) on the critical stresses and strains at layer interfaces. King and May *(King and May 2003)* investigated the effect of bonding on fatigue life using the software BISAR *(De Jong et al. 1973)*. Results of the analysis showed that fatigue life decreases by 50 % when the bond is reduced by 10 %. Roffe and Chaignon *(Roffe and Chaignon 2002)* conducted similar analysis using the French pavement design program ALIZE and concluded that pavement service life can reduce from 20 years to 7 years due to the lack of bond between two asphalt layers.

Tracking, the pick-up of bituminous material by construction vehicle tires, reduces the amount of tack coat in certain areas and creates a non-uniform tack coat distribution between the two construction lifts. This non-uniform tack coat distribution creates localized failures around the low tack coat locations and reduces the overall structural integrity of the pavement structure. In addition, tack coat type, residual application rate, temperature, and existing surface condition (cracked, milled, new, old, or grooved) are the other factors that affect the tack coat performance. By considering all these factors, a QC/QA process needs to be developed to maximize long-term tack coat performance and reduce tracking during construction.

This research study presents a comprehensive field investigation consisting of field and laboratory testing, field coring, and construction sampling of tack coats used in Oregon. Within the study, two new tack coat materials from two companies were, for the first time, evaluated for their performance. Field coring was completed at two different time increments, as well as two

travel lines (wheel path and center of the lane), to capture the effect of traffic loading and time on interlayer shear strength. Recommendations for the most efficient application rate along with interlayer shear strength (ISS) prediction equations based on rheological properties were developed. Results of the evaluation will provide valuable information about correlations between rheological tests and interlayer shear strength, as well as the effects of texture, traffic loads, and application rate on interlayer shear strength.

In this study, tools and methods to reduce tracking were also developed. Weight evaporation experiments were conducted by varying the application rate, air temperature, wind speed, and tack coat type to determine the curing time and the factors that influence it. Tracking was also evaluated by developing a wheel-tracking device that can be used in the field as a visual tool or by collecting weight data via the removable rubber "tires". Data from weight evaporation tests were used to create a linear regression model to predict in-situ curing times and develop a smartphone app (for Android and IOS) using the created model. Prediction of in-situ curing times and not allowing construction vehicles before curing will reduce tracking and improve tack coat bond performance.

In this study, the Oregon Field Torque Tester (OFTT) and the wireless Oregon Field Tack Coat Tester (OFTCT) were also developed to evaluate the long-term post-construction tack coat performance of pavement sections. Correlations between the results of these two field tests and the results of lab shear tests conducted with cores taken from the field were investigated to determine the effectiveness of these new technologies. The peak torque values measured by the OFTT were observed to be highly correlated with the measured lab shear strengths. The OFTT shear strength values calculated by using the torque test results and a theoretical equation were determined to be close to the measured lab shear strengths. It was also determined that the OFTCT can be successfully utilized in the field as a test to quantify the cleanliness of the pavement surfaces before tack coat application. The correlation between OFTCT and lab shear test results is also determined to be statistically significant.

1.2 MAJOR RESEARCH PRODUCTS DEVELOPED IN THIS STUDY

The major research products developed in this study are given as follows:

- Recommended application rates for different tack coat products;
- A smart phone app for Android and IOS to predict tack coat curing time to be used to reduce tracking;
- A wheel tracking device to evaluate tracking during construction;
- The Oregon Field Torque Tester (OFTT) to evaluate and monitor the long-term tack coat performance of pavement sections after construction;
- The Oregon Field Tack Coat Tester (OFTCT), to predict the long-term tack coat performance during construction and quantify the cleanliness of the pavement surfaces before tack coat application;

- A 3D finite element model to determine the impact of structural properties on tack coat performance.

1.3 KEY OBJECTIVES OF THIS STUDY

The main objectives of this study are to:

- Evaluate the factors that influence the bond strength, such as existing surface condition, application rates, tack coat type, surface cleanliness, and temperature, to recommend revisions to current methods and practices;

- Evaluate the performance of "New" tack coat technologies that are developed to reduce tracking and improve bond strength;

- Assess the effects of traffic/time and transverse location (wheel-path vs. center line) on interlayer shear strength;

- Develop methods and equations to predict interlayer shear strength from simple rheological test results;

- Provide recommendations to improve current methods and practices for tack coat application and tracking;

- Develop a smart phone app and a device to determine curing time and reduce tracking;

- Develop a 3D finite element model to determine the impact of structural properties on tack coat performance;

- Develop a low cost and practical technology, the Oregon Field Torque Tester (OFTT), to evaluate and monitor the long-term tack coat performance of pavement sections after construction;

- Develop a device, the Oregon Field Tack Coat Tester (OFTCT), to predict the long-term tack coat performance during construction and quantify the cleanliness of the pavement surfaces before tack coat application.

1.4 ORGANIZATION OF THE REPORT

This report is organized as follows: This introductory chapter is followed by the literature review. Rheological properties of tack coats used in Oregon and the effects of these rheological properties on interlayer shear strength are discussed in Chapter 3. In Chapter 4, tools and methods developed to reduce tack coat tracking are described. Chapter 5 presents the three-dimensional finite element model developed in this study to evaluate the effects of structural characteristics on tack coat performance. The Oregon Field Torque Tester (OFTT) and Oregon Field Tack Coat Tester (OFTCT) devices and test methods developed in this study to improve

tack coat performance are presented in Chapters 6 and 7, respectively. Finally, Chapter 8 presents the conclusions, summary of the work, and recommendations.

2.0 LITERATURE REVIEW

2.1 SLIPPAGE AND DELAMINATION MECHANISM

Tack coats are the bituminous materials applied between pavement lifts to provide an adequate bond between the two surfaces. The adhesive bond between the two layers helps the pavement system to behave as a monolithic structure and improves the structural integrity. The absence, inadequacy or failure of this bond result in a significant reduction in the shear strength resistance of the pavement structure and make the system more vulnerable to many distress types, such as cracking, rutting, and potholes *(Tashman et al. 2006)* (Figure 2.1).

(a)

(b)

Figure 2.1: Pavement distresses due to bond failure (a) Delamination (b) Severe distresses due to the poor bond between two pavement layers *(Willis and Timm 2007)*.

Using computational modeling, Hachiya and Sato *(Hachiya and Sato 1997)* showed that high tension and shear forces created by truck loads can break the bond between the two layers when

the applied stresses exceed the shear and tensile strength of the tack coat. When the bond between the two layers is broken, two layers start to act as independent layers. This change in the pavement structure shifts the critical strain location from the bottom of the asphalt structure to the debonded location *(Mohammad et al. 2012)*. Figure 2.2 shows the critical locations for shear and tensile stresses under truckloads *(Raab and Partl 2004)*. It can be observed that shear stresses created under the truck tire induce tensile stresses in front of the tire. For this reason, laboratory and field experiments focus on both shear and tensile strength of the tack coats to evaluate the long-term resistance.

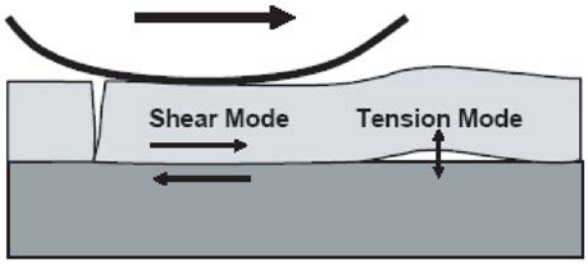

Figure 2.2: Critical stress types at the interface *(Raab and Partl 2004)*.

2.2 TACK COAT MATERIALS AND APPLICATION

2.2.1 Tack Coat Types

Emulsions, paving grade asphalt binders, and cutback asphalts are the materials used as tack coats. Due to environmental concerns, cutback asphalts (asphalts dissolved in solvents such as kerosene) are not allowed to be used as tack coats by many states. Paving grade asphalt binders are also not commonly used since excessive heating of the asphalt cement is required to achieve proper viscosity for spraying *(Leng et al. 2008)*. According to a survey conducted by Mohammad and Button *(Mohammad and Button 2005)*, all of the responding agencies were using asphalt emulsions as tack coats. Asphalt binders were used by 26% and cutbacks were used by 21% of the responding states. In this project, the properties of only asphalt emulsions are investigated since it is the most commonly used tack coat type in Oregon.

Asphalt emulsion is produced by mixing asphalt and water with an emulsifying agent such as soap. The two most commonly used types of asphalt emulsions are anionic and cationic *(Krebs and Walker 1971)*. Asphalt surface charge is negative for anionic emulsions while it is positive for cationic emulsions. Anionic emulsions typically work well with positively charged aggregates such as limestone. Cationic emulsions bond best with negatively charged aggregates such as gravel, sand, and basalt. According to a survey conducted by the International Bitumen Emulsion Federation *(Roffe and Chaignon 2002)*, the most commonly used tack coat type is the cationic emulsion.

Rapid setting (RS), medium setting (MS), and slow setting (SS) are the three general grades used to classify asphalt emulsions *(Krebs and Walker 1971)*. The type and amount of emulsifying agent control the curing (set) time. The most common types of rapid setting emulsions used for

tack coats in the United States are RS-1, RS-2, CRS-1, CRS-2, CRS-2P (polymer-modified), and CRS-2L (latex-modified) while SS-1, SS-1h, CSS-1, and CSS-1h are the most common slow-setting grades *(Mohammad et al. 2012)*. Since the viscosity of slow-setting emulsions can be reduced by dilution, they can be easily sprayed during construction. In addition, slow-setting emulsions are more suitable for lower residual application rates since the total emulsion volume required for the distributor to function can be achieved by dilution *(USACE 2008)*. On the other hand, it might take several hours for slow setting emulsions to break and completely set. Thus, slow-setting emulsions are more vulnerable to slippage during their early life *(USACE 2008)*. Figure 2.3 shows an example for slippage cracking *(Buchanan and Woods 2004)*. Breaking and curing time, change in bond strength over time, and the impact of set time on tracking, the pick-up of bituminous material by construction vehicle tires, should be investigated for different tack coat types to develop a standard for tack coat type selection and application procedures.

Mohammad et al. *(Mohammad et al. 2012)* compared the performance of trackless tack coat (a polymer-modified emulsion with a hard base asphalt cement) to SS-1h, SS-1, CRS-1, and a paving grade asphalt binder (PG64-22). It was concluded that trackless tack coat exhibited the highest shear strength while CRS-1 resulted in the lowest strength. Cortina *(Cortina 2012)* also reported higher shear strength for trackless tack coat. However, improper handling of the trackless tack coat clogged the distributor trucks for several days. Cortina *(Cortina 2012)* recommended a spraying temperature of 175^{o}F to avoid clogging problems.

Figure 2.3: Slippage cracking after overlay construction *(Buchanan and Woods 2004)*.

2.2.2 Tack Coat Application Rates

Using the optimum amount of tack coat is vital to achieving a full bond between two pavement layers. Slippage problems start to arise when an excessive amount of tack coat material is sprayed during construction. On the other hand, inadequate amount of tack coat can result in debonding problems over the design life (especially in the wheel paths) of the pavement structure *(Tashman et al. 2006)*. Thus, optimum residual application rates should be determined by

considering surface (texture and age) and environmental (temperature, humidity, and the wind) conditions. Mohammad et al. *(Mohammad et al. 2012)* recommended to use different residual application rates for i) new or subsequent layers ii) existing relatively smooth, and iii) old, oxidized, cracked, and milled pavement surfaces. Flexible Pavements of Ohio (FPO) *(FPO 2001)* association specified residual application rates for new HMA, oxidized HMA, milled HMA, milled PCC, and new PCC surfaces (Table 2.1). Since surface texture increases with aging and milling, application rates also increase accordingly. Tack coat application rates recommended by Caltrans *(Caltrans 2003)* are given in Table 2.2. It can be observed that slow-setting tack coat application rates for HMA overlays recommended by Caltrans are close to the application rates recommended by Ohio (undiluted) (Table 2.1). Caltrans *(Caltrans 2003)* recommended using higher application rates for open-graded HMA surfaces in order to account for the higher surface texture (Table 2.2).

The effect of application rate on interface shear strength is determined by Mohammad et al. *(Mohammad et al. 2012)* (Figure 2.4). It can be observed that increasing application rates create a considerable increase in interface shear strength for SS-1h and trackless tack coats. However, interface shear strength for CRS-1 is not sensitive to residual application rates. Based on finite element analysis, findings of the field and laboratory experiments, and inputs from state DOTs, Mohammed et al. *(Mohammed et al. 2012)* recommended the residual application rates given in Table 2.3. It should be noted that application rates recommended by Mohammad et al. *(Mohammad et al. 2012)* are within the application rate ranges recommended by the FPO (2001) for all surface types except the application rate for the milled asphalt mixture.

Table 2.1: Typical tack coat application rates for slow setting emulsions in Ohio *(FPO 2001)*.

Pavement condition	Application Rate (gal/yd^2)		
	Residual	Undiluted	Diluted (1:1)
New HMA	0.03~0.04	0.05~0.07	0.10~0.13
Oxidized HMA	0.04~0.06	0.07~0.10	0.13~0.20
Milled Surface (HMA)	0.06~0.08	0.10~0.13	0.20~0.27
Milled Surface (PCC)	0.06~0.08	0.10~0.13	0.20~0.27
PCC	0.04~0.06	0.07~0.10	0.13~0.20

Table 2.2: Recommended tack coat application rates in California *(Caltrans 2003)*.

	Type of Surface	Slow-Setting	Rapid-Setting
HMA Overlay (gal/yd^2)	Dense, smooth surface	0.044~0.077	0.022~0.044
	Textured and aged surface (e.g., milled surface)	0.077~0.199	0.044~0.088
Open-Graded HMA Overlay (gal/yd^2)	Dense, smooth surface	0.055~0.11	0.022~0.055
	Textured and aged surface (e.g., milled surface)	0.11~0.243	0.055~0.121

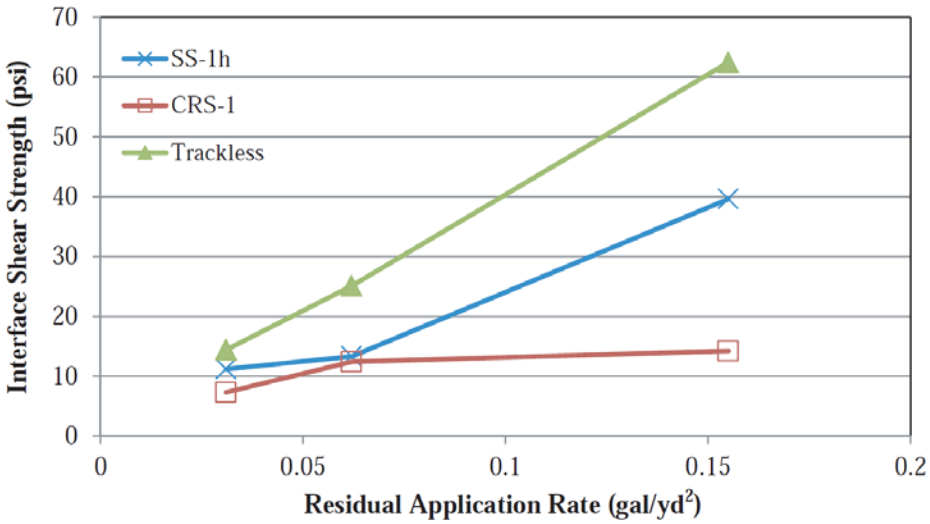

Figure 2.4: Variation of interface shear strength with residual application rates *(Mohammad et al. 2012)*.

Table 2.3: Recommended tack coat residual application rates *(Mohammed et al. 2012)*.

Surface Type	Residual Application Rate (gal/yd^2)
New Asphalt Mixture	0.035
Old Asphalt Mixture	0.055
Milled Asphalt Mixture	0.055
Portland Cement Concrete	0.045

2.2.3 Tack Coat Application Methods

Uniformity and amount of application are two elements required to achieve proper bond strength *(Cortina 2012)*. The factors that are critical to achieving the required application rates and uniformity are summarized as follows *(ASTM Standard D2995 2014; Hachiya and Sato 1997; Mohammad et al. 2012)*:

By placing textile pads along the construction site and weighing them before and after spraying, uniformity and amount of applied tack coat can be measured during construction *(Mohammad et al. 2012; Tran et al. 2012)*. Measured uniformity and spraying rates should be used for tack coat performance evaluation. Distributors should also be modified and maintained to achieve target application rates and uniformity.

2.2.4 Tack Coat Curing Time

There is no consensus on the importance of tack coat curing time. Several research studies *(FPO 2001; TxDOT 2001)* suggested having a cured tack coat layer before constructing the overlay to achieve high bond strengths. Sholar et al. *(Sholar et al. 2004)* evaluated the impact of curing on tack coat shear strength and observed a considerable increase in shear resistance with curing time. On the other hand, several other research studies *(Lavin 2003; USACE 2000)* indicated that since water in the emulsion will immediately evaporate after placing the overlay material on the

tacked asphalt surface, there is no need to wait several hours for the tack coat to cure. Under most circumstances, an emulsion is expected to set in 1 to 2 hours *(USACE 2000)*. Alaska DOT specified a maximum setting period of 2 hours for CSS-1 while Arkansas DOT specified a maximum setting period of 72 hours for SS-1. Texas DOT specified a maximum setting time of 45 minutes for SS-1 *(Mohammad et al. 2012)*. It should be noted that in Europe, asphalt emulsions are applied underneath the paver just before the HMA to minimize tracking problems *(Mohammed et al. 2012)*.

2.3 LABORATORY AND FIELD EVALUATION OF TACK COAT PERFORMANCE

2.3.1 Test Methods

Since pavement interface bond failure is a result of both shear and tensile stresses (Figure 2.2), these two loading modes are used to characterize interface bond strength. Although there are several test types for tack coat performance characterization, the common purpose of all tack coat tests is to determine interface bond strength under shear and tensile forces. In this research project, Florida direct shear test, National Center for Asphalt Technology (NCAT) bond strength test, Louisiana Interlayer Shear Strength Tester (LISST), Texas pull-off test, torque bond test, and Louisiana Tack Coat Quality Tester (LTCQT) are the experiments investigated to develop laboratory and field test devices. In addition, the use of rheological tests (dynamic shear rheometer, rotational viscosity, softening point, and penetration) for tack coat performance characterization is investigated.

2.3.1.1 Florida Direct Shear Test

Florida direct shear test (or FDOT shear tester) is developed by Florida Department of Transportation *(Sholar et al. 2004)* to measure the interface bond strength by applying a shear load in the vertical direction (Figure 2.5a). Two-layered specimens with a diameter of 6 in. (152.4 mm) were tested in shear by moving one of the loading collars (loading frame) in the vertical direction. The gap between the loading frame and the reaction frame was specified to be 4.8 mm. A loading rate of two inches per minute (50.8mm/min.) was used.

Field cores with RS-1 emulsion were tested at 25 ^{o}C. Residual application rates were 0.00, 0.02, 0.05, and 0.08 gal/yd^2. The emulsion was applied on wet and dry surfaces to investigate the effect of water on bond strength. The major conclusions of the study were:

- Water reduced bond strengths. Wet sections with a 0.08 gal/yd^2 application rate have significantly higher bond strengths than the wet sections with lower application rates.
- Tack coats applied on milled surfaces had higher bond strengths.
- The standard deviation of the measured interface bond strengths was determined to be 9.6 psi.

- The interface bond strength difference between the sections with no tack coat (0.00 gal/yd^2) and 0.02 gal/yd^2 application rate were measured to be minimal. However, increasing the application rate to 0.05 gal/yd^2 created a significant increase in measured bond strengths.

2.3.1.2 National Center for Asphalt Technology (NCAT) bond Strength Test

West et al. *(West et al. 2005)* developed NCAT bond strength test (Figure 2.5b) to determine the best tack coat material and optimum application rates. NCAT bond strength test is a shear type test in which shear load was applied with a universal testing machine (UTM). The major difference from the FDOT shear tester is the horizontal load (perpendicular to the direction of shear) applied as a normal (confining) pressure. The major purpose of using normal pressure is to determine the impact of surface texture on bond strength. A loading rate of two inches per minute (50.8mm/min.) was used to be able to conduct the test with a Marshall press (when a UTM is not available).

Two types of emulsion (CRS-2 and CSS-1) and a PG 64-22 asphalt binder were tested at 10, 25, and 60 ^{o}C. Residual application rates were 0.02, 0.05, and 0.08 gal/yd^2. Applied constant normal pressures were 0, 10, and 20 psi. The major conclusions of the study were:

- The normal pressure did not significantly affect the measured bond strengths at 10 and 25 ^{o}C test temperatures. On the other hand, at 60 ^{o}C, increasing normal pressure increased bond strengths.

- CRS-2 and CSS-1 had lower bond strengths than PG 64-22, especially at 60 ^{o}C.

- Increasing temperature reduced bond strengths.

- Tack coats applied on milled surfaces had higher bond strengths.

2.3.1.3 Louisiana Interlayer Shear strength Tester (LISST)

Mohammad et al. *(Mohammad et al. 2012)* developed LISST (Figure 2.5c) to characterize interface bond properties under shear loads. The major difference from the NCAT bond strength test was the reduced loading rate (2.54mm/min) and improved test fixture with less friction. Loading rate was reduced to avoid unrealistically high bond strengths observed under fast loading rates *(Hachiya and Sato 1997)*. Using 2D finite element simulations and laboratory testing at different displacement rates (2in/min, 0.1in/min, and 0.02in/min), Mohammad et al. *(Mohammad et al. 2012)* recommended the use of 0.1 in/min (2.54mm/min) as the displacement rate to be able to effectively simulate the slow rate of loading encountered at the interface in the field. Two-layered specimens with a diameter of 6 in. (152.4 mm) were tested in shear by moving one of the loading collars (loading frame) in the vertical direction. The gap between the loading frame and the reaction frame was specified to be 0.5 in. (12.7mm).

Mohammad et al. *(Mohammad et al. 2012)* conducted several experiments on field-prepared samples under different conditions to investigate the effects of surface type, tack coat type, application rate, cleanliness, water, confinement, and tack coat coverage on interface bond strength. Test factorial is given in Table 2.4 . The major conclusions of the LISST experiments were:

- Trackless tack coat created the highest interface bond strength while CRS-1 had the lowest strength.
- The difference between measured interface bond strengths for confined and unconfined tests was statistically significant. It was concluded that unconfined tests provided a conservative estimate of the bond strengths.
- Dusty conditions exhibited higher bond strength than the clean cases. However, this conclusion was indicated to be a result of the clean sand particles with uniform sizes used for creating the dusty conditions. Sand particles mixed with the applied tack coat formed a mastic which has a higher viscosity than the tack coat. This increased viscosity was indicated to be the reason for increased bond strength.
- The effect of water on bond strength was not statistically significant.
- The increased surface texture was observed to increase bond strength. Measured interface bond strength for milled HMA was the highest followed by Portland cement concrete (PCC), old HMA, and new HMA surfaces.
- Increasing temperature reduced bond strengths.
- Based on the test results, tack coat application rates given in Table 2.3 are recommended.

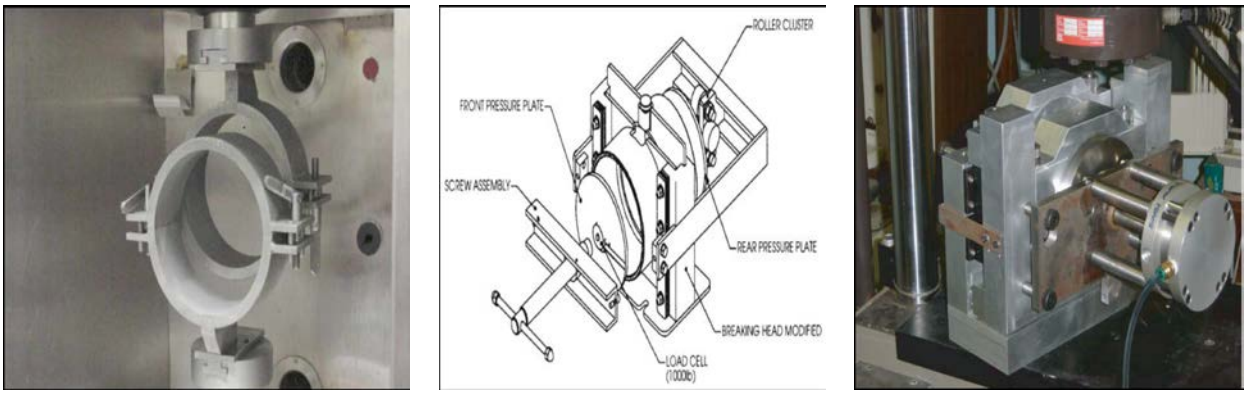

(a) (b) (c)

Figure 2.5: Laboratory shear testers for interface bond strength measurement (a) Florida direct shear tester *(Sholar et al. 2003)* (b) NCAT shear device *(West et al. 2005)* (c) LISST device *(Mohammad et al. 2012)*.

Table 2.4: Test factorial for field-prepared samples (Mohammad et al. 2012).

Variables*	Content	Levels
Pavement surface type	Old HMA, new HMA, grooved PCC, milled HMA	4
Tack coat material	SS-1h, SS-1, CRS-1, Trackless, PG 64-22	5
Residual application rate	0- (No-Tack), 0.031-, 0.062-, 0.155-gal/yd^2	4
Wetness (Rain) condition	Wet, Dry	2
Cleanliness condition	Dusty, Clean	2
Test temperature	25°C	1
Confinement pressure (psi)	0, 20	2
Tack coat coverage	50%, 100%	2
Number of replicates	3	3
Total Number of Samples		474

* Some variables were partially evaluated according to the test factorial.

2.3.1.4 Texas Pull-Off Test

Texas Pull-off test device (Figure 2.6a) was developed at the University of Texas at El Paso (UTEP) *(Deysarkar 2004)* to measure the tensile strength of applied tack coat before constructing a new overlay. After the tack coat is applied on the pavement surface, tack coat layer was left to set. After it is set, the device is placed on the tacked surface. Load plate is lowered to come in contact with the tacked pavement surface. Then, a 40-pound load is applied on the device for 10 minutes prior to testing to create bonding between the test plate and the pavement surface. After 10 minutes, the load is removed and the torque wrench is manually rotated in the counter-clockwise direction to move the plate in the vertical direction (Figure 2.6a). The torque required to break the bond between the plate and the pavement surface is recorded and converted to bond strength using a calibration factor.

Tashman et al. *(Tashman et al. 2006)* conducted several Florida direct shear and Texas pull-off tests on milled and non-milled test sections to investigate the effectiveness of Texas pull-off test for interface bond strength characterization. Test results showed that although measured interface bond strength values for the Florida direct shear test are higher for the milled sections (as expected), tack coat strength values measured by Texas pull-off test during construction appeared to be lower for the milled test sections. This result suggested that smaller contact area for the milled sections (due to high texture) increased the applied stresses and resulted in early failure at lower load levels for the milled sections. Mohammad et al. *(Mohammad et al. 2012)* avoided this problem by attaching a polyethylene foam to the loading plate to increase contact area for milled sections.

2.3.1.5 Torque Bond Test

The torque bond test (Figure 2.6b) was developed in Sweden and used as an in-situ test method to evaluate field bond strength. The test was adopted by the UK as a part of the approval system for tack coats *(Walsh and Williams 2001).* After asphalt overlay is constructed, it is cored about half inch deeper than the interface. Loading plate is glued to the overlay surface using fast setting epoxy. Torque is manually applied to the surface at a constant rate using a torque wrench (Figure 2.6b). Torque at failure is used as a parameter to characterize interface bond shear strength. Torque bond test can also be conducted on laboratory samples under controlled temperature. Manual load application with the torque wrench was later replaced by a servo motor actuator in the ATacker device to improve repeatability *(Buchanan and Woods 2004).*

Although the torque bond test captured the effect of milling on tack coat strength, the correlation between the measured torque values and the bond strength values from the Florida direct shear test was not statistically significant *(Tashman et al. 2006)*. Weak correlation might be a result of the variability and bias introduced by manual load application. In addition, since the limit of the torque wrench was reached for most of the experiments, correlations at high bond strengths were not investigated.

2.3.1.6 Louisiana Tack Coat Quality Tester (LTCQT)

Several research studies have been conducted to develop an in-situ test method to investigate the bonding characteristics of different tack coat types. Texas pull-off and torque bond tests were improved to develop a test method known as the ATacker *(Buchanan and Woods 2004; Mohammad and Buttons 2005)*. Mohammad et al. *(Mohammad et al. 2012)* developed LTCQT (Figure 2-6c) by further improving the ATacker by:

- using a load cell with a lower noise level,
- using a new actuator and driving motor to minimize the errors in displacement rate,
- attaching a polyethylene foam to the loading plate to increase contact area for milled sections.

Mohammad et al. *(Mohammad et al. 2012)* conducted several field experiments to evaluate the effectiveness of LTCQT for tack coat quality evaluation. Tested sections were clean and dry (See Table 2.4). SS-1h, CRS-1, and trackless were the tack coats tested with LTCQT. Residual application rates for the tested sections are given in Table 2.5. More than three replicate tests were conducted on each section. Comparison of LTCQT results to the results of LISST and rheological tests showed that LTCQT is a viable method for tack coat quality evaluation during construction. The LTCQT was recommended to be used as a tool to determine the most effective tack coat application methods and rates in the field. Variability of LTCQT test results was also determined to be acceptable, with an average coefficient of variation of less than 11%. Mohammad et

al. *(Mohammad et al. 2012)* recommended conducting LTCQT at the tack coat base asphalt softening point in order to get comparable results for different tack coat types. Although LTCQT was suggested to be a reliable system for tack coat performance evaluation, practicality, variability, and effectiveness of LTCQT need to be improved to increase the widespread use of this system to evaluate the long-term performance of tack coats.

(a) (b) (c)

Figure 2.6: Interface bond strength devices (a) Texas pull-off test *(Deysarkar 2004)* (b) Torque bond test *(Walsh and Williams 2001)* (c) LTCQT *(Mohammad et al. 2012)*

Table 2.5: LTCQT test sections *(Mohammad et al. 2012).*

Material	Residual Application Rate (gal/yd^2)
SS-1h 50 % Coverage	0.031
	0.155
SS-1h 100 % Coverage	0.031
	0.062
	0.155
Trackless	0.031
	0.062
	0.155
CRS-1	0.031
	0.062
	0.155

2.3.2 Rheological Tests

Mohammad et al. *(Mohammad et al. 2012)* evaluated the correlations between the rheological properties of tack coat materials and the interface bond strength (measured by LISST) by conducting experiments at temperatures ranging from -10 to 60 ^{o}C with a 10 ^{o}C interval. Penetration, absolute viscosity, rotational viscosity, and softening point were the four consistency tests conducted. Results of the consistency tests showed that trackless material was the hardest followed by SS-1h, PG 64-22, and CRS-1. Mohammad et al. *(Mohammad et al. 2012)* also investigated the correlations between rotational viscosity, G*/sinδ , and the softening

point of the tack coat with interface bond strength. Test results showed that rheological properties are correlated with the measured interface bond strength values (Figure 2.7). This result suggested that simple rheological tests can provide important information about the bond strength and performance of tack coats.

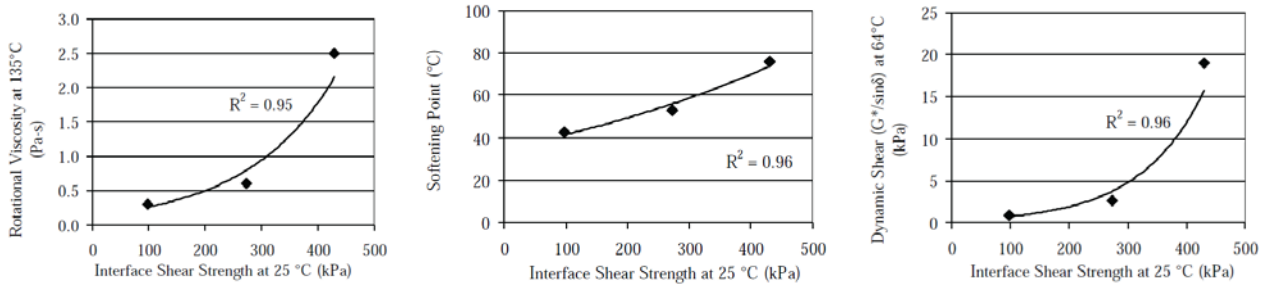

(a) (b) (c)

Figure 2.7: Relationship between interface bond strength and rheological tests *(Mohammad et al. 2012)*.

2.4 COMPUTER MODELS FOR BOND STRENGTH EVALUATION

Several computer models have been developed to investigate the impacts of different variables (such as temperature, layer thicknesses, stiffness, loads, etc) on the critical stresses and strains at layer interfaces. King and May *(King and May 2003)* investigated the effect of bonding on fatigue life using the software BISAR *(De Jong 1973)*. They have modeled 40 kN and 53.4 kN dual tire loads on a flexible pavement structure with two 100 mm HMA layers (an overlay and an existing HMA layer) over a 150 mm aggregate base and a subgrade. Simulations were conducted for several bonding levels ranging from no-slip condition (100 % bonding) to full slip (0 % bonding). Results of the analysis showed that fatigue life decreases by 50 % when the bond is reduced by 10 %. Roffe and Chaignon *(Roffe and Chaignon 2002)* conducted similar analysis using the French pavement design program ALIZE and concluded that pavement service life can reduce from 20 years to 7 years due to the lack of bond between two asphalt layers.

Using 3D finite element modeling, Tayebali et al. *(Tayebali et al. 2004)* investigated the effects of layer thickness and stiffness on the stress-strain-displacements fields. It was concluded that delamination problem can be reduced by increasing overlay thickness. Increased overlay thickness reduces critical interface shear stresses and minimizes the risk of bond failure. The impact of increased layer thickness (higher material costs) and increased fatigue life (longer service life) on pavement life cycle costs should be investigated to evaluate the effectiveness of different design strategies.

Mohammad et al. *(Mohammad et al. 2012)* investigated the effect of tack coat interface bond characteristics on pavement responses using 2D finite element modeling. Aggregate base and subgrade layers were modeled as elastic layers while HMA overlay and the existing layers were modeled as viscoelastic materials using a generalized Kelvin model. Tack coat interface shear bond characteristics were modeled by using the results of laboratory shear tests. Results of the analysis showed that trackless, SS-1h, and PG 64-22 tack coats had the best performance while the sections with CRS-1 tack coat were predicted to experience early fatigue failures. It was also

concluded that tack coat performance is controlled by the pavement design. Tack coat type and application rates are determined to be more important for structures with thin overlays.

2.5 GENERAL PRACTICES IN THE U.S.

This section summarizes the important results of the survey conducted for NCHRP 9-40 project *(Mohammad et al. 2012)*. Responses from 46 states and 4 countries (Denmark, Finland, South Africa, and the Netherlands) were used for deriving conclusions. Important conclusions of the survey are outlined below:

- Emulsified asphalts are, by far, the most commonly used tack coat material followed by asphalt cement and then cutback asphalts.
- SS-1, CSS-1h, SS-1h, and CSS-1 are the most commonly used emulsified asphalts.
- 64% of the respondents achieve above 90% coverage during construction while for only 18% of the respondents, the coverage area is less than 70%.
- 67% of the respondents indicated that pick up of tack coat material is an important problem. According to 38% of the respondents, it is a requirement to have the tack coat material set before haul trucks are allowed on it.
- 73% of the agencies indicated that no specific requirements are used to regulate tack coat application while the amount of spray overlap between adjacent nozzles on the distributor spray bar is a specified requirement for the rest.
- 78% of the respondents do not allow highway traffic prior to HMA placement.
- The amount of time required for setting of the tack coat before overlay construction are:
    - 0 hours (18% of the respondents)
    - 4 hours (12% of the respondents)
    - 12 hours (17% of the respondents)
    - 24 hours (47% of the respondents)
    - 120 hours (6% of the respondents)
- Based on the responses, the factors that affect the break and set times for emulsified asphalts are ranked below in order of importance, from highest to lowest:
    - Ambient temperature,
    - Pavement surface temperature,

- Dilution rate,
- Application rate,
- Humidity,
- Wind velocity, and
- Others.

- 38% of the respondents are requiring a minimum pavement surface temperature for tack coat application (average reported temperature was 3^{o}C). No agency reported a restriction of maximum pavement surface temperature.

- 75% of the respondents do not allow tack coat application on wet pavement surfaces.

- 92% of the respondents indicated that laboratory/field experiments are not conducted to measure bond strength. Texas pull-off and Florida shear tests are the major experiments conducted by the remaining 8%. 18% of the respondents are conducting field/laboratory experiments to evaluate tack coat material quality.

2.6 SUMMARY

A review of the literature indicates that although there are several laboratory shear test methods for interface bond strength evaluation, Florida direct shear, NCAT bond strength, and LISST are the most commonly accepted experiments due to their simplicity. The use of normal pressure in NCAT bond strength test and LISST to simulate in-situ confinement improved the results of experiments conducted at high temperatures *(West et al. 2005; Mohammad et al. 2012)*. Based on the results of laboratory testing and 2D finite element modeling, Mohammad et al. *(Mohammad et al. 2012)* recommended a reduced loading rate (2.54mm/min) for LISST. Although the reduced displacement rate for LISST was reported to minimize the problem of having unrealistically high bond strength values at lower temperatures, the use of lower loading rates avoided the use of a Marshall press for testing.

Texas pull-off, torque bond, and LTCQT are the most commonly accepted laboratory/field experiments used to investigate the bonding characteristics of tack coats. Tashman et al. *(Tashman et al. 2006)* investigated the effectiveness of Texas pull-off test and concluded that Texas pull-off test cannot be used to investigate the bond performance of field sections with milled surfaces. Poor adhesion and smaller contact area for the milled sections (due to high texture) increase the applied stresses and result in early failure at lower load levels. Although the torque bond test captured the effect of milling on tack coat strength, the correlation between the measured torque values and the bond strength values from the Florida direct shear test was not statistically significant *(Tashman et al. 2006)*. Texas pull-off and torque bond tests were improved to develop a test method known as the ATacker *(Buchanan and Woods 2004; Mohammad and Button 2005)*. Mohammad et al. *(Mohammad et al. 2012)* developed LTCQT (Figure 2.6c) by further improving the ATacker by:

- using a load cell with a lower noise level,
- using a new actuator and driving motor to minimize the errors in displacement rate, and
- attaching a polyethylene foam to the loading plate to increase contact area for milled sections.

Although LTCQT is accepted to be a viable method for tack coat quality evaluation during construction, the high cost of LTCQT may restrict its widespread use in overlay construction projects in Oregon. In addition, LTCQT can only be conducted on tack coats before the construction of overlay. An in-situ test device that can be used on overlays should also be developed to periodically monitor interface bond strength.

According to the literature, tack coat type, amount of application, and uniformity are the three important factors required to achieve proper bond strength *(Buchanan and Woods 2004; Tashman et al. 2006; West et al. 2005; Mohammad et al. 2012; Cortina 2012).* According to the survey conducted by Mohammad et al. *(Mohammad et al. 2012)*, emulsified asphalt is the most commonly used tack coat material followed by asphalt cement and then cutback asphalt. SS-1, CSS-1h, SS-1h, and CSS-1 are the most commonly used emulsified asphalt types. Application rates recommended by FPO *(FPO 2001)*, Caltrans *(Caltrans 2003)*, and Mohammad et al. *(2012)* appear to be close for almost all pavement surface types. According to Tran et al. *(Tran et al. 2012)*, uniformity and spraying rates of distributors should be periodically measured during construction. Distributors should be modified and maintained to achieve target application rates and uniformity.

There is no consensus on the importance of tack coat curing time. The setting periods specified by state DOTs and other countries range from 0 to 120 hours. According to the survey conducted by Mohammad et al. *(Mohammad et al. 2012)*, 38% of the respondents indicated that it is a requirement to have the tack coat material set before haul trucks are allowed on it.

Although there are several computer models developed to investigate the impacts of different variables (such as temperature, layer thicknesses, stiffness, loads, etc) on interface bond strength, the impact of increased layer thickness (higher material costs) and increased fatigue life (longer service life) on pavement life cycle costs have never been investigated. The effect of application rate and tack coat type on the performance of tack coats with thin overlays should be investigated.

3.0 EVALUATION OF TACK COAT RHEOLOGICAL PROPERTIES AND THE EFFECTS ON INTERLAYER SHEAR STRENGTH

3.1 INTRODUCTION

CSS-1H emulsions are the most commonly used slow-setting grades in Oregon. “New” emulsions are the engineered emulsions recently developed in Oregon to reduce tracking and increase interlayer shear strength (ISS). The performance of these emulsions, most effective application rates, and the effects of pavement surface texture and traffic on interlayer shear strength are evaluated in this section.

Many studies in the literature have investigated interlayer shear strength (ISS) and the various affecting factors, as well as alternative testing methods to determine the ISS. This section presents a comprehensive field investigation consisting of field and laboratory testing, field coring, and construction sampling of tack coats used in Oregon. Within the study, two new tack coat materials from two companies were, for the first time, evaluated for their performance. Field coring was completed at two different time increments, as well as two travel lines (wheel path and center of the lane), to capture the effect of traffic loading and time on interlayer shear strength. Recommendations for the most efficient application rate along with ISS prediction equations based on rheological properties were developed. Results of the evaluation will provide valuable information about correlations between rheological tests and interlayer shear strength, as well as the effects of texture, traffic loads, and application rate on interlayer shear strength.

Rheological tests were performed on tack coats sampled during construction after binder was extracted via distillation. These tests included softening point, rotational viscosity, penetration, and dynamic shear rheometer. Correlations between rheological tests and shear tests (ground truth) were evaluated, and prediction equations were developed so that in-situ ISS can be predicted from simple rheological test results in the future. Results show that a positive correlation between pavement surface texture and interlayer shear strength exists; therefore, milled surfaces provide significantly higher ISS than non-milled overlay surfaces. For this reason, for milled surfaces, application rates did not have any significant effect on ISS because the surface texture mostly controlled strength. The results indicated that there are positive correlations between rheological tests and interlayer shear strengths from field cores. The results also showed significant variances in application rates by distributor trucks. Hence, there is a need for unified guidelines on tack coat spraying methods and construction practices.

3.2 OBJECTIVES

The major objectives of this part of the study are given as follows:

1. Evaluate the effects of pavement surface texture on interlayer shear strength;

2. Assess the effects of traffic/environmental factors on interlayer shear strength;

3. Develop methods and equations to predict interlayer shear strength from simple rheological test results;

4. Determine the impact of location on interlayer shear strength (wheel-path vs. center line).

5. Determine the most effective application rates and methods to:

    a. Maximize interlayer shear strength

    b. Improve current methods for tack coat application.

3.3 MATERIALS AND METHODS

3.3.1 Experimental Design for Field Testing and Sampling

The general layout of the experimental design is summarized in Table 3.1. In total, testing and sampling were conducted at three locations in the field. Asphalt overlays were constructed with two lifts. First lift (2.5 inches thick) was placed on a milled surface while the second lift (2 inches thick) was built on the new lift (without any milling) about a month after the construction of the first lift. Each location had the same tests performed for the milled and overlay surfaces. A test location consisted of three 200-foot sections, each of which contained a different target application rate (Table 3.1). Location 1 and Location 2 were operating at normal highway speeds, northbound and southbound lanes respectively. Vehicle speeds on Location 3 were lower because it was located within a turning lane at an intersection. The six tack coat types considered in this study are shown in Table 3.1. Generic tack coat type labels are used to conceal the identity of the company providing the material. CSS-1H emulsions are the most commonly used slow-setting grades in Oregon. "New" emulsions are the engineered emulsions recently developed in Oregon to reduce tracking and increase interlayer shear strengths.

Table 3.1: Site layout for field testing

Surface	Location	Day	Tack Coat Type	Application Rates (gal/yd^2)
Milled	1	Day 1	CO1_CSS 1H_a	0.08, 0.10, 0.12
	2	Day 2	CO1_New_a	0.08, 0.12, 0.16
	3	Day 3	CO2_New	0.08, 0.12, 0.16
Overlay	1	Day 4	CO1_CSS 1H_b	0.05, 0.07, 0.10
	2	Day 5	CO1_New_b	0.05, 0.07, 0.09
	3	Day 6	CO2_CSS 1H	0.05, 0.07, 0.10

3.3.2 Field and Laboratory Experiments

Sampling of tack coat from the distributor truck was performed during construction before tack coat application (Figure 3.1a). Sampling was done according to ASTM D140 *(ASTM D140*

2015). On each construction day, three 5-gallon buckets were filled, labeled, and sealed with electrical tape. This extra step to seal the buckets ensured a reduction in bias due to evaporation of water from the emulsion during storage. Buckets of sampled emulsion were then taken to the laboratory for the rheological experiments to be performed. Before sampling emulsions from the buckets in the lab, buckets were agitated for at least 10 minutes to achieve uniformity.

Sand patch testing was conducted during construction to measure the macrotexture depth of the pavement surface for both milled and overlay surfaces according to ASTM E965 *(ASTM E965 2015)* (Figure 3.1b). A known volume of sand was carefully spread over the pavement surface in a circular pattern to fill surface voids. Diameter readings of the circle were recorded on four axes, and the values were averaged. Calculated values were then used to calculate the Mean Texture Depth (MTD). Eight tests were performed at random spots within each of the three site locations.

Application rate measurements were taken by placing 12 inch by 12-inch textile pads end to end in the travel lane in the transverse direction (Figure 3.1c). An application rate was calculated by using the weight of the textile pad before and after spraying. These calculated application rates were then compared to the target application rates to evaluate the overall accuracy of application rates *(ASTM Standard D2995 2014)*. Company distributor trucks (new truck) were used for all milled surface spraying and Location 1 and 2 of overlay surfaces. The contractor's distributor truck (old truck) was used for Location 3 overlay surface spraying.

(a) **(b)** **(c)**

Figure 3.1: Experiments conducted to evaluate tack coat application methods and procedures (a) emulsion sampling for laboratory tests (b) sand patch texture measurements (c) application rate measurement

All binder residues were extracted from sampled emulsions according to ASTM D6997 *(ASTM D6997 2012)* (Figure 3.2a). Measured emulsion densities and water contents are given in Table 3-2. Softening point and rotational viscosity tests were performed according to ASTM D36 *(ASTM D36 2014)* (Figure 3.2b) and ASTM D4402 *(ASTM D4402 2015)*(Figure 3.2c), respectively. Penetration and dynamic shear rheometer (DSR) tests were also performed according to ASTM D5 *(ASTM D5 2013)* (Figure 3.2d) and ASTM D7175 *(ASTM D7175 2015)* (Figure 3.2e), respectively.

Distillation was performed at two temperatures (170 and 260 °C) for several emulsions to determine the impact of distillation temperature on measured performance parameters for all tack coat types (See Table 3.2 for densities). Results of the experiments showed that the correlation

between viscosities at different distillation temperatures is significant, which indicates that the distillation temperature had minimal effect on the performance properties (Figure 3.3).

Although a lower distillation temperature (170^{o}C) was used to recover binder residue from Day 5, CO1_New_b emulsion, both the standard temperature (260 ^{o}C) and the reduced temperature resulted in the burning of the sample and massive amounts (76%) of water being collected. For this reason, rheological experiments could not be performed on CO1_New_b.

Table 3.2: Emulsion densities and water contents

Surface	Location	Day	Tack Coat Type	Density (g/mL)	Water Distilled (mL)	Percent Water (%)
Milled	1	Day 1	CO1_CSS 1H_a	0.930	102	51
	2	Day 2	CO1_New_a	0.928	147	73
	3	Day 3	CO2_New	0.889	123	62
Overlay	1	Day 4	CO1_CSS 1H_b	0.873	94	47
	2	Day 5	CO1_New_b	0.909	152	76
	3	Day 6	CO2_CSS 1H	0.914	110	55

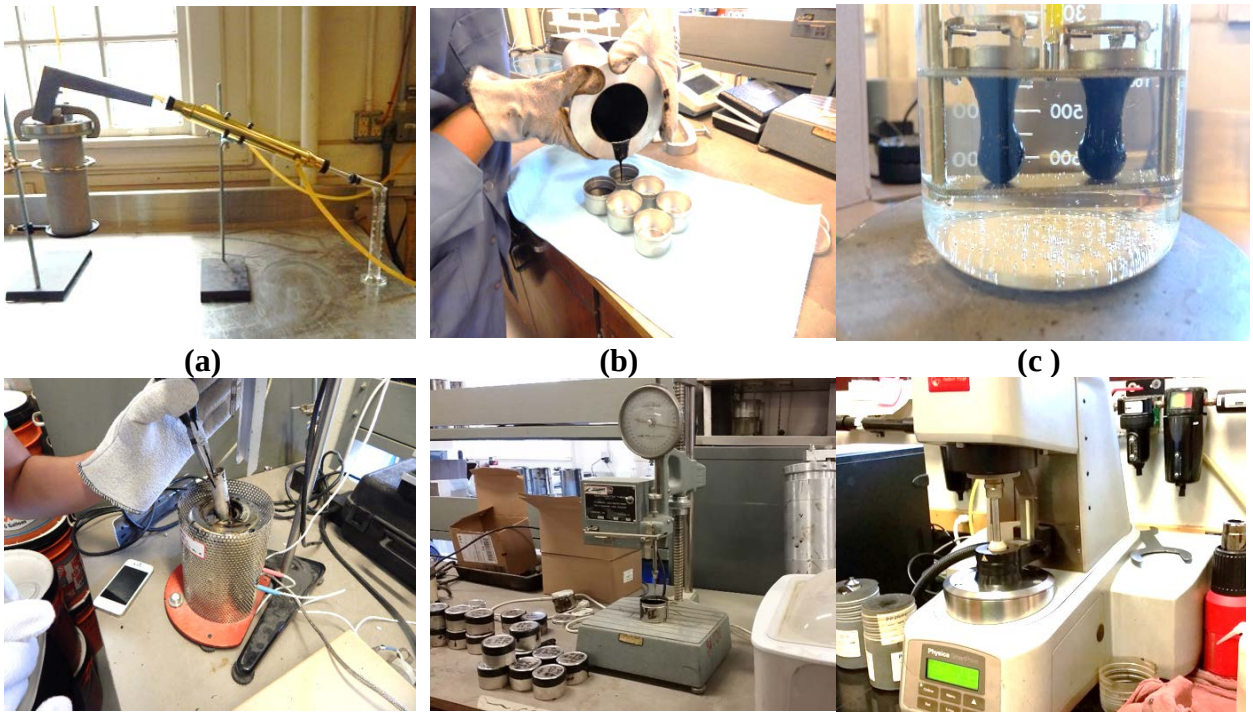

(a) **(b)** **(c)**

(d) **(e)** **(f)**

Figure 3.2: Series of rheological tests performed (a) distillation apparatus (b) resulting binder residue from distillation (c) determination of softening point (d) determination of viscosity using a rotational viscometer (e) determination of penetration (f) dynamic shear rheometer

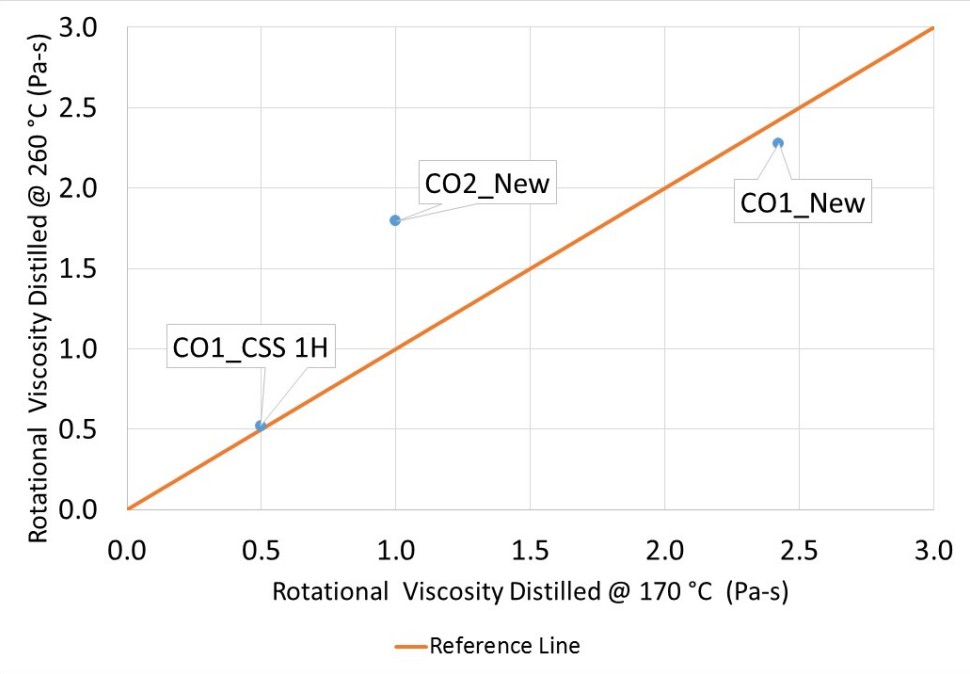

Figure 3.3: Effect of distillation temperature on the viscosity of tack coats

3.3.3 Experimental Design for Field Coring and Testing

3.3.3.1 Procedure for Determining Interlayer Shear Strength of Field Cores

To be able to evaluate the correlations between the parameters from simple rheological experiments and in situ (ground truth) interlayer shear strengths, field cores were taken from all 9 field test sections to conduct shear experiments according to AASHTO TP114 *(AASHTO TP114 2015)*. The general procedure for interlayer shear strength sample preparation and testing is illustrated in Figure 3.4. Asphalt concrete cores used in this study were taken from three locations (as described in Table 3.1) along HWY 99 near Monmouth, Oregon. In total, 114 cores were taken (90 cores three months after construction and 24 cores seven months after construction). The followed steps are as follows:

- Before drilling, the location of each core was marked and arrows were drawn to indicate the direction of traffic within the lane (Figure 3.4a). Samples were sheared in the direction of traffic to reduce variability and bias in test results.
- Six-inch field cores were retrieved using a core drill (Figure 3.4b). Specific location labels were applied before cores were transported.
- All cores were left to dry (Figure 3.4c).
- Core diameters and lift heights were recorded (Figure 3.4d).

- Each core was cut, using a large wet stationary saw, to ensure a proper fit inside the testing apparatus (Figure 3.4e).

- A single core was loaded horizontally into the Asphalt Tack Bond Shear Strength Apparatus with the direction of traffic arrow facing down (shearing direction) and the surface on the shearing side *(AASHTO TP114 2015)* (Figure 3.4f). A confining pressure of 20 psi was used for testing.

- Testing apparatus was placed into the loading frame inside the environmental chamber. Vertical and horizontal displacement sensors (LVDTs) were secured (Figure 3.4g), and samples were left to be conditioned at the 25^{o}C test temperature for a minimum of 2 hours *(AASHTO TP114 2015)*.

- Data was collected via computer software, filtered with MATLAB, and exported into Excel (Figure 3.4h).

- Figure 3.4i shows a sample successfully sheared at the pavement lift interface. All samples showed a similar failure pattern.

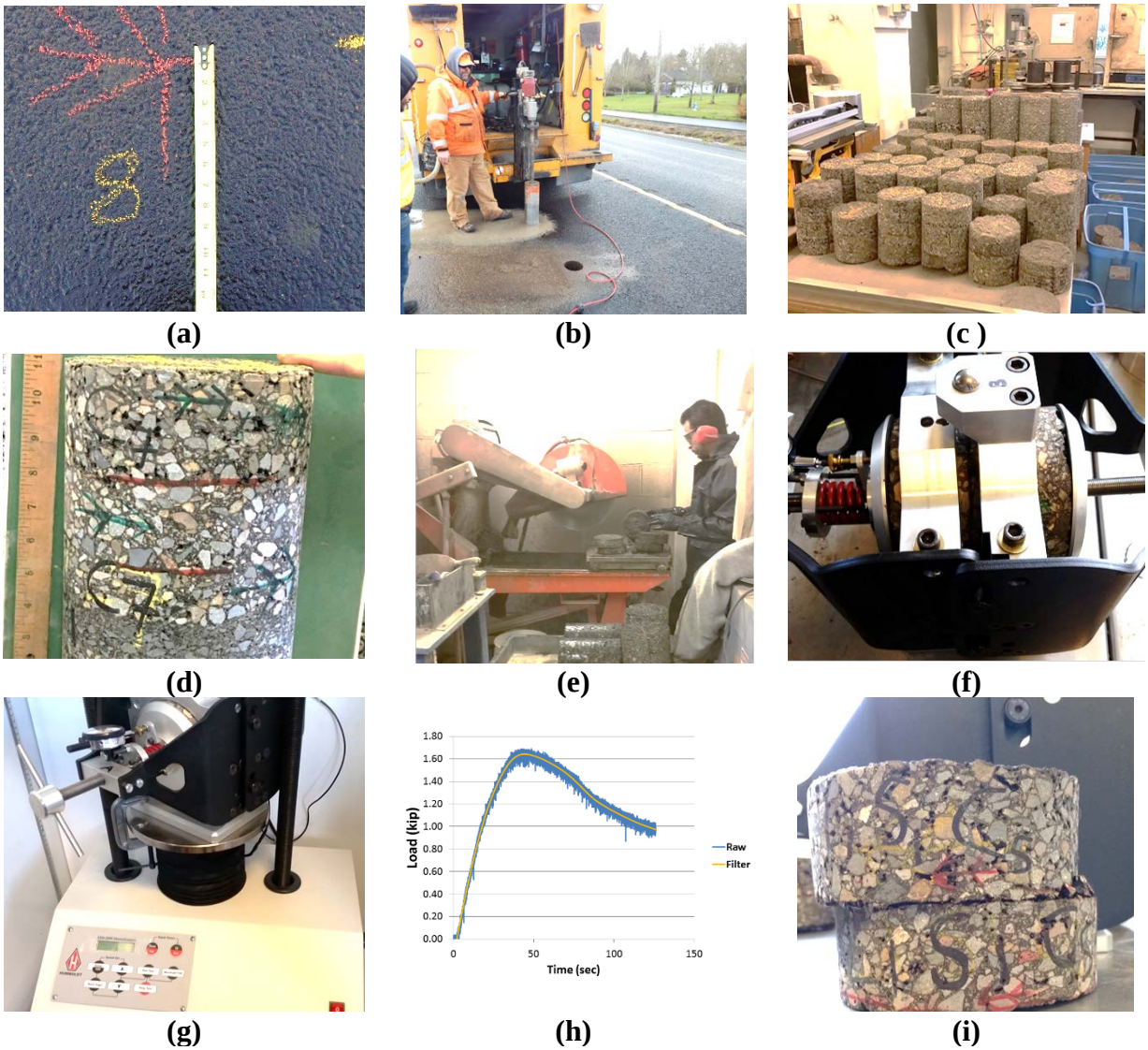

Figure 3.4: General photographic steps used to determine interlayer shear strength of field cores

3.3.3.2 Laboratory Shear Testing to Evaluate the Effect of Traffic on Interlayer Shear Strength

24 cores were taken seven months after construction (four months after taking the initial set of cores) from similar areas within Locations 1 and 2. Of the 24 cores taken, only 16 shear experiments were performed (eight cores were used to conduct torque experiments).Within the locations, only Sections 2 and 3 had cores taken from them. The purpose of the second round of field cores was to quantify the changes in interlayer shear strength due to environmental factors and traffic loading. To capture this effect, only the top layer (overlay surface) interfaces were tested for interlayer shear strength and then compared to values obtained four months earlier.

The first round of coring took ten cores from each section (for a total of 90), with six in the wheel path nearest the fog line and four in the center of the travel lane. The use of two locations in the transverse direction would help identify changes in interlayer shear strength depending on location. The second round of coring deviated from the previous pattern due to top layer separation during coring in Location 1 and coordination of results with field torque testing happening at the same time. Location 1 cores were taken from the center of the travel lane for both sections 2 and 3, while Location 2 cores were taken from the wheel path for both sections 2 and 3.

3.4 RESULTS AND DISCUSSION

3.4.1 Effects of Surface Texture on Interlayer Shear Strength

Effects of pavement surface texture on interlayer shear strength were investigated by determining the surface texture based on the sand patch test method according to ASTM E965 *(ASTM E965 2015)* and investigating the correlations between the measured surface texture and measured interlayer shear strength. Sand patch test method was adopted for its ease of use in the field and for its production of results that are highly correlated with the results from high-cost laser texture scanners. A 2004 report by Hanson and Prowell of the National Asphalt Center for Technology (NCAT) evaluated the Circular Texture Meter (CT Meter) and compared this laser-based device to the simple volumetric method known as the "sand-patch" method. CT Meter and Sand Patch measurements were taken at five random locations on 45 different asphalt pavement sections at the NCAT test track. The high coefficient of determination ($R^2 = 0.95$) indicated a strong relationship between values obtained from the two different test methods *(Hanson and Prowell 2004)*.

Mean texture depths for the field sections measured by following the sand-patch method are given in Figure 3.5. Results showed that milled surfaces had a significantly higher mean texture depth than the overlay surfaces that were not exposed to milling during construction (Figure 3.5). Each box plot represents the spread of texture values obtained from the eight tests performed at each location. Average surface texture values were recorded as the mean of these eight tests for each location for milled and overlay surface types. The overlay surfaces had a considerably smaller (82% less) mean texture depth (MTD) than the milled surfaces. The milled surface exhibited higher variance in MTD values across the three locations when compared to the overlay surface MTD variance.

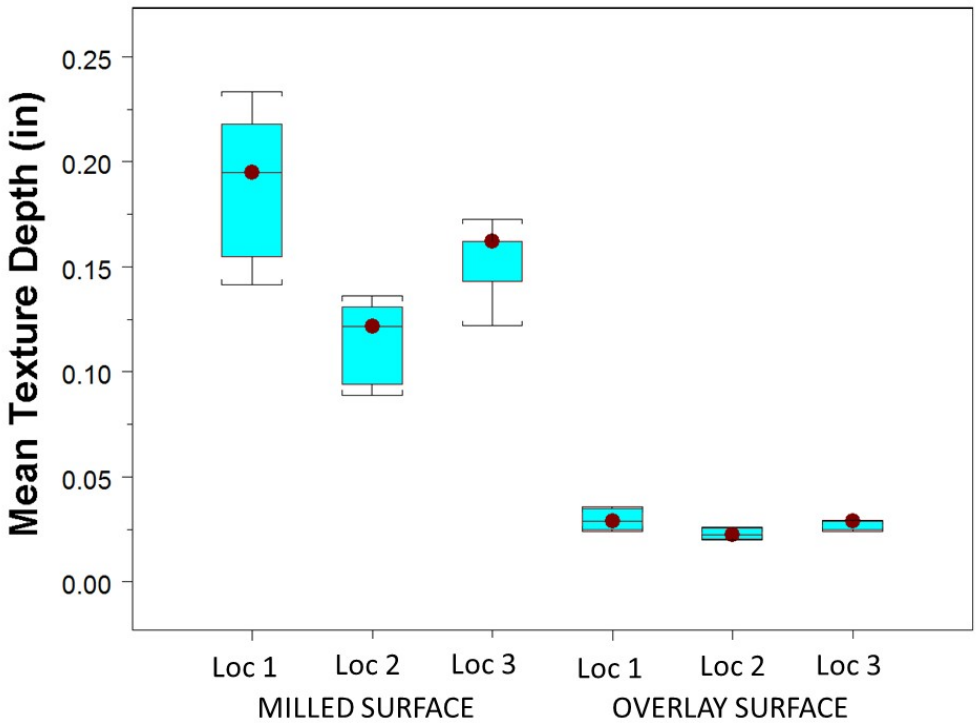

Figure 3.5: MTD results from sand patch measurements

The purpose of determining the surface texture was to compare the measured texture to the measured interlayer shear strength (ISS) values to determine the impact of texture on ISS. Figure 3.6 shows the relationships between surface texture values and the interlayer shear strengths of field cores. Results show a strong positive correlation between texture and ISS. Each point in Figure 3.6 represents the average interlayer shear strength for an entire test location as described in Table 3.1 and the average MTD for the corresponding location. Independently, milled surface test results also showed a positive relationship, as texture increases so do interlayer shear strength. Because of the strong correlation between texture and ISS, conclusions about tack coat materials and application rates derived from results involving the overlay surface can be expected to be more reliable than the conclusions made from milled surfaces. Texture has too much influence on the ISS results for milled surfaces to extract clear relationships and milled surfaces exhibit higher variance in texture values.

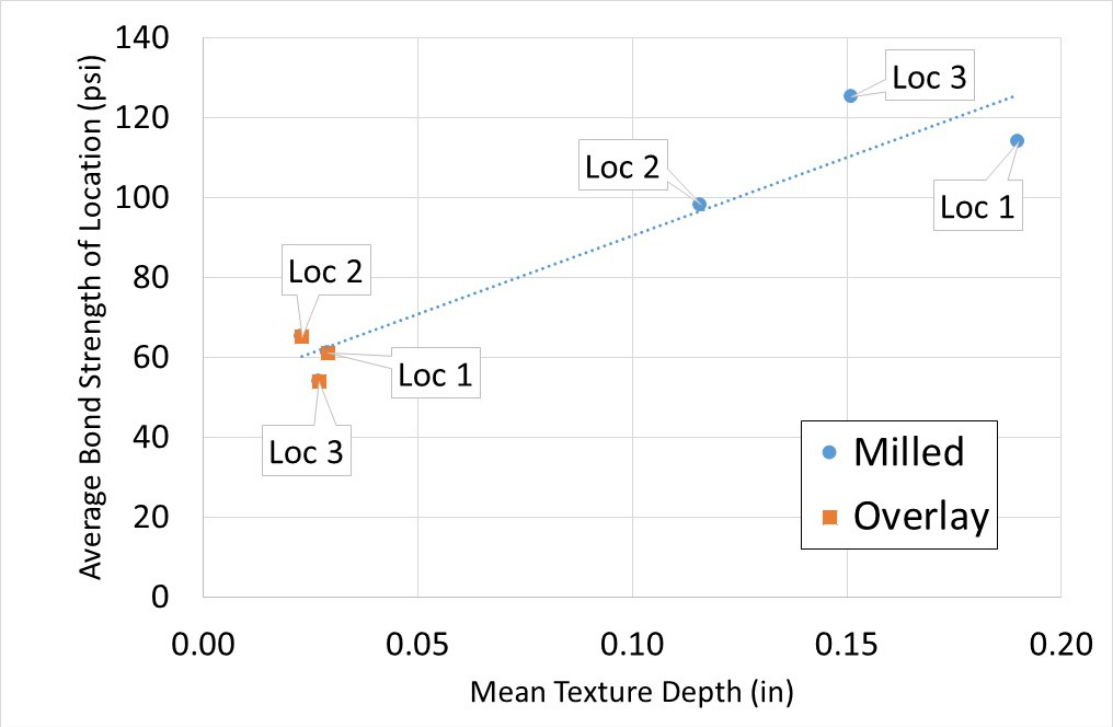

Figure 3.6: Effects of pavement surface texture on interlayer shear strength

3.4.2 Measured Rheological Properties and Correlations with Measured Interlayer Shear Strength

3.4.2.1 Rheological Properties of Tack Coats

Results of the rheological experiments are shown in Figure 3.7. Relationships between softening point, rotational viscosity, penetration, and DSR values were investigated. Test results for five of the six tack coats are presented since CO1_New_b was unable to be distilled. Therefore, rheological tests could not be performed with CO1_New_b. Figure 3.7a shows that tack coat materials with higher softening points have less penetration given the testing conditions. Figure 3.7b demonstrates the relationship between rotational viscosity and penetration. Materials with higher viscosities were observed to provide less penetration, as expected. CO1_New_a was the most viscous material followed by CO2_New, CO1_CSS 1H_a and b, and CO2_CSS 1H. Figure 3.7c relates rotational viscosity to softening point. It can be observed that tack coats with higher viscosities exhibit higher softening point temperatures. The ranking of materials from the stiffest to softest was CO1_New_a, CO2_new, CO1_CSS 1H_a and b, and CO2_CSS 1H (Figure 3.7b). Results of DSR experiments also align with the relationships described above (Figure 3.7d).

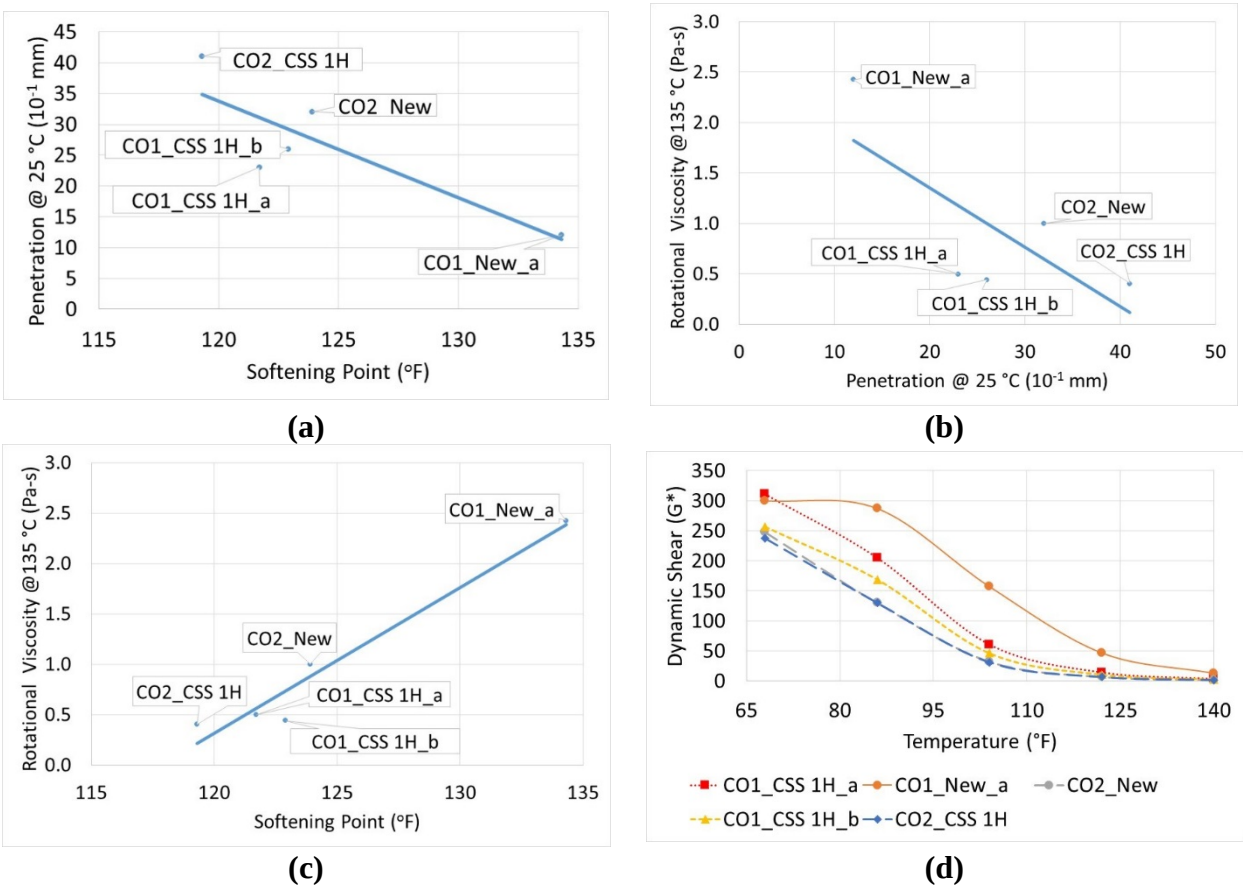

Figure 3.7: Average rheological test results and relationships

3.4.2.2 Effects of Rheological Properties on Interlayer Shear Strength

Effects of rheological properties of tack coats on interlayer shear strength (ISS) were investigated by comparing rheological test results with the results obtained from overlay surface ISS tests. These tests were conducted with samples taken three months after construction. Milled surface interlayer shear strength results were not used due to the significant texture effect on ISS. The purpose was to develop methods and equations to predict in-situ interlayer shear strengths from simple rheological test results. Figure 3.8 shows relationships between rotational viscosity, G*/sinδ, penetration, and softening point of residue asphalt binder with interlayer shear strength at application rates of 0.05 gal/yd^2 and 0.07 gal/yd^2 represented by the dashed and solid lines, respectively. Each grouping of data points, in the vertical direction (along the y-axis), accounts for a different location and respective tack coat material.

For example, in Figure 3.8a there is a grouping of points at a viscosity of 0.402 Pa-s and a grouping at 0.440 Pa-s. The first grouping (0.402) represents Location 3-CO2_CSS 1H, while the second grouping (0.440) represents Location 2-CO1_CSS 1H. Location 1 is not presented due to failed attempts to extract binder residue from CO1_New_b. Equations to predict the ISS using rheological properties are also given in Figure 3.8a-d. Location 2 and Location 3 both consisted of sections with 0.05 gal/yd^2 and 0.07 gal/yd^2 application rates. Therefore two equations are provided.

Overall, positive correlations were observed between the tack coat properties and the interlayer shear strength results. The strength at the interface is increased as the tack coat rotational viscosity, softening point, and DSR stiffness parameter (G*/sinδ) increased, as expected. Similar results (correlations) are observed at both application rates. For penetration, as ISS increased, values decreased, which is expected given the trends of other rheological tests.

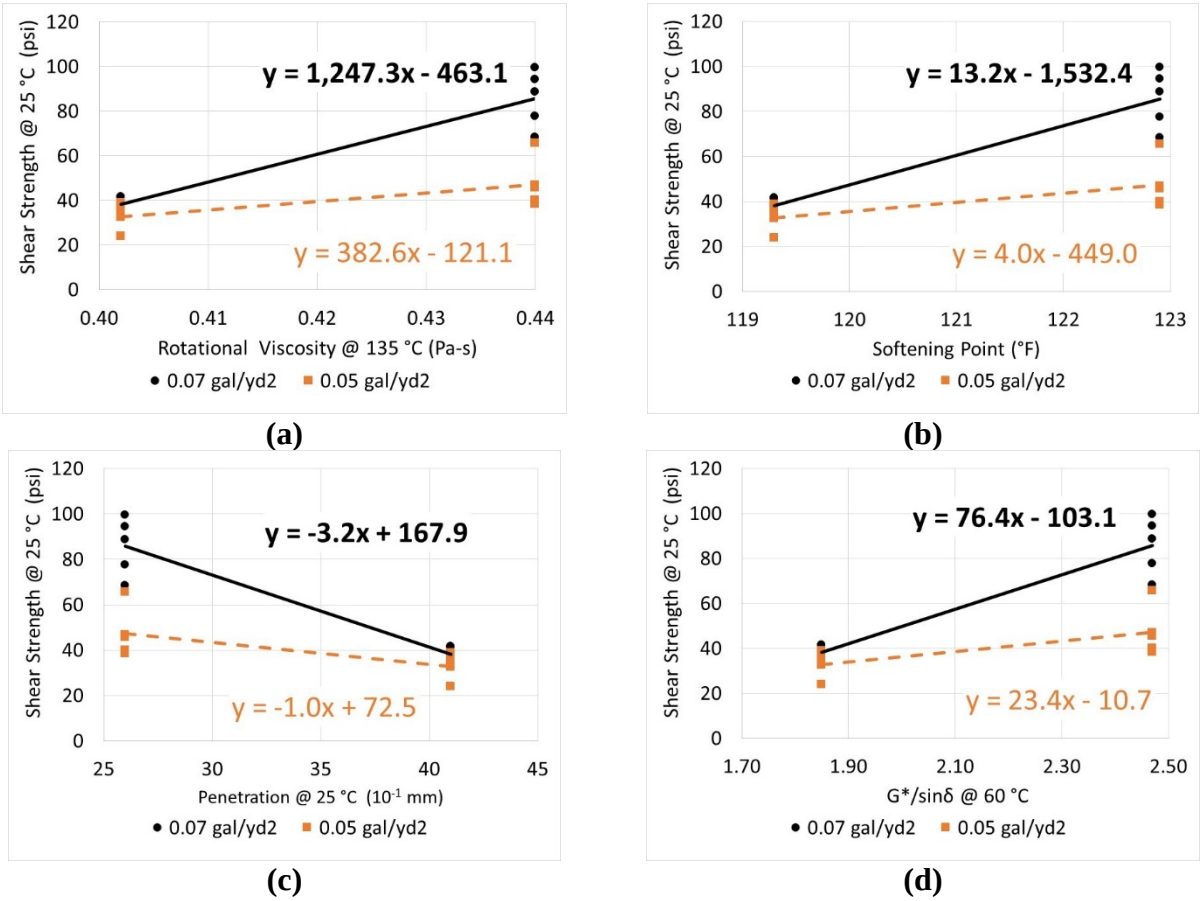

Figure 3.8: Relationship between overlay surface interlayer shear strength and average rheology test results (a) rotational viscosity (b) softening point (c) penetration (d) dynamic shear rheometer

3.4.2.3 Effects of Traffic and Environmental Factors on Interlayer Shear Strength

Effects of traffic loading and environmental factors on the interlayer shear strength of pavement layers were investigated by taking field cores four months after the first round of cores were taken (seven months after initial construction) and comparing the measured strength values from the two sets of samples collected. The purpose was to see how the interlayer shear strength between layers would change over time due to traffic loading and the environment. Figure 3.9 illustrates the reduction in average ISS of field cores taken at three months and seven months after construction for one of the tack coat types and one application rate (Location 1, Section 3). Tabulated values for all sections and the corresponding strength reductions are summarized in Table 3.3.

In total 16 shear experiments were performed with the cores taken seven months after construction. Results for Location 1, sections 2 and 3 and Location 2, sections 2 and 3 are tabulated in Table 3.3. Only the bond between overlay surfaces was tested and compared. Of the results obtained, reduction in average interlayer shear strength varied from 0 (no effect) to 39%, with larger reductions seen in Section 3 than in Section 2 (Table 3.3).

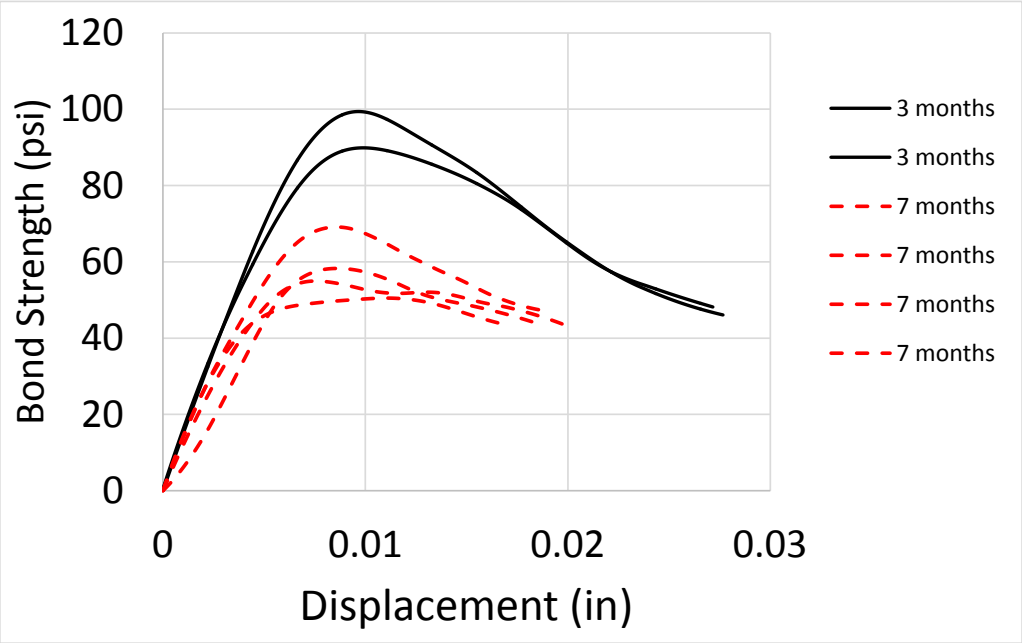

Figure 3.9: Effects of traffic and environmental factors on average ISS with 0.10 gal/yd2 and CO1_New tack coat

Table 3.3: Reductions in average ISS due to traffic loading and environmental factors

Location	Date	Tack Coat	Line	0.07 gal/yd^2	0.10 gal/yd^2
L1	3 mo.	CO1_New	CL[1]	69	95
	7 mo.	CO1_New	CL	69	58
	Reduction (%)			***0***	***39***
Location	**Date**	**Tack Coat**	**Line**	**0.09 gal/yd^2**	**0.07 gal/yd^2**
L2	3 mo.	CO1_CSS 1H	WP[2]	45	94
	7 mo.	CO1_CSS 1H	WP	38	76
	Reduction (%)			***16***	***19***

Note: [1] CL: Centerline – center of the lane, [2] WP: Wheel path – south side of lane, near fog line

3.4.2.4 Effects of Location in Trasverse Direction and Texture on Interlayer Shear Strength

Effects of transverse location on interlayer shear strength were evaluated by taking cores from two different travel lines within the travel lane (center-line and wheel-path). The results of statistical analysis of travel lines (wheel-path and center of travel lane) show that there is no difference in interlayer shear strength between the two transverse locations for an initial set of cores taken three months after construction. On the other hand, the difference in interlayer shear strength for the milled and overlay (top and bottom) interfaces was statistically significant (Figure 3-10 and Table 3-4). A statistical summary of the two sample t-tests performed is listed in Table 3-4. Tests were a Welch Modified Two-Sample t-test with unequal variance and 95% confidence (alpha = 0.05). For Test 1, the null hypothesis, that the difference in means is equal to zero, was rejected, meaning that there is evidence to suggest that the sample means are statistically different. The null hypothesis was rejected because of the high t-stat (10.959) and the small two-sided p-value (0). Test 2 failed to reject the null hypothesis, meaning that there is no evidence to suggest that the samples have a statistical difference in means (sample means are the same).

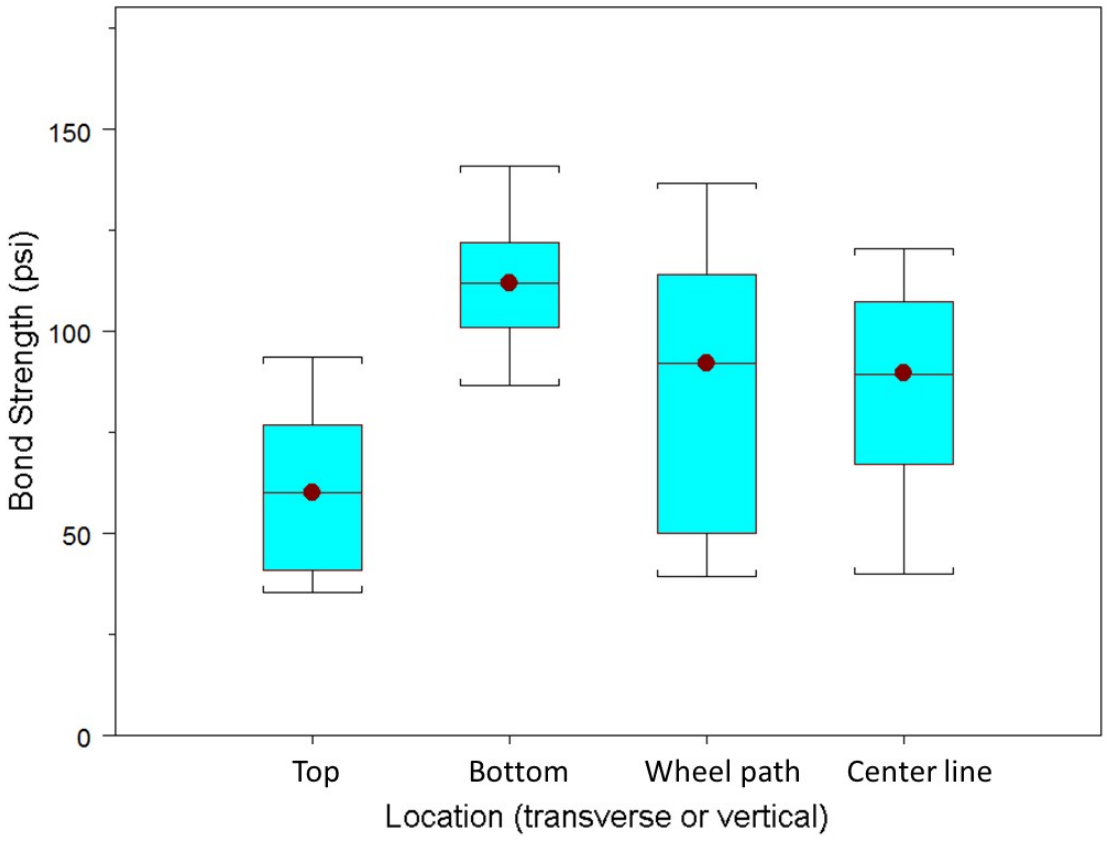

Figure 3.10: Effects of transverse location and texture on ISS

Table 3.4: Summary statistics for transverse location and texture on ISS

Test	Test 1-Texture		Test 2-Location	
Sample	Top	Bottom	Centerline	Wheel path
Min	24.0	59.0	24.0	31.0
Mean	60.2	112.3	84.9	87.1
Median	60.0	112.0	89.0	92.0
Max	104.0	166.0	132.0	166.0
Total N	54.0	54.0	54.0	54.0
Std Dev.	22.1	23.1	29.4	37.8
t	10.959		-0.305	
df	87.840		85.855	
p-value	0.000		0.761	

3.4.3 Most Effective Application Rate to Maximize Interlayer Shear Strength

To determine the most effective application rate to maximize interlayer shear strength (ISS), application rate measurements were performed according to ASTM D2995 *(ASTM D2995 2014)* first to determine the accuracy of the distributor trucks during tack coat application. Large differences in target rates (specified rates) and actual application rates were observed, as shown in Figure 3.11. Each boxplot represents the variance of application rates captured by the line of textile pad squares placed in the transverse direction (Figure 3.1c) for each of three sections within each test location.

Results show that there is a significant lack of control in tack coat application rates. Actual tack coat application rates for milled surfaces were consistently above the target values (Figure 3.11a) and showed an increasing trend from one rate to the next. Overlay surface spraying exhibited this same pattern only at Location 1. Location 2 overlay spraying showed that actual rates are consistently above the target value, but there was no increasing trend from one rate to the next. Overlay surface spraying at Location 3 showed that application rates were consistently above the target values, but a decreasing trend was observed (Figure 3.11b). An increasing trend from one rate to the next, similar to Location 1 of the milled surface, is expected. Observable differences in actual application rates can be seen from the boxplots in all the milled surface locations and the overlay surfaces at Locations 1 and 2. These significant differences in target application rates allow the effects of application rate on interlayer shear strength to be observed. Overlay surface results at Location 3 exhibit no increasing trend from one rate to the next, which is unexpected. Results related to the effects of application rate on interlayer shear strength at Location 3-Overlay were inconclusive due to inaccurate tack application. Inaccurate application rates for Location 3-Overlay may be attributed to the use of the contractor's distributor truck (old truck) for this location only. Figure 3.12 illustrates the non-uniform tack coat application with the contractor's distributor truck.

Figure 3.13a summarizes the interlayer shear strength values obtained from field cores taken three months after construction for the various application rates and tack coat materials used in this study. A significant difference in interlayer shear strengths can be seen in those tack coats used on the milled surface (bottom lift) and overlay surface (top lift). The interlayer shear

strength of the tack coats used on the milled surface was on average 112 psi, while those used on the overlay surface was on average 60 psi. The most effective application rate maximizing the interlayer shear strength of pavement layers was selected by finding the largest strength value and the corresponding application rate using Figure 3.13a. In cases where differences in interlayer shear strength were minimal (for example CO1_New_b), the most effective rate was selected as the lowest rate to provide a more economical choice. Table 3.5 lists the recommended application rates that are the most effective to maximize the interlayer shear strength of pavement layers for selected Oregon tack coat materials. It can also be observed from Figure 3.13 that the section with inconsistent rates and non-uniform application (Location 3-Overlay - Figure 3.12) has significantly lower ISS than all other sections. This result points out the importance of developing a quality control process and standard for tack coat application.

Figure 3.13b also shows the relationship between ISS and target application, but after being normalized to include the effect of texture using the equation from Figure 3.6. A calculated ISS was determined using this equation and used as a reduction factor for each measured ISS. Normalizing the interface strength values in this way gives a more realistic comparison between bond strengths of bottom (first lift) and top (second lift) interfaces. After normalizing the ISS for each tack coat material, CO2_CSS1H exhibits lower values for two of the three application rates than all other materials. CO1_CSS_1H_a, CO1_New_a, and CO1_New_b exhibit more similar ISS values (grouped closer together on the plot) after normalizing. CO1_CSS_1H_b and CO2_New exhibit similar ISS values (approximately 70 psi) for different application rates (Figure 3.11b).

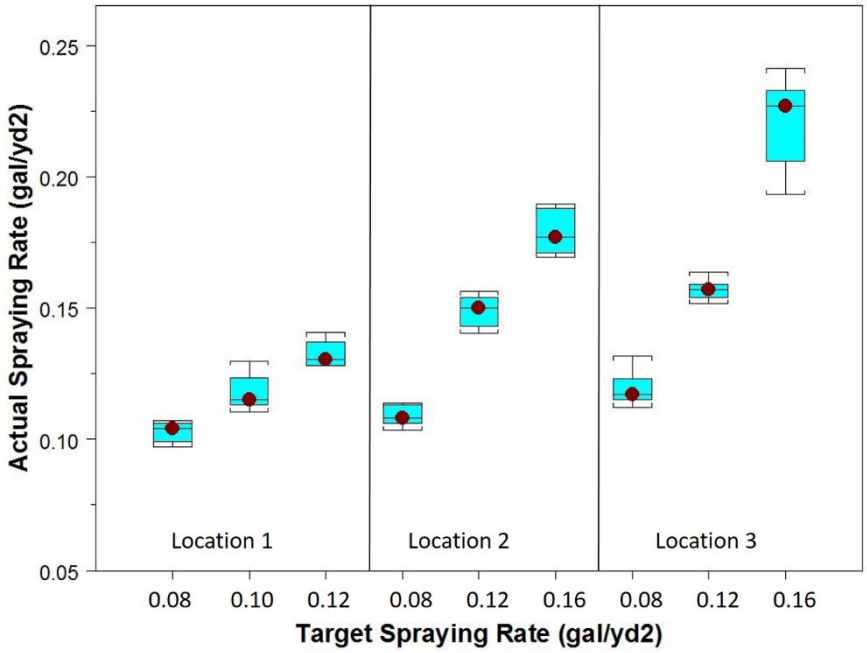

(a)

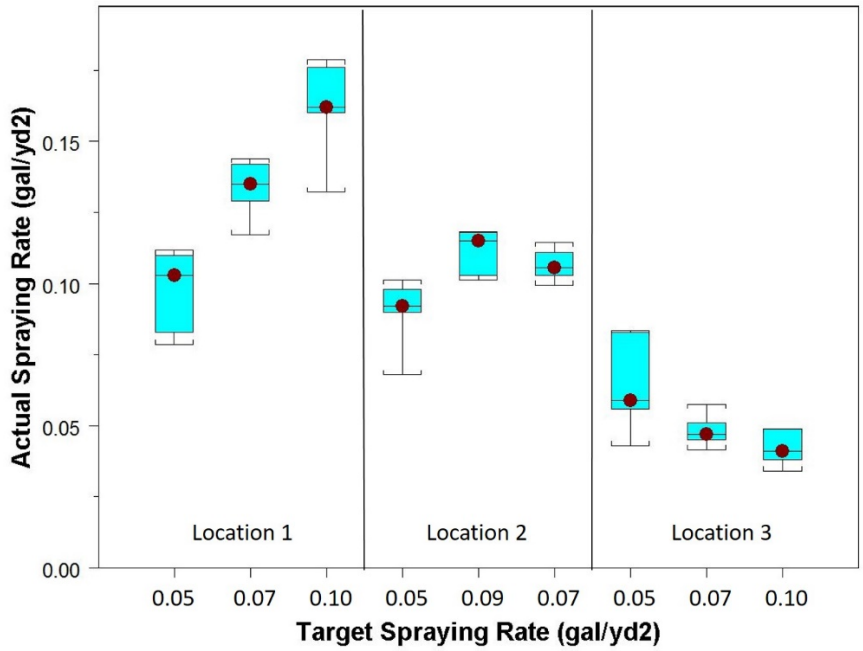

(b)

Figure 3.11: Differences in target application rate vs. actual application rate in the field (a) milled surface (b) overlay surface

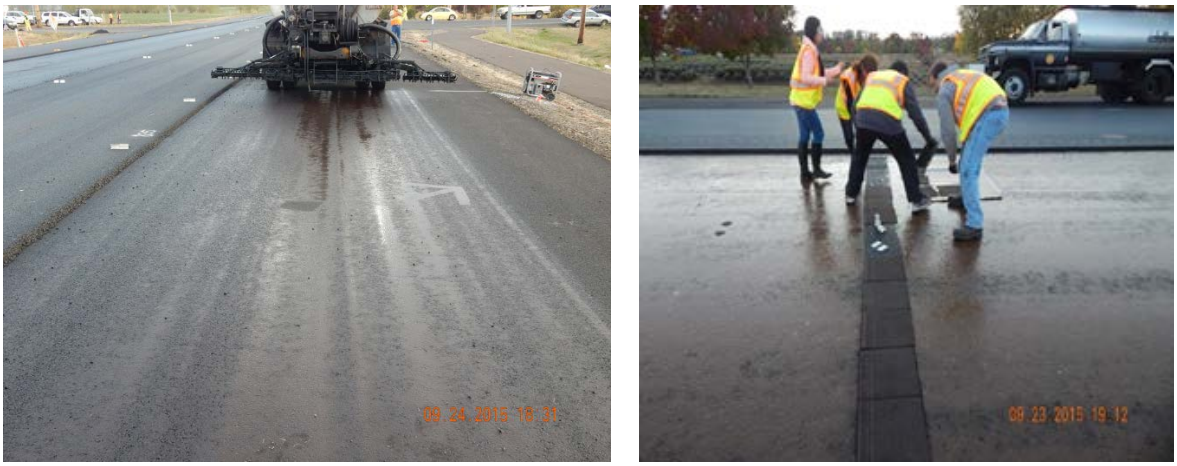

(a) **(b)**

Figure 3.12: Impact of distributor truck on tack coat uniformity (a) Non-uniform application with streaks (contractor's distributor truck) (b) Uniform application with the new distributor truck

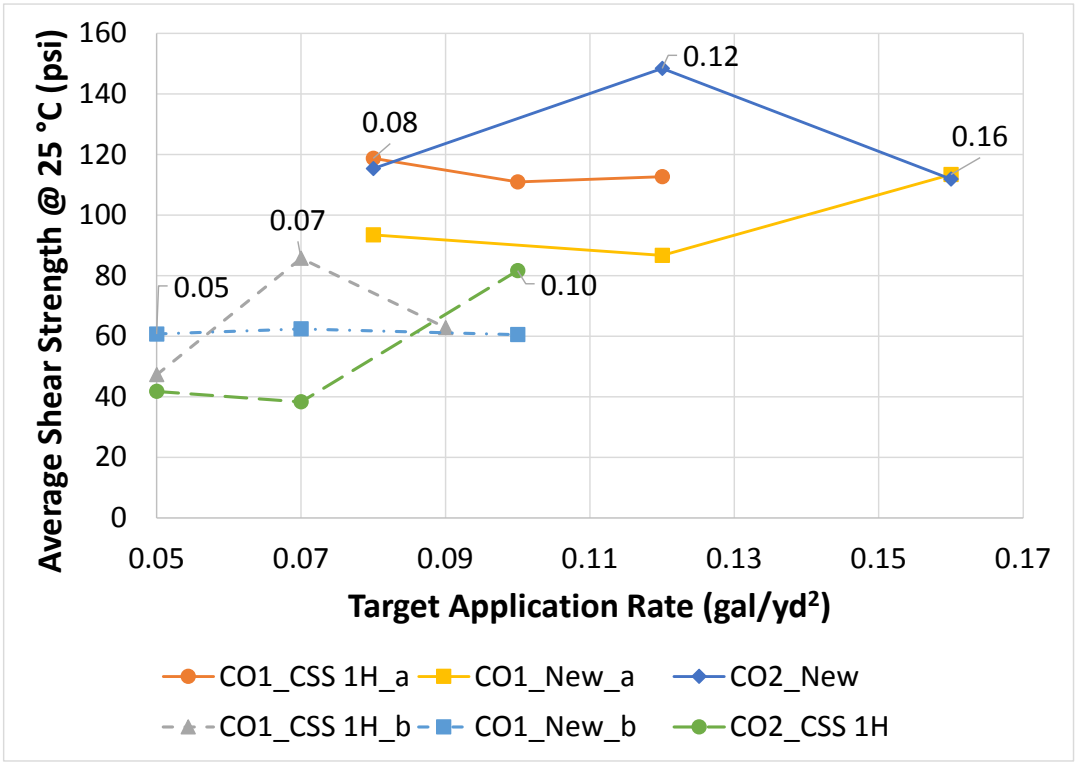

(a)

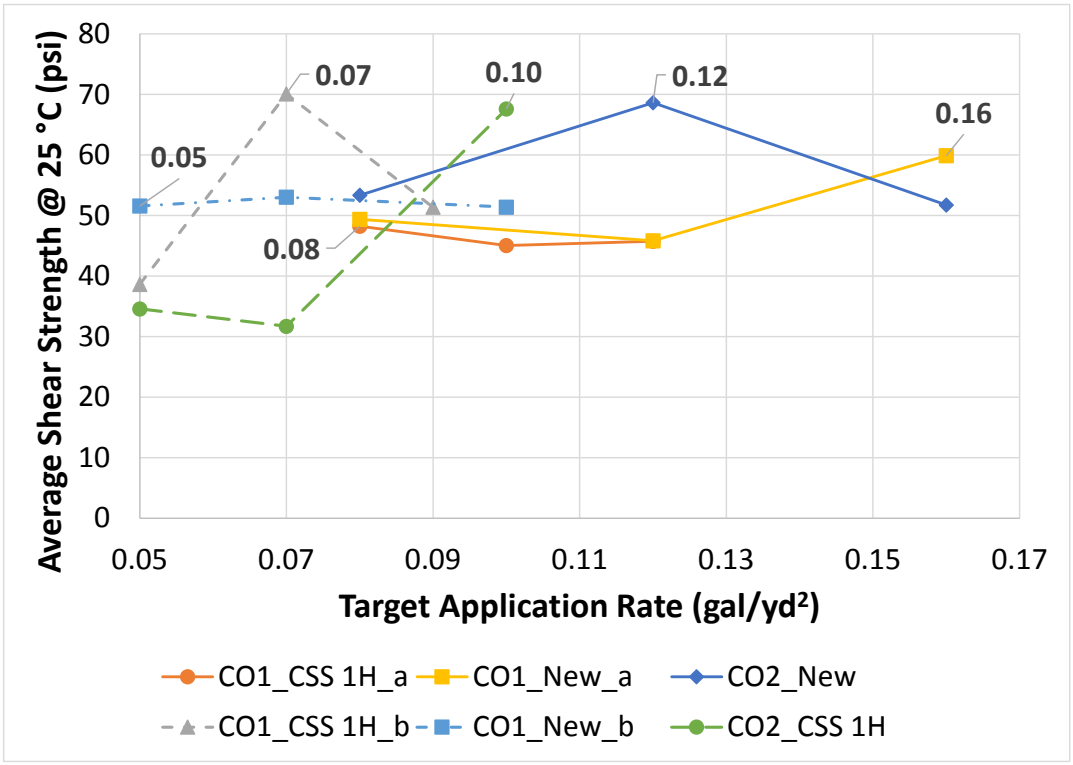

(b)

Figure 3.13: Relationship between ISS and target application rate (a) Measured response (b) Normalized response to exclude the effect of texture on ISS.

Table 3.5: Most effective application rates for Oregon tack materials on milled and overlay surfaces

Tack Coat Material	Surface Type	[1]Effective Rate (gal/yd2)
CO1_CSS 1H_a	Milled	0.08
CO1_New_a	Milled	0.16
CO2_New	Milled	0.12
CO1_CSS 1H_b	Overlay	0.07
CO1_New_b	Overlay	0.05
CO2_CSS 1H	Overlay	0.10

Note: [1] All suggested, "effective rates" are application rates and not residual rates.

3.5 SUMMARY AND CONCLUSIONS

Oregon's most commonly used slow-setting grade emulsions, CSS 1H, and "New" engineered emulsions from two companies were investigated for their performance. The performance of these emulsions, most effective application rates, and the effects of pavement surface texture, transverse location, and traffic on interlayer shear strength were evaluated in this study. Results were used to develop equations to predict bond shear strengths from simple rheological test results.

The conclusions drawn from the results of this study are:

- Milled pavement surfaces were measured to have a significantly higher mean texture depth (MTD) when compared to overlay pavement surfaces.

- A positive correlation between pavement surface texture and interlayer shear strength exists. The influence of surface texture on measured ISS limited results to be confined to overlay pavement surfaces only when comparisons of tack coat materials were to be made regarding performance.

- The results of statistical analysis of travel lines (wheel-path and center of travel lane) show that there is no difference in interlayer shear strength between the two transverse locations for an initial set of cores taken three months after construction. On the other hand, the difference in interlayer shear strength for the milled and overlay (top and bottom) interfaces is statistically significant.

- The difference in interlayer shear strength for the milled and overlay (top and bottom) interfaces is statistically significant.

- Tack coat materials with higher viscosities exhibit higher softening point temperatures and lower penetration values. For overlay pavement surfaces in this study, positive correlations between rheological test results and interlayer shear strength of field cores taken three months after construction exist.

- For overlay pavement surfaces in this study, positive correlations between rheological test results and interlayer shear strength of field cores taken three months after construction exist.

- Traffic loading and environmental factors can create a significant reduction in interlayer shear strength.

- Large consistency issues are present in tack coat application rates via distributor trucks, and there is a need for QC/QA for tack coat application rates and methods during construction. Issues with tack coat application was observed to reduce ISS.

- Most effective application rates in many cases were the middle rates

- .

4.0 DEVELOPMENT OF A SMARTPHONE APP AND DEVICE TO REDUCE TACK COAT TRACKING

4.1 INTRODUCTION

Oregon slow-setting grade and "New" engineered emulsions were investigated to evaluate their tracking resistance, the pick-up of tack coats by construction vehicle tires during construction activities. Tracking reduces the amount of tack coat in particular areas and creates a non-uniform tack coat distribution between the two construction lifts. This non-uniform tack coat distribution leads to localized distresses and even complete failure of the bond between lifts. The magnitude of this effect is dependent on tack coat type, application method, and curing time. By avoiding construction vehicle traffic before the calculated curing time, tracking can be minimized. For this reason, reducing tracking, by determining the appropriate curing time becomes vital to the longevity of the pavement structure.

In this study, weight evaporation experiments were conducted by varying the application rate, air temperature, wind speed, and tack coat type to determine the curing time and the factors that influence it. Tracking was also evaluated by developing a wheel-tracking device that can be used in the field as a visual tool or by collecting weight data via the removable rubber "tires". Data from weight evaporation tests were used to create a linear regression model to predict in-situ curing times and develop a smartphone app (for Android and IOS) using the created model. Prediction of in-situ curing times will reduce tracking and improve current QC/QA. Results show that lower temperatures and increased application rates lead to longer curing times while higher wind speeds will reduce curing times. The results indicate that tracking will decrease with increased curing time.

4.2 OBJECTIVES

The main objectives of this part of the study are to:

1. Provide recommendations to improve current methods for tack coat application and tracking;

2. Make recommendations to reduce tracking;

3. Develop a device to measure tack coat tracking and determine in-situ curing time;

4. Develop a smartphone application for tack coat curing time prediction to be used during construction;

5. Determine the tracking resistance of "New" tack coat technologies developed in Oregon.

4.3 MATERIALS AND METHODS

4.3.1 Tack Coat Materials and Curing Time Test Plan

Four different types of emulsions (CO1_CSS 1H, CO1_New, CO2_CSS 1, and CO2_New) are tested in this study to determine the curing time. Generic tack coat type labels are used to conceal the identity of the company providing the material. CSS 1H emulsions are the most commonly used slow-setting grades in Oregon. "New" emulsions are the engineered emulsions recently developed in Oregon to reduce tracking and increase bond strengths.

Tack coat curing time was evaluated in the laboratory through evaporation experiments in a temperature controlled chamber using three application (spraying) rates and two testing temperatures (Table 4.1). Experiments were conducted with steel plates (no texture), open-graded (OG) (high texture) asphalt cores, and dense graded (DG) (medium texture) asphalt cores to determine the impact of texture on measured curing time. A summary of the experimental plan is shown in Table 4.1. A total of 48 steel plate samples were prepared, along with 48 asphalt concrete core (AC) samples (24 each of OG and DG), for a total of 96 experiments.

As a part of the test plan, tack coat densities were determined by measuring out a predetermined volume (100 mL) and using a high accuracy scale to determine the emulsion weight for the measured volume. Calculated densities are listed in Table 4.2. These densities, along with application rates from Table 4.1, were then used to determine the emulsion weight to be applied to the samples during testing for a specific surface area. Calculated application weights for the various application rates are listed in Table 4.3 and were calculated by using the general equation as follows:

$$\textit{Target weight} = \textit{Application rate} \times \textit{Sample surface area} \times \textit{Density of tack coat} \quad \textbf{(4.1)}$$

AC core surface texture, mean texture depth (MTD), was measured for all samples before testing to use as a variable in the regression analysis to evaluate the effect of texture on tack coat curing time. Texture experiments followed a modified procedure from ASTM E965 *(ASTM E965 2015)*. Fine sand was lightly applied to each sample to cover the surface completely. By using the before and after the weight of the core sample, the mass of sand applied was determined. The mass of the sand was converted to a volume with the known density. The following equation was then used to calculate the MTD for each sample:

$$MTD = \frac{4V}{\pi D^2} \quad \textbf{(4.2)}$$

Where;

MTD = mean texture depth of pavement surface, in.
V = sample volume, in^3 and
D = measured diameter of AC core, in.

Table 4.1: Summary of test plan for tack coat curing time determination

Parameter	Experimental Setting
Emulsion	CO1_CSS 1H, CO1_New, CO2_CSS1, CO2_New
Temperature (°F)	Low: 59, High: 95
Application Rate (gal/yd^2)	0.045 (L), 0.105 (M), 0.164 (H)
Texture	Open grade (OG), dense grade (DG), steel plate (SP)

Table 4.2: Measured tack coat densities

Emulsion Type	CO2_CSS 1	CO2_New	CO1_CSS 1H	CO1_New
Weight of emulsion (g)	80.38	85.29	88.12	95.41
Volume of emulsion (mL)	100	100	100	100
Density (g/mL)	0.8038	0.8529	0.8812	0.9541

Table 4.3: Summary of target application weights for samples used in tack coat curing time tests (in grams)

Rate (gal/yd^2)	0.045		0.105		0.164	
Sample	**Steel Plate**	**AC Cores**	**Steel Plate**	**AC Cores**	**Steel Plate**	**AC Cores**
CO2_CSS 1	3.80	1.33	8.88	3.10	13.86	4.84
CO2_New	4.04	1.41	9.42	3.29	14.71	5.13
CO1_CSS 1H	4.17	1.46	9.73	3.40	15.20	5.30
CO1_New	4.52	1.58	10.53	3.68	16.45	5.74

4.3.2 Procedure for Determining Tack Coat Curing Time

The general procedure followed for tack coat curing time measurement, and data analysis are illustrated in Figure 4.1. Steel plate and asphalt cores were cleaned for excess debris and left to dry before testing. The steps for determination of curing time are as follows:

- Samples were placed on a high accuracy scale (capable of measuring the 0.01g change in weight) inside of an environmental chamber (Figure 4.1a). After calibrating the scale for the chamber temperature, the scale was initialized to zero.
- An application weight, calculated by converting a specified application rate to grams using the calculated density, was applied via paintbrush to the surface of the sample (Figure 4.1b)
- Samples were left on the scale, inside the closed chamber, while data was collected via computer connection (Figure 4.1c)
- Tests were conducted at low (59°F) and high temperatures (95 °F) while the temperature was controlled by the chamber (Figure 4.1d).

- An excel template was created to collect data at 10-second intervals from the scale using a software package (Figure 4.1e).

- Data was collected continuously at 10-second intervals as the weight of the applied tack coat decreased due to evaporation of water. Termination of the test was conducted once a visible horizontal line was present in the data collection plot (Figure 4-1e). After the completion of the test, the surface color of the tack coat appears black in color (the weight will be constant) (Figure 4.1f).

- Due to the ambient vibrations, the data had a certain level of high-frequency noise. To filter out high-frequency noise, a low-pass filter available in MATLAB R2015b is used (Figure 4.1g).

- The filtered signal is then rounded to a single decimal point and plotted. The rounded data reflects reduced accuracy that may be experienced in the field when the curing time is measured by a lower accuracy scale (capable of measuring the 0.1g change in weight). The curing time is then determined by locating the first time stamp that the rounded data curve has reached the lowest recorded weight (shown with a red arrow in Figure 4.1h).

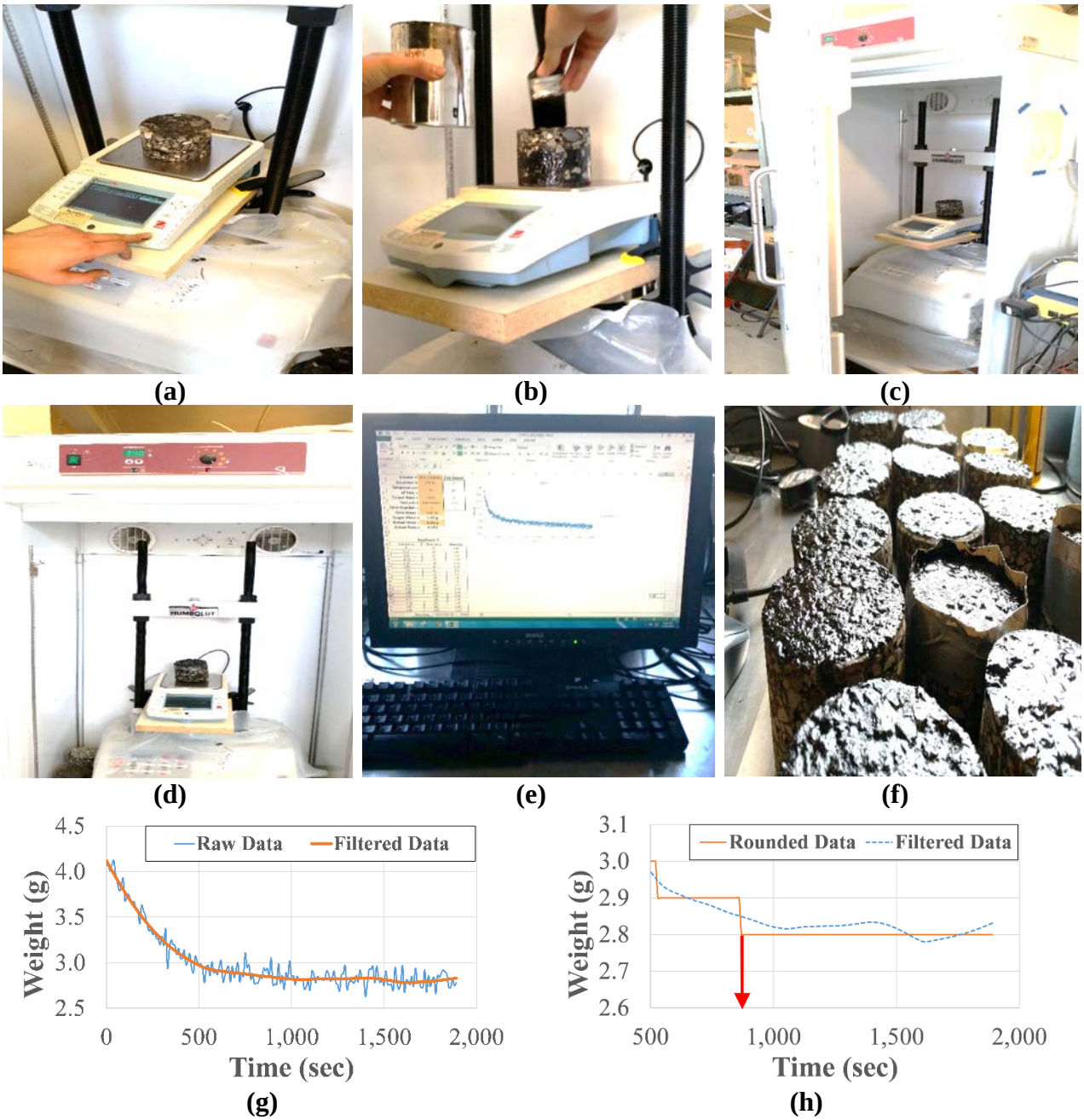

Figure 4.1: General procedure for tack coat curing time determination

4.3.3 Development of a Smartphone App

4.3.3.1 Linear Regression Model for App

This portion of the study focused on the development of regression equations to determine emulsion curing time in the field. By avoiding construction vehicle traffic before the calculated curing time, tracking can be minimized. Ultimately, accurately predicting the emulsion curing time will reduce tracking and decrease delays seen in construction. The equations developed from this portion of the study will also serve as

the beginnings of a quality-assurance and quality-control process to maximize tack coat performance throughout the design life. A field tack coat curing time measurement tool (a smartphone app) was developed using test results and the regression equations.

Simple linear regression analysis was conducted to generate the models. The model selection procedure included the following steps:

1. Prepare a scatter (pairs) plot matrix to inspect possible relationships amongst predictor variables;
2. Construct a correlation matrix of all variables to assess relationships further;
3. Develop an Analysis of Variance (ANOVA) table to identify significant variables;
4. Apply regression analysis to develop linear equations;
5. Plot the residuals to determine if regression model is suitable for the data being used.

Regression models were developed for four different scenarios:

- All AC cores (dense and open grade)
- Steel plates:
- Using two replicates
- Using a single replicate
- Combined dataset: AC cores and steel plates.

Steel plate experiments were performed to determine whether texture has an effect on the curing time. Two separate steel plate regression models (all steel plate replicates vs. replicate one only) were developed to determine if performing replicate experiments increased the accuracy of the model. The results provided an indication as to whether replicate tests for AC cores were necessary or not.

Monte Carlo simulations were conducted with several of the model equations (AC Core w/ no texture and AC core plus Steel plate w/ no texture) developed to generate a distribution of curing times and determine which model produced more reliable results. Tests were also conducted to determine the effect of the wind on the curing time to improve the accuracy of the linear model. It was determined that increasing the wind reduced the curing time. Therefore the model was adjusted with a Wind Adjustment Factor. Several experiments were conducted using the procedure given in Figure 4-1 at a

test temperature of 32 °F to see how well the model worked outside of the initial testing temperatures. It was determined that the relationship between curing time and temperature be linear. Therefore no adjustments were needed for low temperatures.

4.3.3.2 Summary of Procedure to Develop the Smartphone App

The mobile application linked to this project has an Android and iOS version. The Android version was developed using Android Studio while the iOS version was developed using Swift. Both were developed by using a C++ program for testing purposes only. The C++ program was set up to keep both versions as similar as possible in concept. During this process, the bounds for the regression equation changed as well as the minimum time that could be calculated. The temperature was given a range appropriate to Oregon climate.

The wind was automatically set to 4 mph for cases when the wind speed is anything higher than 4 mph since the maximum wind speed simulated in the laboratory was limited. Even with the bounds set, there were times when the set time was still calculated to be 5 minutes or lower. The cases were rare but considering the data that was collected that was unrealistic. If the calculation for the set time is anything less than 25 minutes, it is then automatically set to 25 minutes to give the tack coat enough time to cure in the field.

Next came the aesthetics of the application. Several sketches were prepared to show the details of the layout for the application. The design of both applications is relatively similar. Spinners, or drop down menus, vary when it comes to iOS and Android, so the best fitting one is what ended up being in the app depending on the application. Units for the various inputs were also incorporated into the app.

After the initial layout and icon design had been created for the mobile application, it was then handed over for testing to the research group as well as other mobile application developers. According to the feedback from the research group and other app developers, both applications were revised and finalized. Both IOS and Android versions will be available in app stores soon.

4.3.4 Development of a Device to Measure Tack Coat Tracking

In this part of the study, the goal was to develop a small-scale device to evaluate tack coat tracking in the field. Initial design parameters were based on ASTM D711, *Standard Test Method for No-Pick-Up Time of Traffic Paint (ASTM D711 2010)*. The design from ASTM D711 developed by Clark et al. *(Clark et al. 2012)* and Wilson et al. *(Wilson et al. 2015)* to test trackless tack coats in Virginia and Texas was modified to develop the device.

Different from previous studies, the device in this study was designed to match the tire pressure of a full-size construction truck, assumed to be 720 kPa. The footprint of the tire was assumed to be square. A scaled load was determined by using the tire pressure and contact area (cross section of the O-rings used as tires = 9.5mm). A factor of safety was used to increase the applied load by 50% to a value of 20 kg. The calculated weight was converted into a volume using the

density of steel (7.5 g/cm^3). The device had a fixed diameter of 130 mm. Thus, the height of the cylinder was determined to be 190 mm. Two rubber O-rings (tires) were placed 50 mm from each end and 90 mm from each other (Figure 4.2a). Each tire has the capability to be removed after use with the purpose of taking weight measurements to record the amount of tack coat picked up (Figure 4.2b). Testing is performed by placing the wheel on the sprayed tack coat and rolling the wheel using the handle to complete one revolution (Figure 4.2c).

Similar to ASTM D711 testing procedure, the time at which no tack coat is picked up (visually or based on measured weight) is indicated as the curing time of the tack coat. This value serves as an indicator of the in-situ curing time of various tack coat materials within this study.

(a) **(b)** **(c)**

Figure 4.2: Tack coat wheel tracking device (a) schematic (b) removing O-rings in field (c) use of wheel device during a field test

4.4 RESULTS AND DISCUSSION

4.4.1 Evaluation of tack coat curing time

4.4.1.1 Laboratory Curing Time Determination

Tack coat curing time was determined by conducting laboratory evaporation tests inside a temperature controlled chamber using a high-accuracy scale. Testing followed the procedure shown in Figure 4.1. Steel plate samples were flat, smooth squares with an area of 36 square inches. AC core samples had a diameter of 4 inches with open and dense-graded surface types. The purpose was to obtain the curing time of various tack coats to aid in the development of linear regression models embedded in the smartphone apps that would predict in-situ curing times.

Figure 4.3 shows general results of the curing time experiments for a steel plate sample at two different temperatures. Results for all 96 experiments are given in Appendix A. For steel plate experiments, CO1_New had a significantly higher curing time than all other emulsions regardless of the conditions (different application rate, low or high temperature). Graphically, the tack coat with the shortest curing time was not observable, but statistical analysis revealed that CO2_New was on average curing faster than all other tack coat types considered. Average curing times for steel plate experiments are listed in Table 4.4.

Results of the AC core curing time experiments were divided by texture (open graded and dense graded). Graphically, similar results were observed in the steel plate experiments. CO1_New had the longest curing time for both dense and open graded samples. Again, CO2_New was revealed to have the shortest curing time, for both dense and open graded specimens. These results suggest that texture does not have a significant impact on the curing time of these particular tack coat types. ANOVA results showing the insignificant effect of texture on curing time is given in section 4.4.1.2. Average curing times for AC core experiments are listed in Table 4.5.

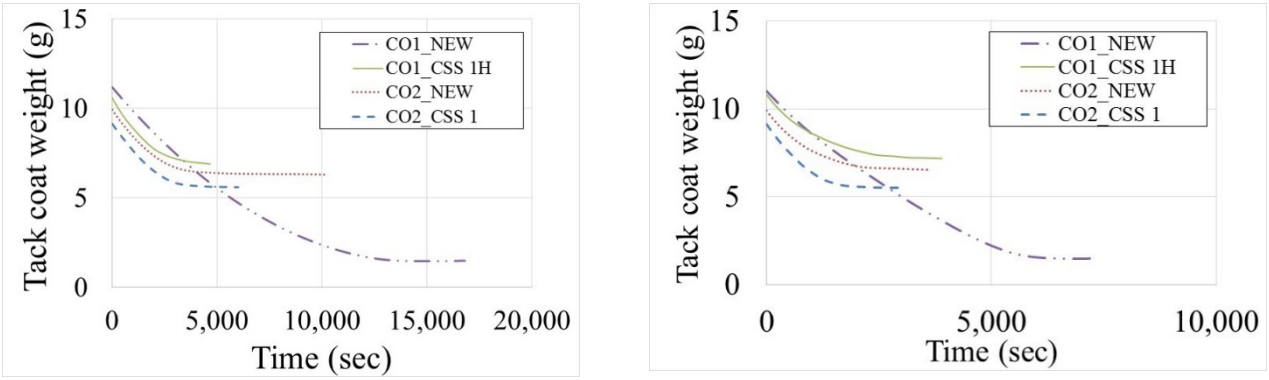

(a) **(b)**

Figure 4.3: Steel plate emulsion evaporation curves with medium rate (0.105gal/yd^2) (a) 59 °F (b) 95 °F

Table 4.4: Average laboratory curing time of tack coats on steel plates

Tack Coat Type	Avg. LT[1] Curing time (min)	Avg. HT[2] Curing time (min)	Avg. LR[3] Curing time (min)	Avg. MR[4] Curing time (min)	Avg. HR[5] Curing time (min)
CO2_CSS 1	72.53	52.31	37.46	58.79	91.00
CO2_New	74.53	39.83	25.04	66.38	80.13
CO1_CSS 1H	73.44	50.14	31.33	62.96	91.08
CO1_New	188.75	95.64	86.42	157.71	164.63

Note: LT[1]: Low temperature – 59 °F, HT[2]: High temperature – 95 °F, LR[3]: Low application rate – 0.045 gal/yd^2, MR[4]: Medium application rate – 0.105 gal/yd^2, HR[5]: High application rate – 0.164 gal/yd^2

Table 4.5: Average laboratory curing times of tack coats on AC cores (dense and open grade)

Tack Coat Type	Avg. LT[1] Curing time (min)	Avg. HT[2] Curing time (min)	Avg. LR[3] Curing time (min)	Avg. MR[4] Curing time (min)	Avg. HR[5] Curing time (min)
CO2_CSS 1	66.56	64.58	44.00	62.96	89.75
CO2_New	58.17	59.94	27.42	44.50	105.25
CO1_CSS 1H	78.75	66.03	33.42	87.83	95.92
CO1_New	183.43	134.72	74.29	144.42	258.53

Note: LT[1]: Low temperature – 59 °F, HT[2]: High temperature – 95 °F, LR[3]: Low application rate – 0.045 gal/yd^2, MR[4]: Medium application rate – 0.105 gal/yd^2, HR[5]: High application rate – 0.164 gal/yd^2

4.4.1.1 Linear regression model

In this study, the dependent variable used for model development is the emulsion curing time (measured in seconds), and the independent variables are those that describe the emulsion type being used (emulsion type and rate applied), surface texture and surrounding environment (temperature). A correction factor for wind speed was later incorporated into the model.

For the first scenario described in section 4.3.3.1, only AC cores were utilized for model development to extract possible relationships between the emulsion curing time and the independent variables considered. Results of this model via ANOVA indicated that texture (MTD) did not have a significant effect on curing time (p-value = 0.9711), while temperature, emulsion type, and application rate were significant. As for the steel plate models, the next scenario, the similarities in regression model coefficients of the two models with (R^2= 0.85) and without replicates (R^2= 0.84) demonstrate that the models are relatively similar to each other. Overall, using a replicate test did not improve the accuracy and precision of the regression models. Therefore replicate experiments were not conducted for testing AC cores. The analysis of scenarios one and two, lead to the development of the final model (scenario three), which was a combined dataset of AC cores and steel plates (no texture). Table 4.6 shows the variables used for the development of the final regression model (combined dataset of AC cores and steel plates with no texture) and their numerical ranges.

Table 4.6: Dependent and independent variables used for AC core + Steel plate model

Variable Type	Variable	Description	Range
Dependent	SET	Curing time of applied emulsion in seconds	510-18,880
Independent	TEMPF	Temperature of chamber during test in degrees Fahrenheit	59, 95
	MTD	Mean Texture Depth, a measure of the texture of each tested sample in inches	0.0177-0.1281
	EMUL	Indicator of which emulsion was used for the test	CO2_CSS 1, CO2_New, CO1_CSS 1H, CO1_New
	ACTR	The amount of emulsion applied to the sample during testing, measured in gal/yd^2	0.044-0.175

Figure 4.4 is a matrix of scatter plots which depict the interactions between the dependent and independent variables that were used in model development. Several trends are illustrated in Figure 4.4, for example, higher temperatures result in shorter curing times, emulsion CO2_New has the largest range of curing times, and higher application rates yield longer curing times. It can also be observed that independent variables are not correlated and can be used for regression model development.

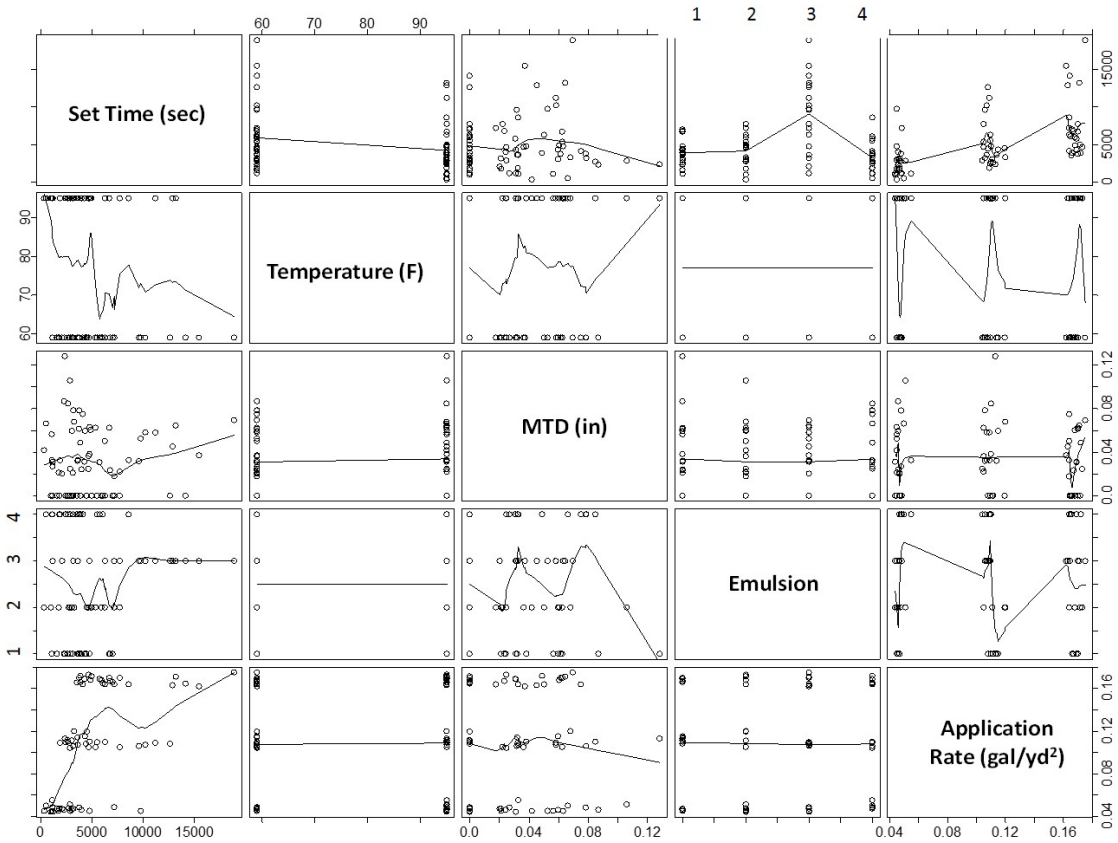

Figure 4.4: Scatter plot matrix for AC core + Steel plate test results
Note: 1: CO2_CSS 1, 2: CO1_CSS 1H, 3: CO1_New, 4: CO2_New

Table 4.7 shows the Analysis of Variance (ANOVA) results for the estimation of emulsion curing time using the combined dataset (AC cores and steel plates). For this model, Temperature, Emulsion, and Application Rate are found to be significant and have the most important effect on the curing time (large F-values and small p-values), while MTD does not have any considerable effect on emulsion curing time (low F-value and high p-value). Since the variable MTD was found not to be significant according to the ANOVA table shown in Table 4.7, another regression model was developed omitting the texture effect. The equation without the texture variable (MTD) can be considered to be more practical since it may not be practical to conduct sand patch tests during the construction to measure surface texture. All regression equations developed in this study are given in Appendix A. The resulting equation used in the smartphone app is given below:

$$SET=3{,}054.59 - 45.79\times TEMPF + 266.94\times CO1\_CSS\ 1H + 5{,}305.85\times CO1\_New - 499.74\times CO2\_New + 39{,}970.96\times ACTR \quad \textbf{(4.3)}$$

$$R^2=0.71$$

As seen in the equation, terms with negative signs indicate that an increase in this variable will decrease the curing time (SET). For example, higher temperatures and using

emulsion CO2_New will decrease the curing time. Since each emulsion type has a corresponding coefficient and term within the equation, not all of the terms are used when a specific emulsion type is selected. For example, to find the curing time of emulsion type CO1_CSS 1H, simply insert a one (1) into the equation where CO1_CSS 1H appears and zeros (0) for the other emulsion types, eliminating the unused coefficients and leaving the one of interest. Similarly, to find the curing time for CO2_CSS 1, insert zeros (0) for all the emulsion terms. The calculated R^2 value, which gives an estimate of the strength of the relationship between the independent variables of the linear regression model and the curing time, was 71%. Although this value gives an indication of a good fitting model, residual plots must still be assessed to determine any bias, overfitting issues, and outliers.

Figure 4.5 illustrates the greater detail of the regression model. Figure 4.5a shows the fitted values versus the residuals. The residual values should be close to zero for a reliable model. Also, if the residuals present a constant trend (linear, parabolic, hyperbolic), the mathematical function used for model development must be changed. For this regression model, the pattern of the residual plot is acceptable, indicating a linear relationship is adequate. Figure 4.5b shows the same residual plot where the square root absolute value of residuals is plotted to compare the negative and positive residuals. Figure 4.5c represents the final model fit on a line of equality (predicted vs. measured). Figure 4.5d shows that the distribution of residuals is very close to normal, meaning a majority of the points fall on the dotted line. In Figure 4.5e, the range of the fitted values is higher than the residuals, which also proves the statistical strength of the model. Figure 4.5f demonstrates the potential outliers encountered during model development by using a Cook's Distance plot.

Table 4.7: ANOVA results of combined data regression model

	Degrees of Freedom	**Sum of Squares**	**Mean Squares**	**F-Value**	**P-Value**
Temperature (°F)	1	45,961,676	45,961,676	10.58	0.0018
Mean Texture Depth (in)	1	1,858,407	1,858,407	0.43	0.5155
Emulsion	3	392,072,912	130,690,971	30.07	0.0000
Application Rate (gal/yd2)	1	281,691,882	281,691,882	64.82	0.0000
Residuals	65	282,484,572	4,345,916		

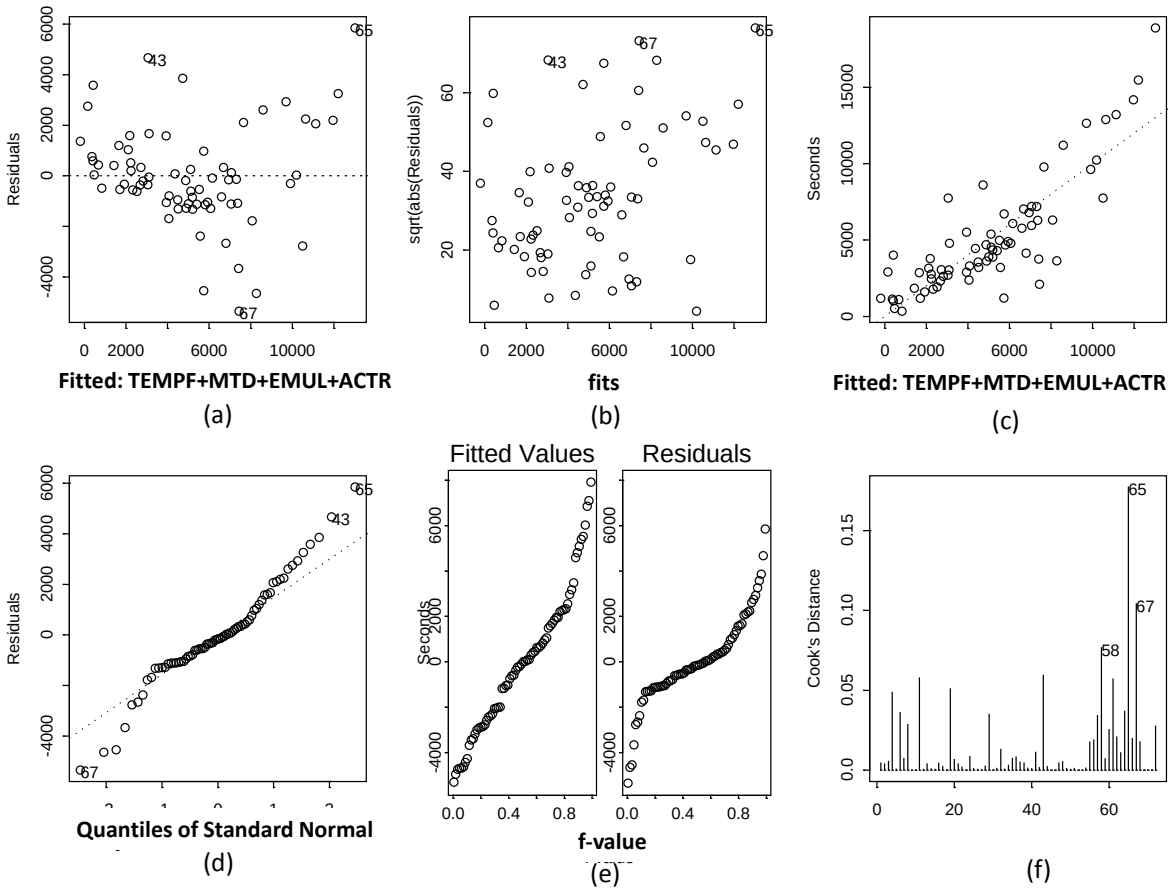

Figure 4.5: Residual plot for final model (combined data)

4.4.1.2 Adjustments to Regression Model

Effects of the wind on tack coat curing time were investigated by conducting several additional curing time experiments with a target application rate of 0.105 gal/yd^2 using CO1_CSS 1H. The tack coat was applied via paintbrush (approximately 7.64 grams) to a 6-inch diameter asphalt core measuring 2 inches thick and placed in front of a box fan. The distance from the core and power of the fan were adjusted until the target wind speed was measured via a hand-held anemometer. Tests were conducted at speeds of 0, 2, 4, 6, and 8 mph. Weight measurements were recorded at every 5 minutes until no significant change in weight occurred. Curing time was determined as the time at which the weight readings remained constant. Results were plotted to show how wind speed affects the curing time of tack coats (Figure 4.6).

Because the regression model was developed without considering the wind, an equation was developed to calculate an adjustment factor to incorporate the impact of wind into the predictions of developed linear regression equation. Each curing time value from the developed linear regression equation should be modified using the following equation:

$$Set\ Time\ Final = Set\ Time * Wind\ Factor \quad \textbf{(4.4)}$$

Where;

$$Wind\ Factor = \frac{-9.75 * Wind\ speed\ (mph) + 129}{129} \quad \textbf{(4.5)}$$

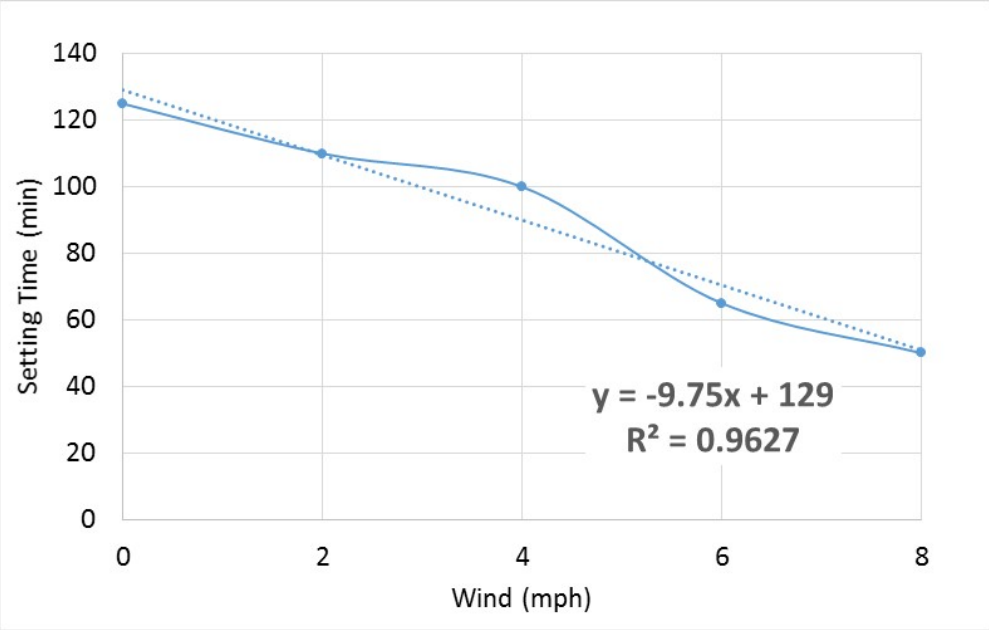

Figure 4.6: Effect of the wind on tack coat curing time

4.4.1.3 Smartphone App

IOS and Android apps were developed to calculate tack coat set time in the field. The IOS app screenshot in Figure 4.7 is showing the input screen and the output screen with the timer. The app sends a notification (with vibration) to the contractor saying "Tack coat is set!" when the timer reaches zero. Both IOS and Android apps will be available in app stores.

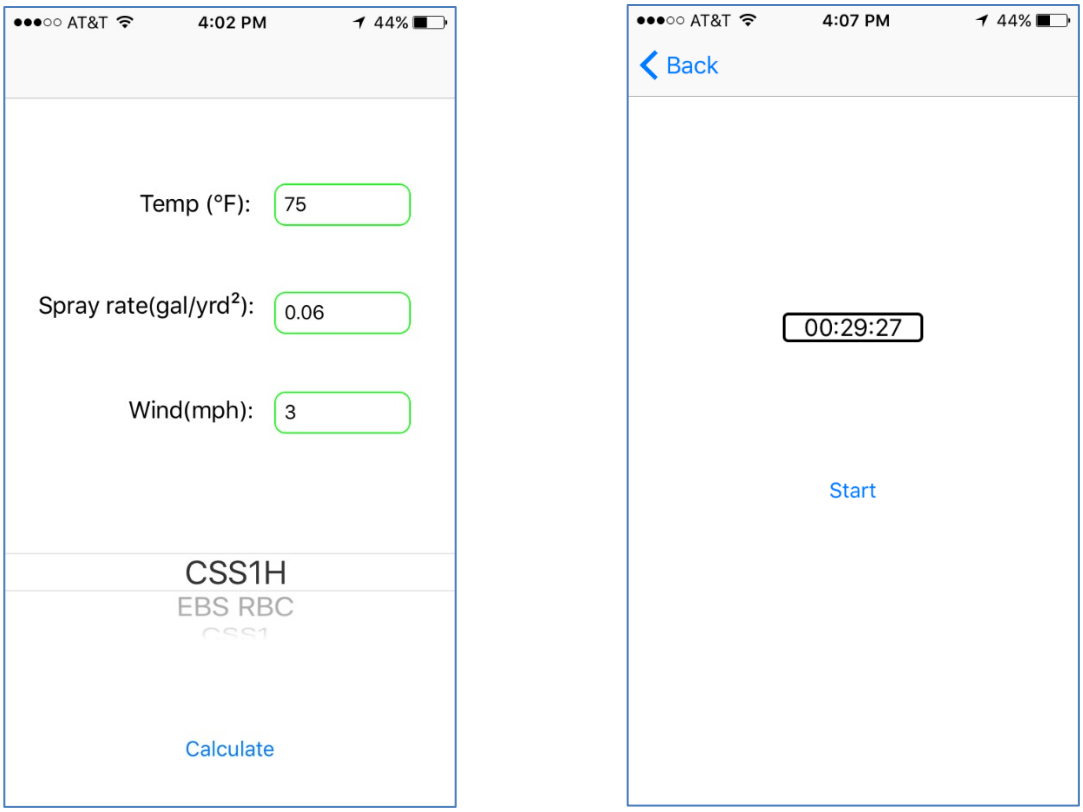

(a) **(b)**

Figure 4.7: Screenshot taken from smartphone app (IOS) developed for tack coat curing time (a) user input (b) countdown timer

4.4.2 Evaluation of Tack Coat Tracking

Tack coat tracking was also investigated in a parking lot experiment on an asphalt surface and in a field experiment on milled and overlay surfaces by using the wheel device developed for this study. Each experiment consisted of placing the wheel on the applied tack coat some known amount of time after spraying and making one pass of the wheel (one revolution of the wheel). The purpose was to measure tack coat tracking using this device to determine the in-situ curing time and provide recommendations to reduce tracking during construction. Figure 4.8 depicts the average amount of tack coat tracked by the developed wheel device over time for several tack coat types for the parking lot tests (non-milled surfaces) conducted with an application rate of 0.07 gal/yd^2. Tack coat tracking also serves as an indicator of the actual curing time of that specific tack coat material. As the amount being tracked decreases, the tack coat approaches a cured state ready for haul vehicles to drive on. The amount tracked decreased as time increased. This result suggests that wheel tracking device can be a useful tool to determine tack coat curing time in the field and can be used to reduce tracking by not allowing construction vehicle traffic on the applied tack before an appropriate amount of time has passed. Tack coat CO2_New showed the highest initial amount of tracking while CO1_CSS 1H showed the lowest amount of tracking (Figure 4.8).

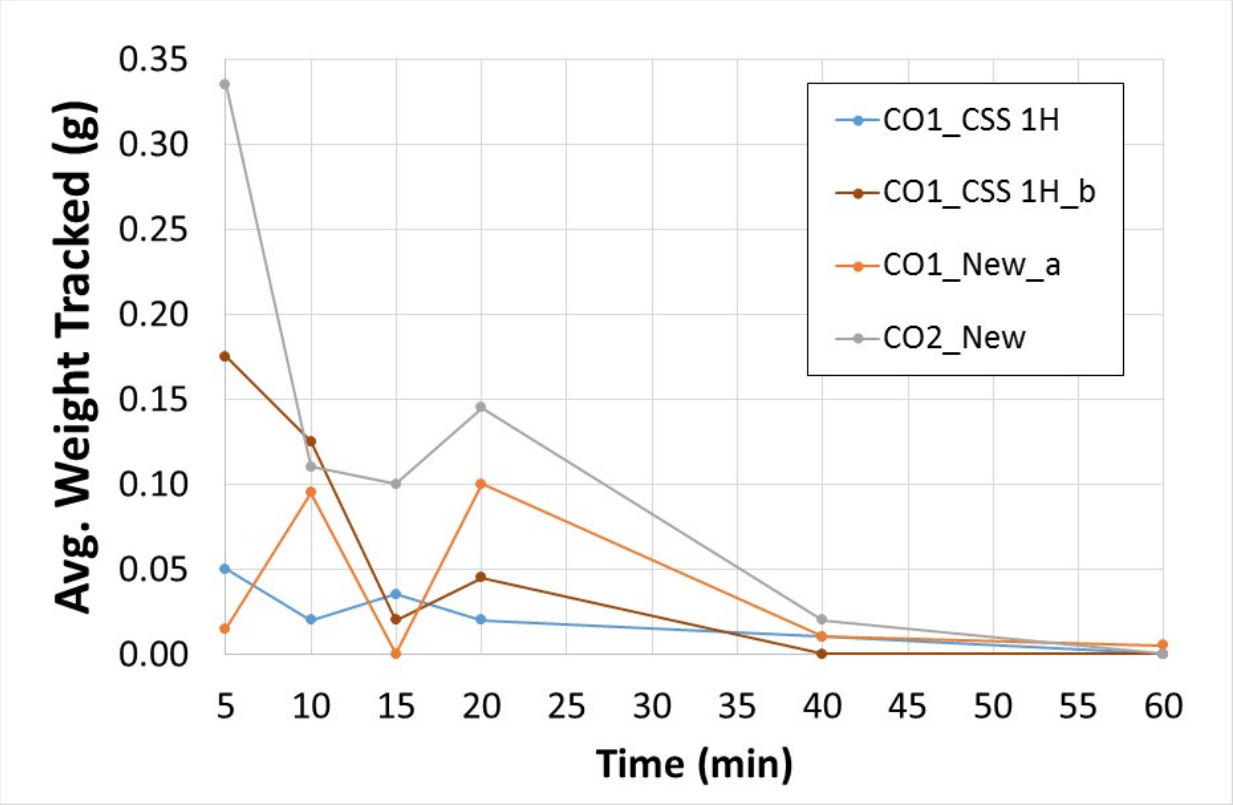

Figure 4.8: Parking lot tracking of tack coats over time with 0.07 gal/yd2

Field experiments were also conducted on a highway construction of new HMA. Milled and overlay surfaces were evaluated at various application rates at approximately the same time after spraying occurred. Figure 4.9 shows the relationship of tack coat tracking for an application rate at approximately 50 minutes after spraying for the two surface types considered. Figure 4.9a and Figure 4.9b show tack coat tracking in the field of milled and overlay surfaces, respectively, by a visual inspection. Visual inspection (without weighing the tires with a high accuracy scale) can be performed to give an indication of whether or not the tack coat is cured. Less tracking measured by tire weighing or less material on the tires of the wheel device (observed by visual inspection) indicates that the tack coat is approaching the curing time. Milled surfaces tracked significantly more than overlay surfaces both in visual inspection and by tire weighing (Figure 4.9c and Figure 4.9d). CO1_CSS 1H_a tracked the most on the milled surface, followed by CO1_New_a and CO2_New. In the field experiments, “New” engineered emulsions appear to be tracking less than the traditional tack coat materials (Figure 4.9).

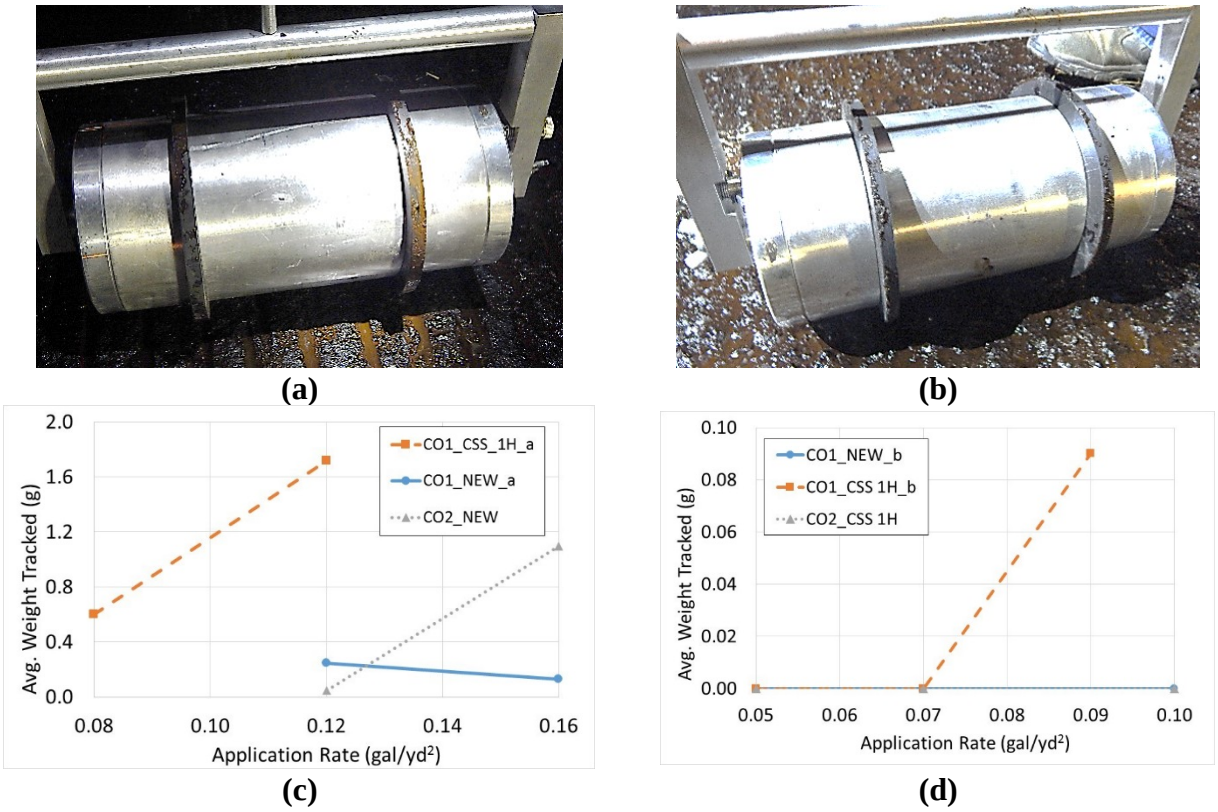

Figure 4.9: Tack coat tracking relationship with application rate (a) visual inspection on milled surface (b) visual inspection on overlay surface (c) measured tracking on milled surface (d) measured tracking on overlay surface

4.5 SUMMARY AND CONCLUSIONS

The tracking potential of Oregon's CSS 1H and "New" engineering emulsions from two companies were investigated. Curing time was evaluated by performing weight evaporation tests in a laboratory. Data from evaporation tests were used to develop a linear regression model to predict curing times and develop a smartphone application. Tracking evaluation of selected tack coats was completed by using a wheel tracking device developed in this study. Tests were conducted in the parking lot and field on milled and overlay surfaces. Development of two new technologies (smartphone app and wheel device) for the state of Oregon are expected to improve construction practices, reduce tracking, and improve the bond strength between pavement layers.

The conclusions of this study are:

- Higher temperatures lead to shorter curing times for all tack coat types;
- Increased application rates lead to increased curing times;
- Regression analysis revealed that mean texture depth (MTD) did not have a significant effect on curing time;

- CO1_New illustrated the longest curing time in laboratory experiments, followed by CO1_CSS 1H, CO2_CSS 1, and CO2_New for all testing conditions (temperatures and application rates);

- Increased wind speeds will result in reduced curing time;

- Tack coat tracking, the amount picked up, decreases with curing;

- Milled surfaces exhibit more tracking, due to tack coat accumulating in grooves of texture, when compared to overlay surfaces; and

Wheel tracking device can be effectively used to determine tack coat curing time during construction.

5.0 THREE DIMENSIONAL FINITE ELEMENT MODE TO EVALUATE THE EFFECTSA OF STRUCTURAL CHARACTERISTICS ON TACK COAT PERFORMANCE

5.1 INTRODUCTION

This portion of the study focused on development of a 3D viscoelastic finite element (FE) model to evaluate the effects of asphalt overlay (OL) thickness, existing asphalt layer (AC) thickness, aggregate base layer (AB) thickness, subgrade (SG) stiffness, and temperature (Temp.) on tack coat layer's displacement and shear strain distributions. Tack coat layer is assumed to be between the existing AC layer and the OL.

5.2 GENERAL PROCEDURE FOR MODEL DEVELOPMENT

A viscoelastic finite element (FE) model was developed to calculate displacement and shear strain under different conditions. Energy dissipation due to the subgrade damping is not simulated in the model. In the developed viscoelastic FE model, only the linear behavior is considered (small strain domain). The material constituting the base is considered isotropic linear elastic.

The temperature dependency of the asphalt mix is defined by using the Williams-Landel-Ferry (WLF) equation, given as follows *(Ferry 1980)*:

$$\log(aT) = \frac{-C_1\left(T - T_{ref}\right)}{C_2 + \left(T - T_{ref}\right)} \quad \textbf{(5.1)}$$

Where;

aT = the time-temperature shift factor,
C_1 and C_2 = regression coefficients,
T_{ref} = the reference temperature, and
T = test temperature.

To optimize the regression coefficients C_1 and C_2, the modulus data were first fitted to a sigmoid function, in the form of:

$$\log\left(G(\xi)\right) = \delta + \frac{\alpha}{1 + e^{\beta + \gamma \log \xi}} \quad \textbf{(5.2)}$$

Where;

α, β, γ, δ = regression coefficients, and
ξ = reduced time.

Shift factors are calculated by fitting the measured modulus to the sigmoidal function (5-2). One shift factor is calculated at each test temperature while the shift factor for the reference temperature (19^{o}C) is set at zero. A MATLAB code was developed to optimize the regression coefficients α, β, γ, δ and shift factors for all temperatures. Regression coefficients C_1 and C_2 are calculated by simply fitting the WLF equation (5-1) to the calculated shift factors.

The generalized Maxwell-type viscoelastic model is used in this study to simulate the time dependency. The model consists of two basic units, a linear elastic spring and a linear viscous dash-pot. Various combinations of these spring and dashpot units define the type of viscoelastic behavior. In this study, one spring and five Maxwell elements in parallel were used for the mastic model (Figure 5.1). Measured shear modulus (G*) values were separated into storage modulus [G'(ω)] and loss modulus [G"(ω)] components based on the measured phase angles (δ) using the following equations *(Papagiannakis et al. 2002)*:

$$G'(\omega) = G^*(\omega)\cos\delta \quad \textbf{(5.3)}$$

$$G''(\omega) = G^*(\omega)\sin\delta \quad \textbf{(5.4)}$$

Where;

ω = loading frequency in rad/s,
G*(ω) = complex shear modulus in MPa, and
δ = phase angle between strain and stress.

Storage modulus and loss modulus can be expressed as follows *(Baumgaertel and Winter 1989)*:

$$G'(\omega) = G_e + \sum_{i=1}^{N} g_i \frac{(\omega\lambda_i)^2}{1+(\omega\lambda_i)^2} \quad \textbf{(5.5)}$$

$$G''(\omega) = \sum_{i=1}^{N} g_i \frac{\omega\lambda_i}{1+(\omega\lambda_i)^2} \quad \textbf{(5.6)}$$

Where;

N = number of Maxwell units,
G_e = equilibrium modulus,
g_i = relaxation strengths (spring constants of Maxwell units), and
λ_i = relaxation times.

$$\lambda_i = \frac{\eta_i}{g_i} \quad \textbf{(5.7)}$$

Where;

η_i = dashpot constants of Maxwell units (Figure 5.1)

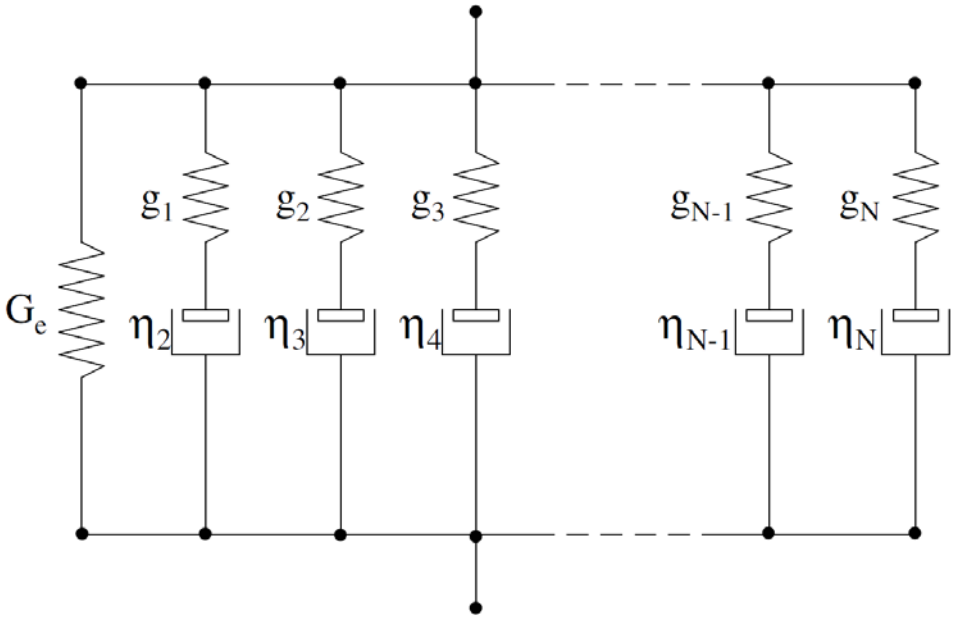

Figure 5.1: Schematic of the generalized Maxwell model *(Coleri and Harvey 2012).*

By fitting equations (5.5) and (5.6) to measured G' and G" data, the parameters of a discrete relaxation spectrum can be determined. A genetic algorithm was used to optimize these model parameters (G_e, g_i and λ_i) by minimizing the calculated residual sum of squares (RSS) *(Tsai et al. 2004)*. In this study, the following fitness function was used to calculate the RSS for optimization:

$$RSS = \sum_{j=1}^{m} \left(\left[\frac{G'(\omega_j)}{\hat{G}'_j} - 1 \right]^2 + \left[\frac{G''(\omega_j)}{\hat{G}''_j} - 1 \right]^2 \right) \quad \textbf{(5.8)}$$

Where;

$\hat{G}'_j$ and $\hat{G}''_j$ are the measured data at m frequencies.

To predict the global viscoelastic behavior of the asphalt mixture, time-temperature dependent FE analysis was conducted. Abaqus™ software is used for model development. The pavement structure is represented by a 6 m long and 2.5 m wide slab (Figure 5.2a). The finite-element mesh consists of Lagrange brick elements with a second-order interpolation function. The mesh is refined under the wheel path (Figure 5.2b).

The bottom side of the model is clamped. The symmetry condition in the transversal direction imposes a boundary condition on one side. To ensure the continuity of this slab with the rest of

pavement, only vertical displacement is allowed for other lateral sides. Perfect bonding is assumed between different pavement layers.

In order to simulate moving wheel loading in the viscoelastic FE model, the trapezoidal impulsive loading method (quasi-static) is used *(Yoo et al. 2006).* Figure 5.2 shows the displacement field at two time points under the moving truck tire. The tire is assumed to have a square contact area and the distribution of load on the tire is assumed to be constant. A truck tire pressure of 760 kPa and a tire load of 37.9 kN is used for modeling. Viscoelastic asphalt material properties are simulated using the results of a laboratory dynamic modulus test conducted on dense graded asphalt concrete samples (PG64-22).

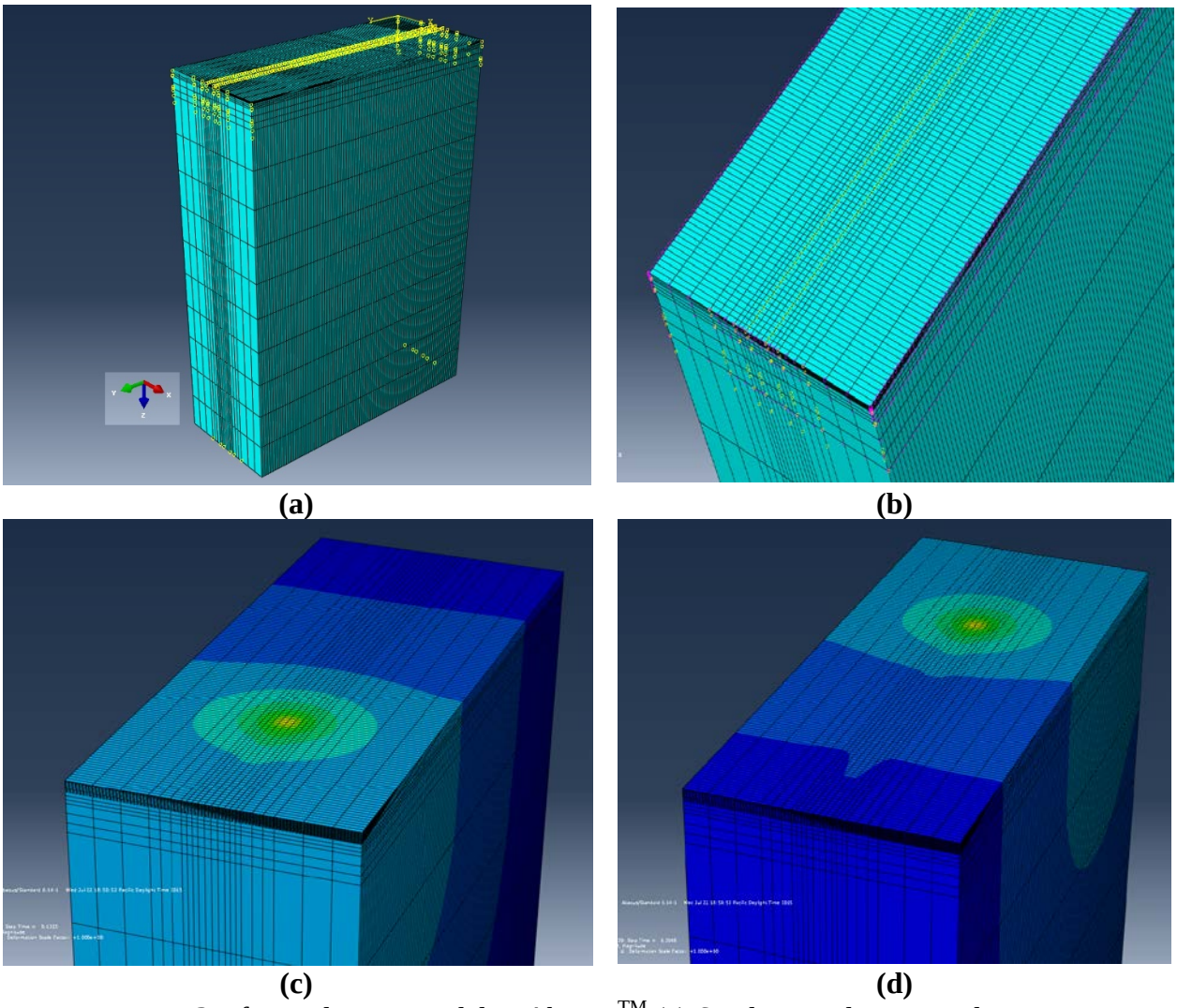

(a) **(b)**

(c) **(d)**

Figure 5.2: 3D finite element model in Abaqus™ (a) 6 m long and 2.5 m wide pavement structure with subgrade, aggregate base, asphalt and asphalt overlay layers (b) Meshed 3D FE model (truck wheel is travelling in the middle part which has a refined mesh) (c, d) Displacement field at two time points under the moving truck tire.

5.3 FACTORIAL DESIGN FOR 3D FE MODELING

A total of 32 cases were simulated to evaluate the impact of OL thickness, AC thickness, AB thickness, SG stiffness, and Temp. on displacement and shear strain distributions on tack coat layers. Simulated cases are given in Table 5.1: Factorial for 3D FE modeling. It should be noted that when a critical stress and displacement level is exceeded under a truckload, tack coat will be broken. Broken tack coat will change stress and strain distribution in the pavement structure and result in early failure *(King and May 2003; Roffe and Chaignon 2002).*

Table 5.1: Factorial for 3D FE modeling

Case	H_{OL} (in.)	H_{AC} (in.)	H_{AB} (in)	E_{SG} (psi)	Temp. (^{o}F)
1	2	4	10	5,800	86
2	2	4	10	5,800	113
3	2	4	10	14,500	86
4	2	4	10	14,500	113
5	4	4	10	5,800	86
6	4	4	10	5,800	113
7	4	4	10	14,500	86
8	4	4	10	14,500	113
9	2	12	10	5,800	86
10	2	12	10	5,800	113
11	2	12	10	14,500	86
12	2	12	10	14,500	113
13	4	12	10	5,800	86
14	4	12	10	5,800	113
15	4	12	10	14,500	86
16	4	12	10	14,500	113
17	2	4	16	5,800	86
18	2	4	16	5,800	113
19	2	4	16	14,500	86
20	2	4	16	14,500	113
21	4	4	16	5,800	86
22	4	4	16	5,800	113
23	4	4	16	14,500	86
24	4	4	16	14,500	113
25	2	12	16	5,800	86
26	2	12	16	5,800	113
27	2	12	16	14,500	86
28	2	12	16	14,500	113
29	4	12	16	5,800	86
30	4	12	16	5,800	113
31	4	12	16	14,500	86
32	4	12	16	14,500	113

Note: H: Thickness; E: Stiffness; Temp.: pavement temperature.

5.4 RESULTS AND DISCUSSION

Critical (highest) strain under the simulated rolling truck wheel for all 32 cases are summarized in Figure 5.3. Analysis of variance (ANOVA) technique, which measures the variance within groups to the variance between groups, is used to determine the effects of OL thickness, AC thickness, AB thickness, SG stiffness, and Temp. On simulated critical tack coat shear strain values (Table 5.2). The most important parameter in ANOVA is the F-value which is a measure of the independent variables importance to define the dependent variable. Larger F-values represent those variables that are more significant in affecting the critical shear strain. It can be observed from Table 5.2 that temperature is the most significant factor that affects critical shear strain while overlay thickness also has a significant effect. On the other hand, the effects of existing layer thickness, AB layer thickness, and subgrade stiffness are insignificant when compared to the effects of overlay thickness and temperature. This result suggests that tack coat quality and spraying rates must be modified depending on the climate and overlay design thickness. For this reason, tack coat resistance and strength become more important for thin overlays.

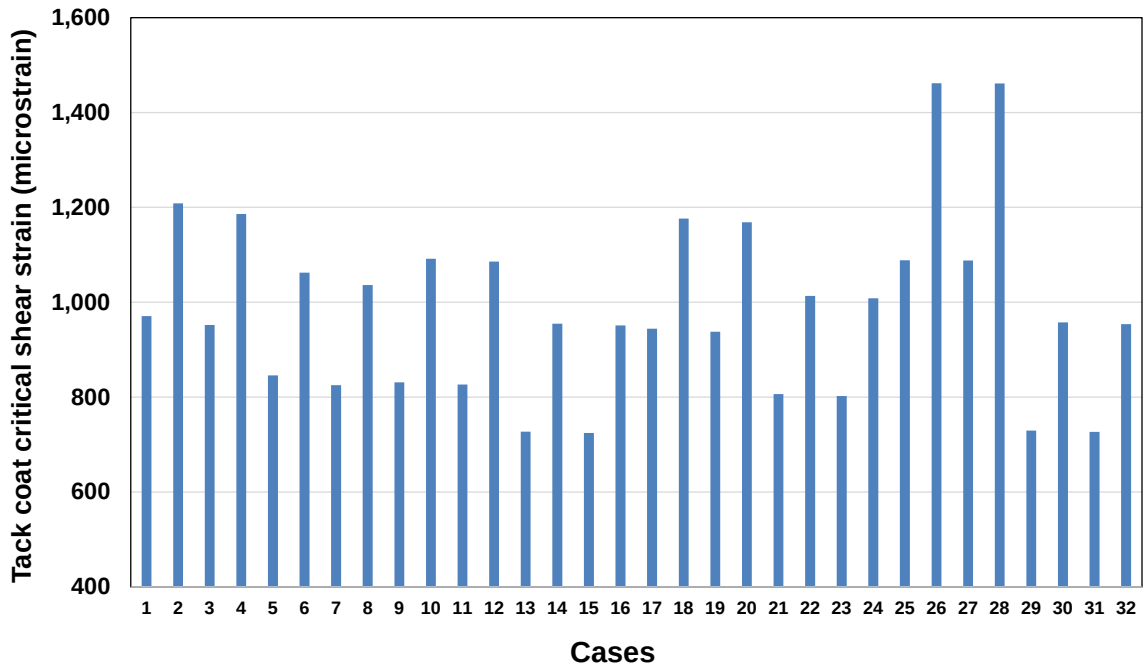

Figure 5.3: Tack coat critical (highest) shear strain under the simulated truck wheel (information for each case is given in Table 5-1).

Note: AB layer thickness is positively correlated with predicted shear strain since larger AB layer thickness shifts the shear strain distributions up and localizes shear strain around the tack coat area.

Table 5.2: ANOVA table for critical tack coat shear strain values

Variables	Df	Sum of Sq	Mean Sq	F Value	Pr(F)
H_{OL} (in.)	1	351558	351558	40.61	0.0000
H_{AC} (in.)	1	2530	2530	0.29	0.5934
H_{AB} (in.)	1	34132	34132	3.94	0.0577
E_{SG} (psi)	1	565	565	0.07	0.8003
Temp. (^{o}F)	1	487548	487548	56.32	0.0000
Residuals	26	225086	8657		

Distributions of shear strain (E13) and vertical displacement (U3) along with some of the simulated sections are given in Figure 5.4 through Figure 5.9. All plots are snapshots of the pavement cross-section when the truck wheel is in the middle of the 3D FE model. It can be observed from Figure 5.4 that increasing overlay thickness creates a significant reduction in shear strain. In addition, thick overlay shifts the critical shear strain location from the tack coat area (OL and AC interface) to mid-overlay area. Figure 5.5 shows the significant impact of overlay thickness on the simulated deflection basin. Increasing the overlay thickness from 2in. to 4in. creates a significant reduction in observed displacement.

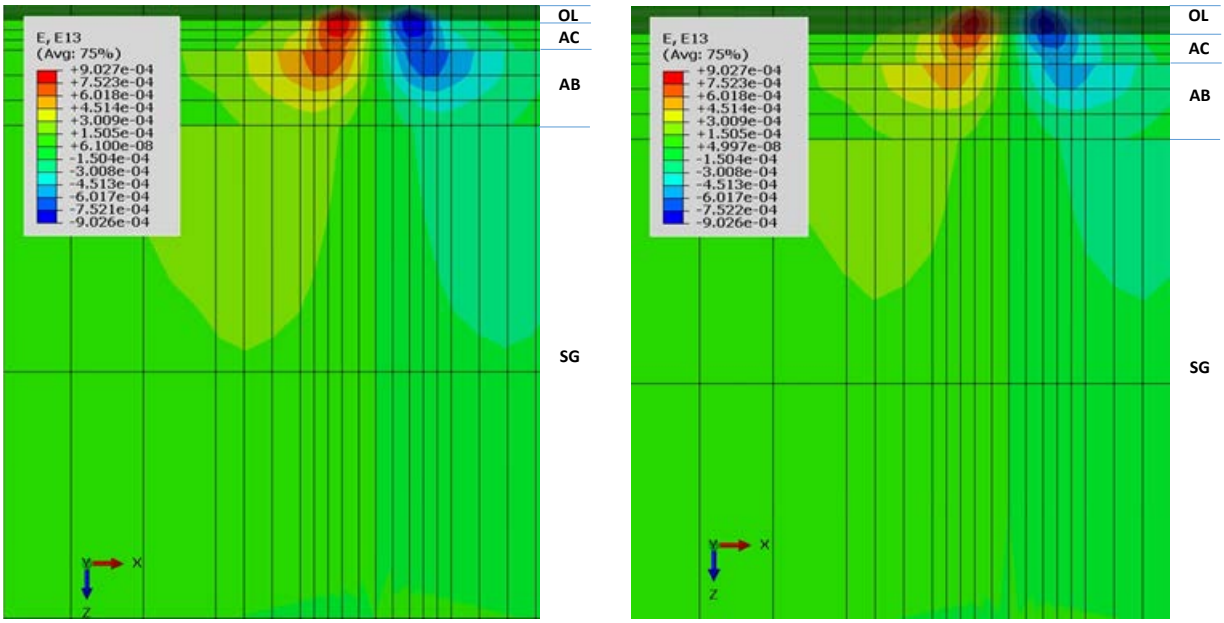

(a) (b)

Figure 5.4: Overlay thickness effect on shear strain (a) CASE 1: H_{OL}= 2 in., H_{AC}= 4 in., H_{AB}= 10 in., E_{SG}= 5,800psi, Temp.=86^{o}F (b) CASE 5: H_{OL}= 4 in., H_{AC}= 4 in., H_{AB}= 10 in., E_{SG}= 5,800psi, Temp.=86^{o}F.

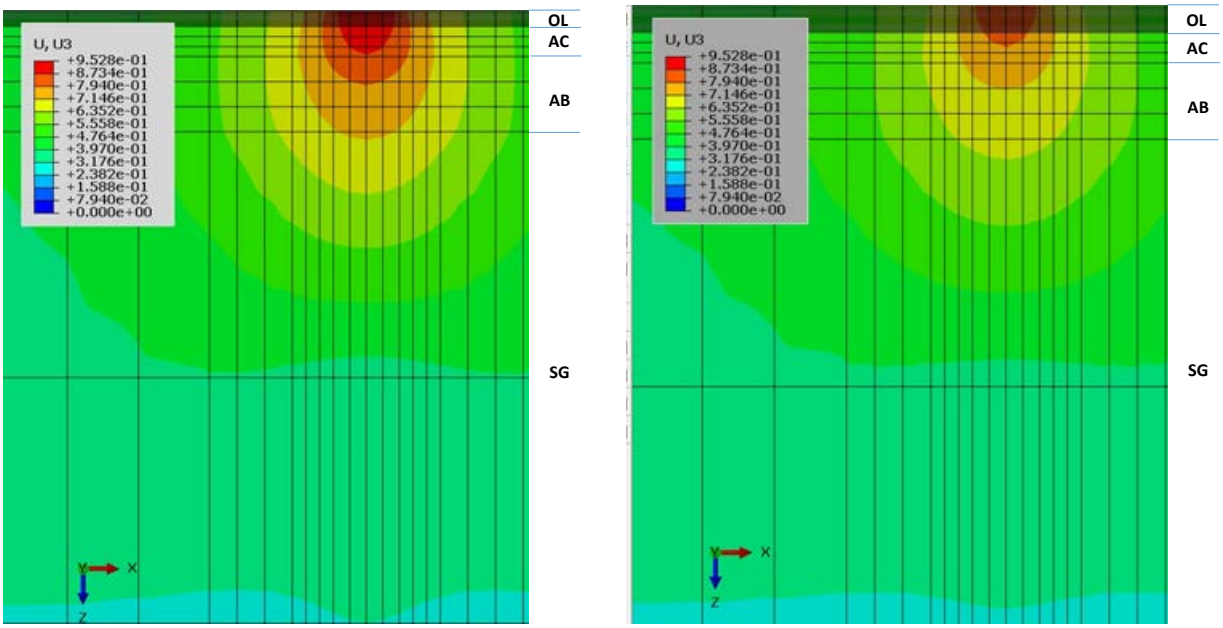

(a) (b)

Figure 5.5: Overlay thickness effect on displacement (a) CASE 1: H_{OL}= 2 in., H_{AC}= 4 in., H_{AB}= 10 in., E_{SG}= 5,800psi, Temp.=86^{o}F (b) CASE 5: H_{OL}= 4 in., H_{AC}= 4 in., H_{AB}= 10 in., E_{SG}= 5,800psi, Temp.=86^{o}F.

Figure 5.6 shows the impact of existing AC layer thickness on shear strain distribution. Although increasing the existing AC layer thickness reduces the observed shear strain along the section, critical shear strain observed on the tack coat does not significantly change (Table 5.2). In other words, increased existing AC layer thickness does not create a shift in the strain distribution.

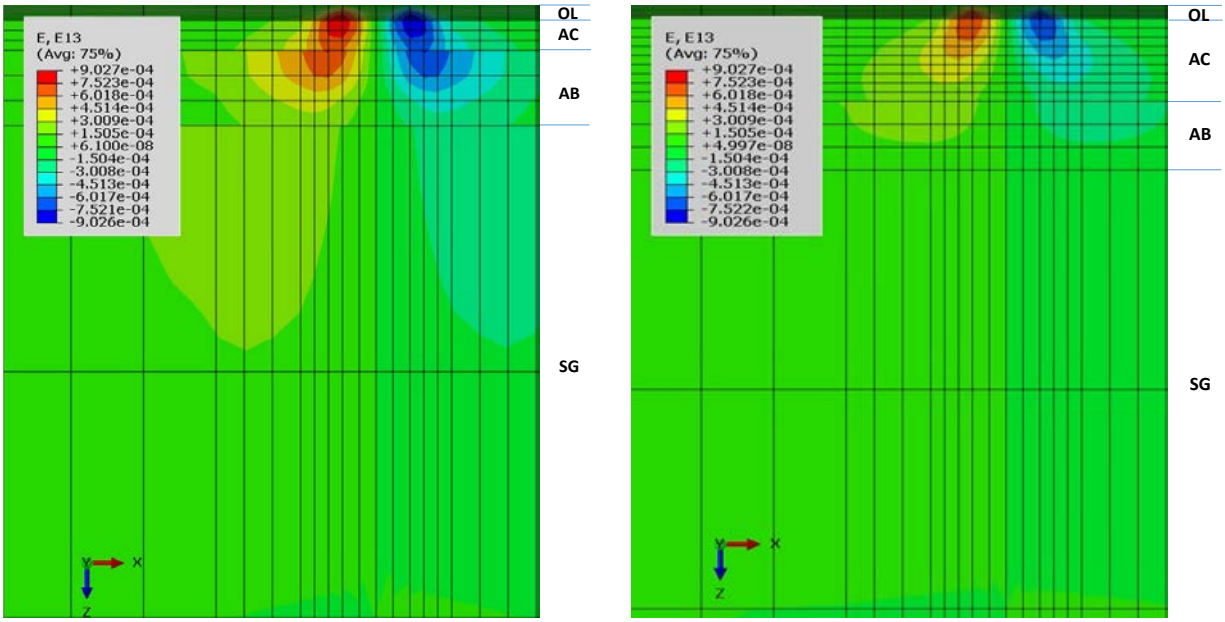

(a) (b)

Figure 5.6: Existing AC layer thickness effect on shear strain (a) CASE 1: H_{OL}= 2 in., H_{AC}= 4 in., H_{AB}= 10 in., E_{SG}= 5,800psi, Temp.=86^{o}F (b) CASE 9: H_{OL}= 2 in., H_{AC}= 12 in., H_{AB}= 10 in., E_{SG}= 5,800psi, Temp.=86^{o}F.

Increasing AB layer thickness reduces the average shear strain observed along the pavement cross-section (Figure 5.7). However, AB layer thickness is observed to be positively correlated with predicted tack coat shear strain (Figure 5.3) since increasing AB layer thickness shifts the shear strain distributions up and localizes higher shear strain around the tack coat area (Figure 5.7). This result suggests that increasing the strength and thickness of underlying (unbound) layers do not necessarily reduce critical tack coat shear strain values.

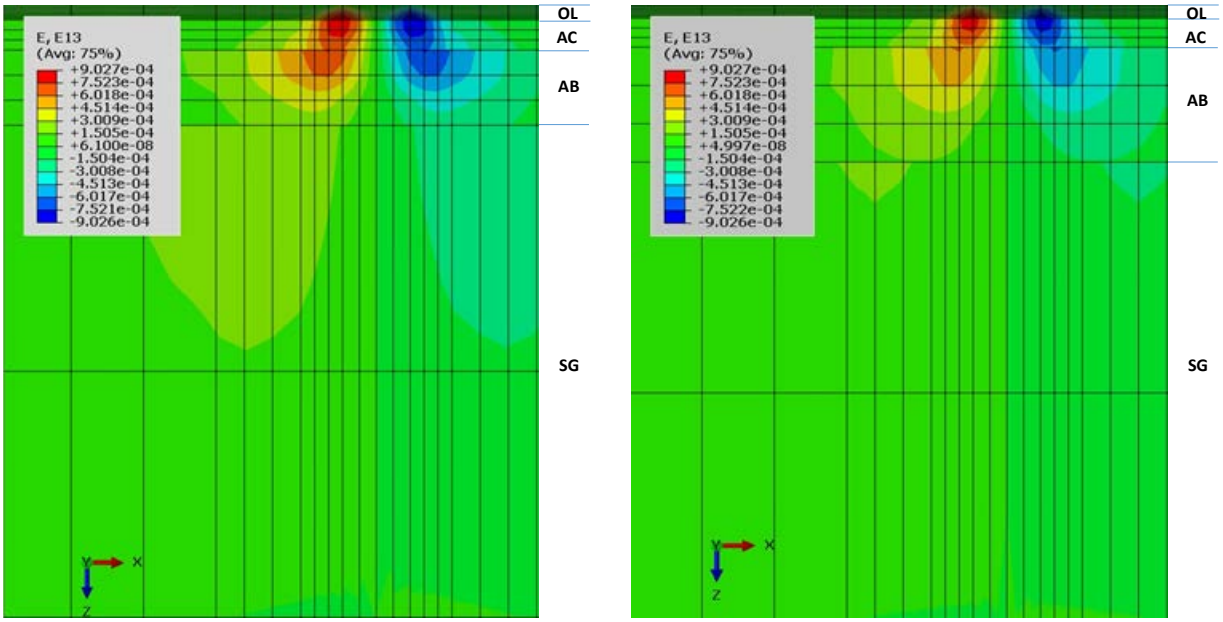

(a) (b)

Figure 5.7: AB layer thickness effect on shear strain (a) CASE 1: H_{OL}= 2 in., H_{AC}= 4 in., H_{AB}= 10 in., E_{SG}= 5,800psi, Temp.=86^{o}F (b) CASE 17: H_{OL}= 2 in., H_{AC}= 4 in., H_{AB}= 16 in., E_{SG}= 5,800psi, Temp.=86^{o}F.

It can be observed from Figure 5.8 that increasing subgrade stiffness does not create a considerable impact on shear strain distributions. However, increasing the temperature from 86^{o}F to 113^{o}F results in a significant increase in shear strain (Figure 5.9). This result suggested that at high summer temperatures tack coat bond failures are likely to occur. However, results from laboratory shear tests with field cores should be evaluated to determine whether the observed critical shear strain values are higher or lower than the failure strain levels.

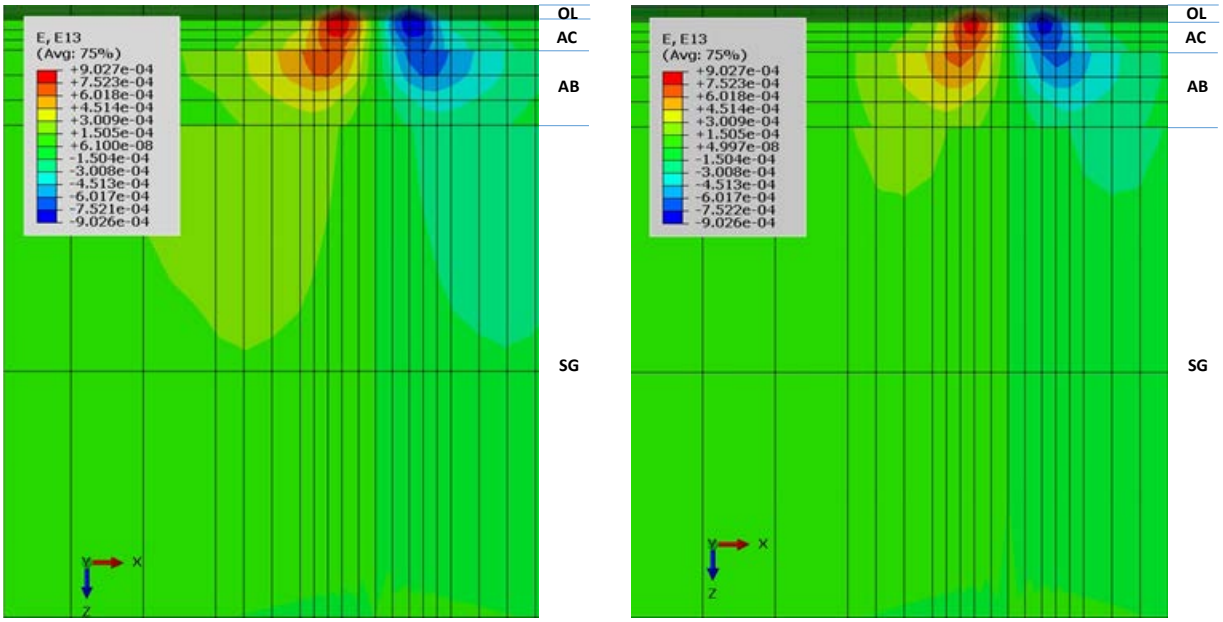

(a) (b)

Figure 5.8: SG layer stiffness effect on shear strain (a) CASE 1: H_{OL}= 2 in., H_{AC}= 4 in., H_{AB}= 10 in., E_{SG}= 5,800psi, Temp.=86^{o}F (b) CASE 3: H_{OL}= 2 in., H_{AC}= 4 in., H_{AB}= 10 in., E_{SG}= 14,500psi, Temp.=86^{o}F.

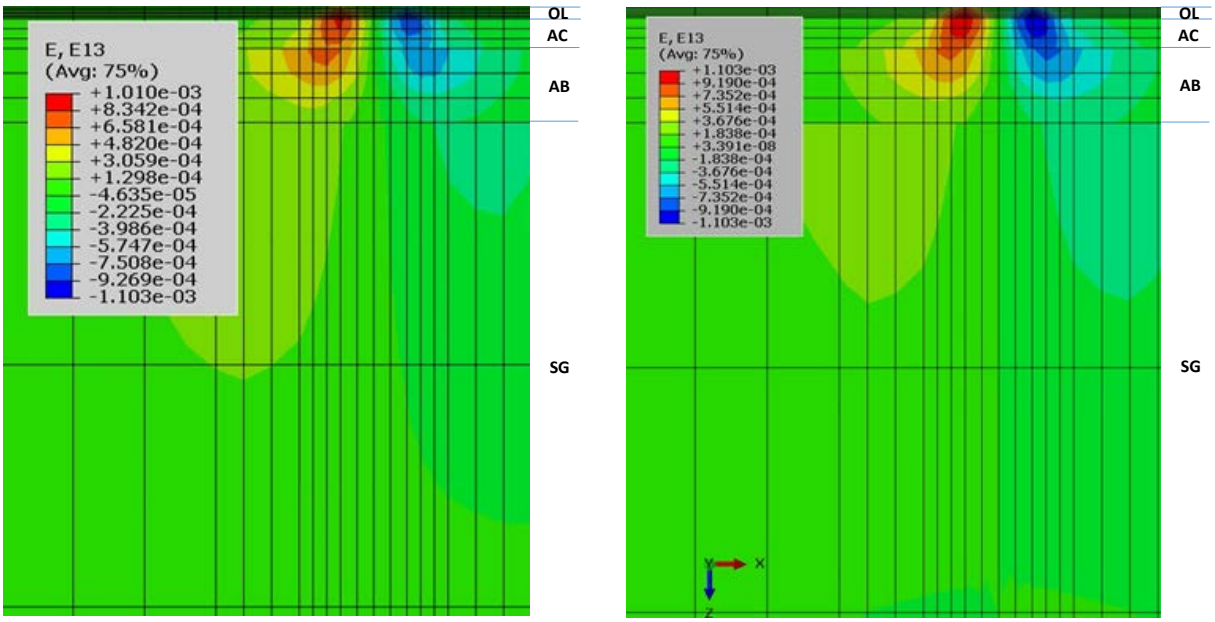

(a) (b)

Figure 5.9: Pavement temperature effect on shear strain (a) CASE 1: H_{OL}= 2 in., H_{AC}= 4 in., H_{AB}= 10 in., E_{SG}= 5,800psi, Temp.=86^{o}F (b) CASE 2: H_{OL}= 2 in., H_{AC}= 4 in., H_{AB}= 10 in., E_{SG}= 5,800psi, Temp.=113^{o}F.

5.5 SUMMARY AND CONCLUSIONS

This portion of the study focused on the development of a 3D viscoelastic FE model to evaluate the effects of OL thickness, existing AC thickness, AB thickness, SG stiffness, and Temp. On tack coat layer's displacement and shear strain distributions.

The analysis presented in this report have yielded the following conclusions:

- Temperature is the most significant factor that affects critical shear strain while overlay thickness also had a significant effect. On the other hand, the effects of existing layer thickness, AB layer thickness, and subgrade stiffness are insignificant when compared to the effects of overlay thickness and temperature. This result suggests that tack coat quality and spraying rates must be modified depending on the climate and overlay design thickness.

- Increasing overlay thickness shifts the critical shear strain location from the tack coat area (OL and AC interface) to mid-overlay area. This phenomenon creates a significant reduction in critical tack coat shear strain with increasing overlay thickness. For this reason, tack coat resistance and strength become more critical for thin overlays.

- Although increasing the existing AC layer thickness reduces the average shear strain along the section, critical shear strain observed on the tack coat does not significantly change.

- Increasing AB layer thickness reduces the average shear strain observed along the pavement cross-section. However, AB layer thickness is observed to be positively correlated with predicted tack coat shear strain since increasing AB layer thickness shifts the shear strain distributions up and localizes higher shear strain around the tack coat area.

- Increasing temperature from 86^{o}F to 113^{o}F results in a significant increase in shear strain. This result suggested that at high summer temperatures tack coat bond failures are likely to occur.

6.0 DEVELOPMENT OF A FIELD TORQUE TEST TO EVALUATE IN-SITU TACK COAT PERFORMANCE

6.1 INTRODUCTION

Monitoring the performance of the interlayer shear strength (ISS) during the use phase and identifying bond failures are critical to improving pavement management systems and develop more efficient pavement design strategies. It is crucial to monitor the performance of tack coats regularly and measure the changes over time. However, testing cores taken from roadways in the laboratory is not economical and practical. In addition, removal of full depth cores can affect the structural integrity of the pavement and can create localized failures.

In this study, a low cost, practical, and less destructive field test device, the Oregon Field Torque Tester (OFTT), is developed to evaluate the long-term post-construction tack coat performance of pavement sections. Correlations between OFTT field test results and the results of laboratory shear tests conducted with cores taken from the field were investigated to determine the effectiveness of the OFTT tests. The peak torque values measured by the OFTT were observed to be highly correlated with the measured laboratory shear strengths. The OFTT shear strength values calculated by using the torque test results and a theoretical equation were determined to be close to the measured laboratory shear strengths.

6.2 OBJECTIVES

The objectives of this study are to:

1. Develop a new low-cost technology, the Oregon Field Torque Tester (OFTT), to evaluate the long-term tack coat performance of pavement sections after construction. This new technology allows for a more practical test method and is less destructive as compared to the laboratory shear testing;

2. Investigate the effectiveness of OFTT by evaluating the correlations between the laboratory shear and OFTT test results; and

3. Provide recommendations to improve the developed system further.

6.3 CURRENT TORQUE TESTER TECHNOLOGIES

The current laboratory shear testing technologies to determine tack coat bond strength require full depth field cores, which reduce the structural integrity of the pavement. Changing the structural integrity of the pavement by taking cores can damage/weaken the subgrade layer when water penetrates through the core holes. Even though the OFTT developed in this study also requires coring, it is still less destructive when compared to the laboratory direct shear tests,

because full-depth cores are not needed for testing, and the diameter of the cores are only 2.5 inches.

The torque bond test was created in Sweden, and is a testing method used to evaluate field bond strength. The UK adopted this method and it became a part of the approved testing system for tack *coats (Walsh et al. 2001).* After construction, cores were drilled to a depth of half an inch below the layer interface and left in contact with the pavement. Then, the loading platen was glued to the drilled core by using a fast setting epoxy. Then, a constant torque rate was manually applied to the cored surface using a wrench until failure occurs *(Walsh et al. 2001*). This test procedure is based on the British Board of Agreement guidelines document SG3/98/173. However, since it is difficult to control the constant torque rate manually, high variability in test results can be observed. The measured peak torque is used as a parameter to characterize the interlayer shear strength (ISS) at the layer interface.

Another study compared results from Florida's laboratory shear test against those of the manual bond torque test *(Tashman et al. 2006).* It was found that the correlation between the Florida laboratory shear test and the torque bond test results were not statically significant even though the effect of the milled surface on ISS was captured in the data *(Tashman et al. 2006).* However, both tests provided different ISS values at the interface due to the differences in their loading mechanisms. The difficulty of maintaining a constant torque rate manually was another reason for the low correlation. In addition, since the torque bond tester was not able to apply the high torque levels required to break the bonds with high strength levels, it was difficult to get reliable results for cores with high bond strengths.

Muslich *(Muslich 2009)* developed an automatic laboratory torque device to evaluate the tack coat bond strength. In the laboratory test procedure, specimens with 100mm diameter were used. Gluing the cylindrical loading platen, 100mm in diameter and 10mm in thickness, to the top and bottom of the specimens allowed for easy and secure placement into the test frame. After the applied glue had been cured, the core was placed inside a temperature-controlled cabin for five hours. To ensure that the test was conducted at a constant torque rate (600Nm/mm), a constant vertical force was applied to the rack with a steady and continual torque rate. To test the constant rotation rate (180^o/min), a constant vertical displacement rate was applied to the rack. Use of a load cell and an LVDT incorporated into the axial testing machine allowed for measurement of the vertical force and the corresponding displacement. The results from both torque and shear experiments indicated that there was a high correlation ($R^2 = 0.89$) between the two methods and illustrated that the nominal shear strength obtained at 180^o/min was 1.9 times higher than the nominal shear strength measured at 600Nm/mm *(Muslich 2009).* Although the developed torque test equipment provided reliable results, it can only be used to conduct experiments in the laboratory.

6.4 PROPOSED SOLUTION

This part of the study focused on developing a new low-cost technology that would be used to evaluate the long-term post-construction tack coat performance of pavement sections. The OFTT device is specifically designed to measure in-situ ISS comparable to those of other destructive tests. The OFTT combines several proprietary technologies including software and automated rotation rate control, allowing the device to be used easily in the field. This practical software

was developed to control the rotational speed rate and the movement of the platen relative to the cored sample. A small platen of 2.5 inches in diameter was considered to reduce the cost, test timing, and to reach the peak torque with less energy. The reduction of the diameter results in less damage to the pavement structure compared with laboratory shear tests, which requires extracting full-depth 6-inch diameter cores from the pavement. In addition, the developed OFTT device system was designed to carry out multiple experiments in less than two hours in both field and laboratory settings. An adjustable heat gun and temperature control box were also developed to control the temperature for testing. In the final analysis, the device gave acceptable and reliable results; hence, it can be adopted as a test to evaluate the long-term bond performance of pavement structures.

6.4.1 Challenges

The system needed to be designed to overcome several challenges:

- Practical issues such as drying the samples before testing: A blower and a vacuum were used to remove the water from coring and dry the samples without removing them from the pavement.

- Temperature control in the field was a significant concern, hence; a temperature control box with an adjustable heat gun and a thermometer were used to maintain/regulate the temperature.

- A practical software needed to be developed to allow the use of the OFTT device easily in the field.

- The design of a light adjustable frame was required to allow for comfortable mobility.

- All samples were cored at one inch below the interface to avoid the failure at the bottom of the cored specimen. Doing so provided a confining pressure between the lower part of the core and the layers below at comparable stress levels within the pavement structure.

- Multiple platens needed to be developed to be able to conduct more experiments in a shorter period of time.

- The best adhesive significantly stronger than the tack coat bond was necessary to minimize adhesive deformation and failure in the test. In addition, the curing time for the adhesive was required to be less than half an hour to be able to conduct several field experiments in a short period of time.

6.5 MATERIALS AND METHODS

6.5.1 Tack Coat Types and Tested Sections

Field experiments with OFTT were conducted on:

- Overlay-Location 1 on sections sprayed with CO1_CSS 1H_b emulsion at medium and high application rates of 0.07 and 0.10 gal/yd^2 (See Table 3.1);
- Overlay-Location 2 on sections sprayed with CO1_New_b emulsion at a medium application rate of 0.07 gal/yd^2 (See Table 3.1).

6.5.2 OFTT Device

Universally, the tack coat bond failure is characterized by three mechanisms: direct shear, direct tension, and torque shear tests. For the research conducted, the bond strength at the interface between pavement layers was determined using two types of testing: a laboratory direct shear test and an OFTT in-situ torque test.

The OFTT device was developed at Oregon State University. The hardware of the device consists of an automatic step motor, planetary gearbox, transducers, torque sensor and amplifier, data acquisition and control systems, and an adjustable frame as shown in Figure 6.1. Figure 6.2 shows the software that was developed to control the loading and rotation speed of the system. The software was designed to display a real-time plot to allow real-time viewing and analysis of the data.

6.5.2.1 Hardware

Stepper Motor

The initial torque is produced by a Nema Size 34K high torque, bipolar stepper motor rated at 134 in-lbs of torque. Step size can be as large as 1.8 degrees/step or reduced through micro-stepping technology to accommodate the required load rate.

Stepper Driver

The bipolar micro step driver accepts stepper timing, enable and direct signals from the control system and produces the necessary current to drive the stepper motor accordingly. Microstepping technology is used to generate slower rotational speeds along with smoother motion. The rotational speed of the stepper is determined by the frequency of a pulse train generated by the data acquisition and control system.

Planetary Gearbox

The planetary gearbox was designed to interface directly with the NEMA 34K stepper motor. It produces a 50:1 reduction in angular velocity while increasing the available torque by the same ratio. It is important to understand that the maximum torque of drive system is affected by the angular velocity of the stepper motor and the micro stepping.

Torque Sensor, Transducer, and Amplifier

The torque sensor is capable of sensing torques in the range of 0 – 500 in-lbs and outputs a proportional voltage. The amplifier provides gain and conditioning of the torque sensor signal making it suitable to record by a data acquisition system.

Data Acquisition and Control System

The system consists of a laptop running the data acquisition and control software which communicates through a USB interface with a multipurpose device that provides digitization of the torque sensor amplifier signal as well as timing and control signals for the stepper motor driver. The multipurpose device digitizes the incoming torque voltage to 16-bit resolution at a scan rate of 50Hz and sends the digital values to the laptop for logging on a hard drive. The multipurpose device also receives control commands from the laptop and outputs the required digital control signals to the stepper driver.

Environmental chamber

It is used to maintain the core sample at the specified temperature of 25^{o}C using a heat gun.

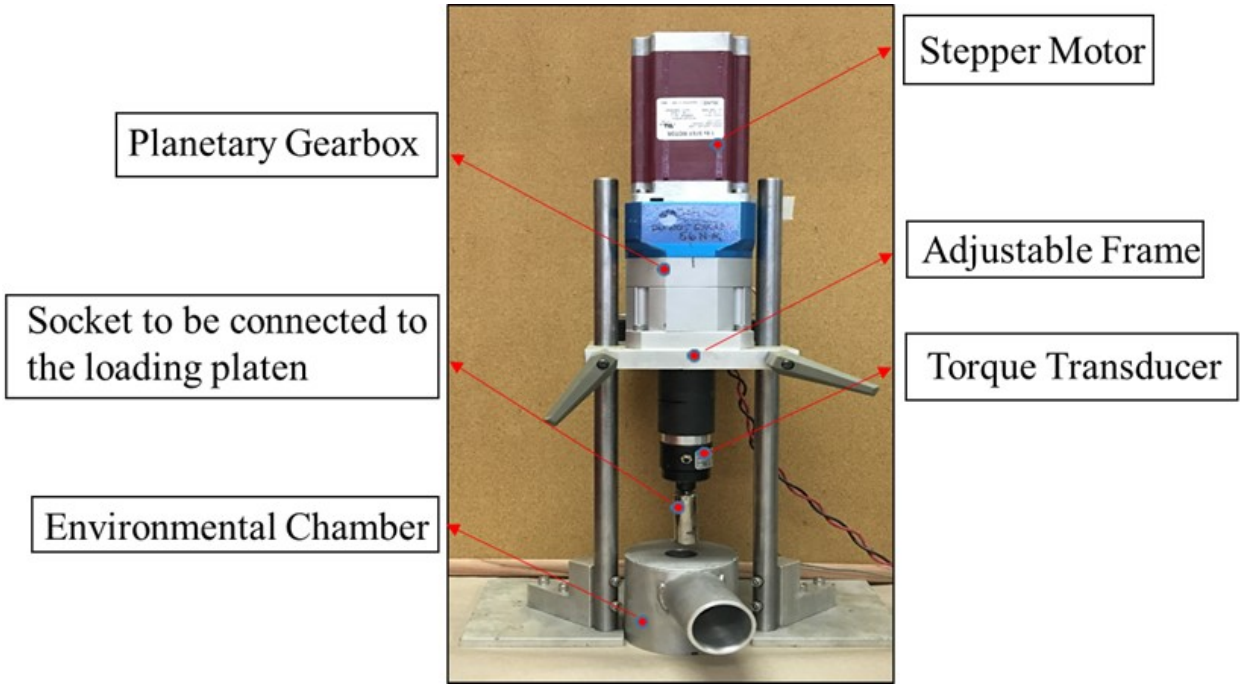

Figure 6.1: OFTT device

6.5.2.2 Software

Control Software

The control software is a GUI written in Laboratory view and allows the operator to enable the stepper, change the direction of rotation as well as the rotational speed. The desired rotational speed is entered by the operator using the simple on/off toggle switches that allow the operator to enable the stepper or change its direction of rotation.

Data Acquisition Software

The data acquisition software is a GUI written in LabVIEW and allows the operator to specify the proper conversion factor for the torque sensor voltage into physical units as well as the data acquisition scan rate and the name of the data output file on the hard drive. A real time plot is also provided during the tests allowing real-time viewing and analysis of the data (Figure 6.2).

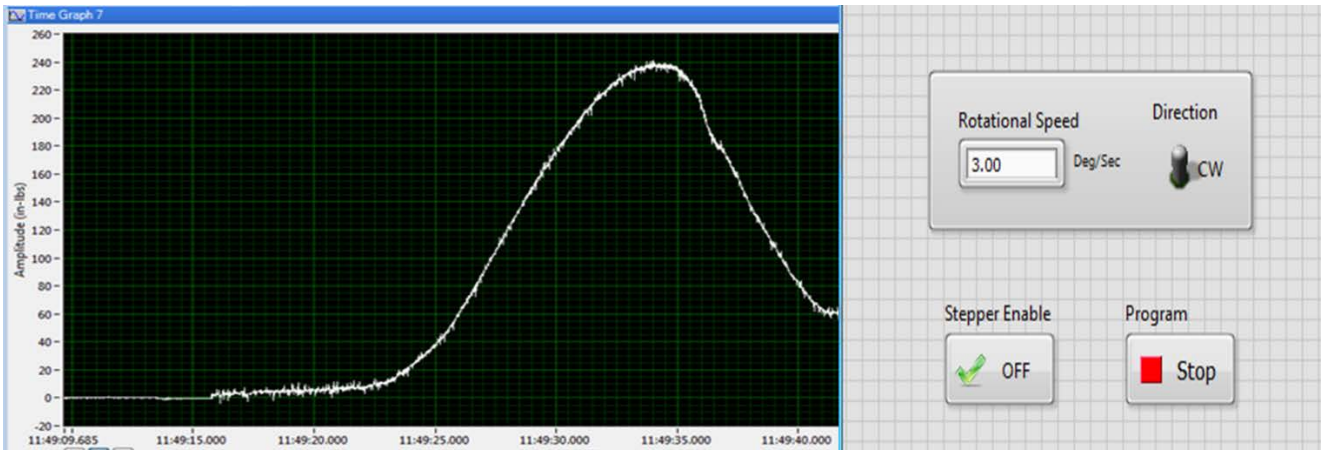

Figure 6.2: OFTT software

6.5.3 Field Test Procedure

The general procedure followed for OFTT field experiments is illustrated with photographs in Figure 6.3. The step-by-step procedure for the OFTT field testing is described as follows:

- Seven months after construction, torque tests were conducted on new asphalt overlays. In order to minimize the effect of spatial variability on laboratory versus in-situ test results comparisons, a total of ten 2.5inch cores were drilled at a distance of one foot from each of the 6inch cores that were used for laboratory shear testing (Figure 6.3a)

- Each of the 2.5-inch diameter cores was drilled to a depth of one inch below the layer interface and at least three locations were drilled on every section (Figure 6.3b).

- After drying the sample area by using a vacuum and blower (Figure 6.3c), a fast setting epoxy mix was used to glue the platen to the cored sample surface (Figure 6.3d).

- Weight was applied for one hour to cure and strengthen the contact surface between the loading platen and core sample (Figure 6.3e).

- Multiple platens were glued to be able to conduct several experiments in a short period of time (Figure 6.3f).

- A thermometer, temperature control box, and portable heat gun were used to maintain/regulate the temperature at 25^{o}C (Figure 6.3g).

- The OFTT experiment was performed to measure the peak torque stress (strength) at the interface between pavement layers (Figure 6.3h).

- Figure 6.3i shows the failure interface after performing the OFTT test. It can be observed that no shear bands were formed on the sample during the test and the maximum measured torque can be expected to provide the actual strength of the tack coat bond.

- After obtaining the peak torque strength for each sample, the measured torque strength (Nm) was converted to OFTT shear strength (kPa) using the equation given below *(Muslich 2009)*:

$$\tau = \frac{12M \times 10^6}{\pi D^3} \quad \textbf{(6.1)}$$

Where;

τ is the interlayer shear strength (OFTT shear strength) (kPa);
M is the peak torque at failure (N.m), and
D is the diameter of the core (mm).

Figure 6.3: General procedure followed for OFTT field experiments

6.5.4 Laboratory Shear Testing

The laboratory shear tests were conducted in accordance with the AASHTO TP114 (2015) specification. Laboratory shear test results were considered as the reference data (ground truth) to evaluate the effectiveness of OFTT results. Details of the laboratory shear test procedure are described in Section 3.3.3. At least three six inch diameter cores from each section were drilled and taken to the OSU pavement laboratory for shear testing.

6.6 RESULTS

Figure 6.4 shows the comparison of results that were obtained by OFTT and laboratory shear tests. The experiments were conducted on sections with two types of emulsions and different application rates. In order to minimize the effect of spatial variability on laboratory vs. in-situ measurement comparisons, all cores for both tests were drilled at a close distance to each other. Results from OFTT and laboratory shear tests for these adjacent cores were compared in Figure 6.4, with the laboratory shear test results being considered as reference bond strength (ground truth data). The peak measured torque was converted to shear strength using equation (6.1). The laboratory shear test results demonstrated that CO1_New_b emulsion with a medium application rate (0.07 gal/yd^2) had the highest shear strength, followed by CO1_CSS 1H_b with a high application rate and CO1_CSS 1H_b with a medium application rate. These results were similar to that of the OFTT shear test results. From Figure 6.4, it can be observed that the correlation

between the OFTT test results and laboratory shear strength test results is statistically significant with a coefficient of determination (R^2 value) of 0.6544. It should be noted that for the first field OFTT experiment, the research team had problems in setting up (leveling) the portable core drill to prepare the first 2.5 inch core. For this reason, result from the first core is not presented in Figure 6.4.

Figure 6.5 illustrates the correlation between the measured strength averages from all cores in one section for both OFTT and laboratory shear strength tests. At least three replicate tests were conducted per section for both OFTT and laboratory shear strength experiments. A high correlation (with an R^2 of 0.972) was observed between the average section results from both tests.

It should be noted that parameters such as stiffness below and above the interface, thickness of the layers, material properties, and a limited number of tests can increase the variability in test results. Climate, traffic loads, and non-uniform application of tack coats during construction can also lead to non-uniformity and poor bonding, which results in increased test results' variability. The impact of test results variability on measured ISS can be reduced by increasing the number of replicate tests in the field.

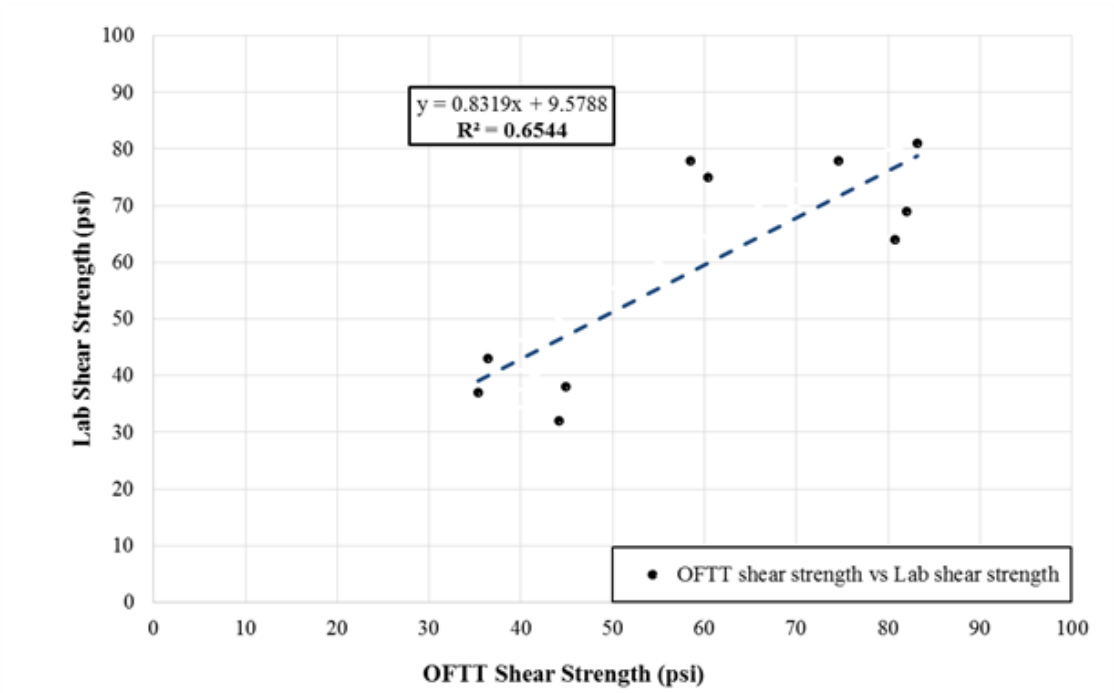

Figure 6.4: Correlation between OFTT shear strength (psi) and laboratory shear strength (psi)

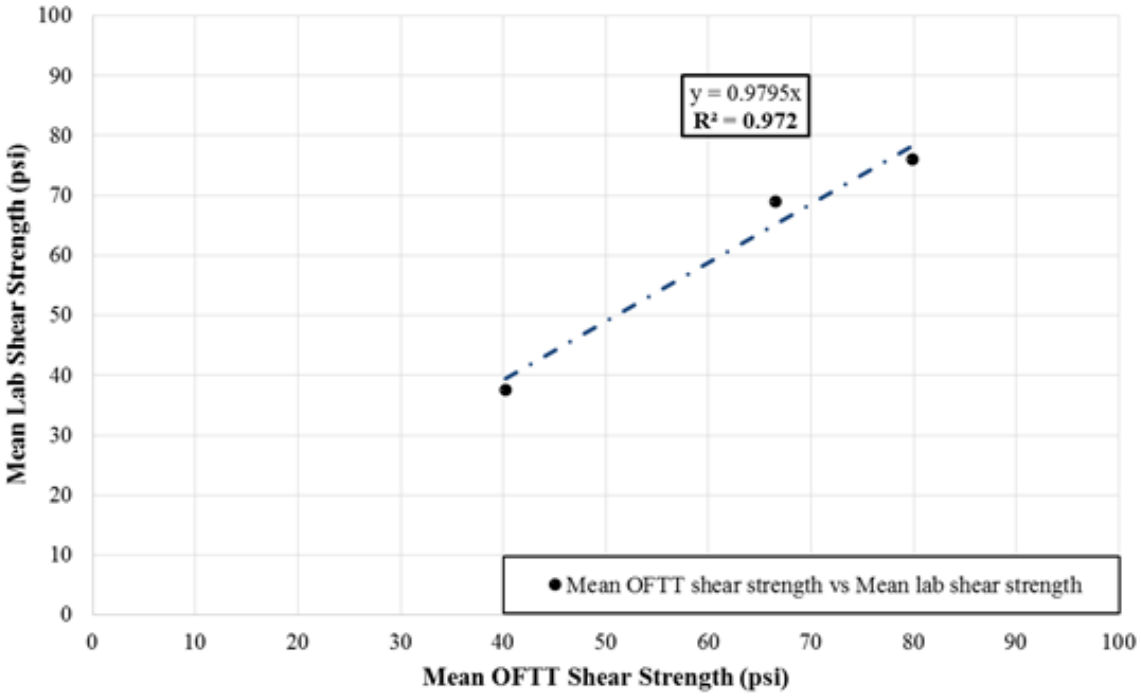

Figure 6.5: Correlation between average OFTT shear strength (psi) vs. average laboratory shear strength (psi)

6.7 SUMMARY AND CONCLUSIONS

In this study, a low cost, practical, and less destructive field test device, the Oregon Field Torque Tester (OFTT), is developed to evaluate the long-term post-construction tack coat performance of pavement sections. Correlations between OFTT field test results and the results of laboratory shear tests conducted with cores taken from the field were investigated to determine the effectiveness of the OFTT. The peak torque values measured by the OFTT were observed to be highly correlated with the measured laboratory shear strengths. The OFTT shear strength values calculated by using the torque test results and a theoretical equation were determined to be close to the measured laboratory shear strengths.

The new technology allows for a more practical test method and is less destructive compared with the typical laboratory shear test. Correlation between the OFTT test results and laboratory shear strength test results was observed to be statistically significant with a coefficient of determination (R^2 value) of 0.6544. When the correlation between the measured strength averages from all cores in one section for both OFTT and laboratory shear strength tests were investigated, a significantly higher correlation (with an R^2 of 0.972) was observed. These strong correlations suggest that OFTT can be an effective, low-cost, less destructive, and practical technology to monitor long-term in-situ bond strength.

Both laboratory shear and OFTT tests yielded the same conclusion, which is that the CO1_New_b emulsion with medium application rate (0.07 gal/yd^2) had the highest shear strength among the three residual application rates. This was followed by CO1_CSS 1H_b with a high application rate and CO1_CSS 1H_b with a medium application rate.

6.8 FUTURE WORK

The following future work is required to improve the OFTT and start using it for long-term tack coat performance monitoring:

- Conduct additional experiments and identify practicality issues to improve the OFTT.
- Develop a wireless system to allow more practical testing. The wireless system could be developed by creating a tablet application that allows for the control of the OFTT device wirelessly.
- Conduct more experiments on thin asphalt layers to investigate the effectiveness of the OFTT device on thin overlay sections.
- Conduct tests at different temperatures to determine the effect of temperature on bond strength and test results' variability.

7.0 DEVELOPMENT OF A WIRELESS FIELD TACK COAT TESTER TO EVALUATE IN-SITU TACK COAT PERFORMANCE

7.1 INTRODUCTION

In this part of the study, Oregon Field Tack Coat Tester (OFTCT) was developed by using the Louisiana Tack Coat Quality Tester (LTCQT) device as a reference in order to create a practical method and test system to evaluate and improve the long-term tack coat performance. The OFTCT system was developed to predict the long-term performance of tack coat bonds based on the results of tests conducted during construction. In addition, the OFTCT device was used to evaluate the impact of pavement surface cleanliness before tack coat application on bond strength. Wireless sensors installed on the OFTCT significantly improved the mobility and practicality of the device in the field. In order to reduce the tack coat's curing time in the field and control temperature during testing, an adjustable heat gun, and environmental chamber were developed. The results indicated that the new temperature control system resulted in a 12% reduction in measurement variability. The results further revealed that using the new heating system provided consistent and reliable temperature control, and prevented excessive heating of the tacked surface. It was also determined that the OFTCT can be successfully utilized in the field as a test to quantify the cleanliness of the pavement surfaces before tack coat application. The correlation between OFTCT and laboratory shear test results is determined to be statistically significant ($R^2 = 0.5189$). However, more field experiments need to be conducted to implement it as a test to predict in-situ interlayer shear strength (ISS). It should be noted that OFTCT was able to identify the tack coat type with the highest ISS.

7.2 CURRENT TECHNOLOGIES

Several research studies were conducted in order to develop an in-situ test method to investigate the bonding characteristics of different tack coat types. Texas pull-off, Torque bond, and LTCQT tests are the major devices developed for tack coat performance evaluation. Texas pull-off, Torque bond, and LTCQT test methods are described in Sections 2.3.1.4, 2.3.1.5, 2.3.1.6, respectively.

7.3 CHALLENGES AND PROPOSED SOLUTIONS

The prior results from the Texas pull-off tests indicated that the presence of dust on the pavement surface before tack coat application results in lower bond strengths *(Tashman et al. 2006)*. In our study, proof-of-concept testing was conducted at the OSU parking lot to determine the possibility of using OFTCT as a quality control (QC) and quality assurance (QA) test during construction to evaluate the degree of cleanliness of pavement surfaces before tack coat application. The developed procedure is expected to provide a method to quantify pavement surface cleanliness before tack coat application, improve bond strength, and increase pavement life.

In addition, research showed that using an infrared reflective heating lamp in the field results in less control of the temperature during the field tests and a significant increase in the variability of measured tack coat bond strength. This was due to the difficulty of controlling the tacked surface temperature at the softening point temperature during the tests and exposure to excessive heating. In this study, an adjustable heat gun and an environmental chamber were developed to maintain a steady temperature during the field tests.

The OFTCT device was developed at Oregon State University. A user-friendly software and wireless sensors (controlled via a tablet computer) were used to maintain a constant displacement rate and accurately control the movement of the loading platen. These contributions improved the reliability and repeatability of the experiments and enhanced the practicality of the OFTCT in the field. Finally, the development of the OFTCT device was very economical compared to the cost of the current technologies. The device gave acceptable and reliable results; hence, it can be adopted as a QC/QA test to evaluate the cleanliness of the pavement surface before tack coat application and predict the long-term performance of tack coats in the field.

7.4 MATERIALS AND METHODS

7.4.1 Tack Coat Types and Tested Sections

OFTCT experiments were conducted on all 9 field test sections given in Table 3.1. Tests were conducted during construction after tack coat application. Four to six replicate experiments were conducted on every section to reduce the impact of spatial variability on calculated average strength values.

7.4.2 OFTCT Device

7.4.2.1 Hardware

The main device has the following components (Figure 7.1):

- The load cell (S-shape) was attached with three displacement transducers (pots) to measure the displacement rates of the very bottom plate. The average of the readings was automatically calculated to ensure that the displacement rate is applied accurately.

- Upper plate, which was used as a reference plate to measure the vertical displacement.

- Stepper modder, which creates the up and down movement. It was attached to power the phase of the stepper (Electric sensor for load and displacement).

- Frame with three adjustable legs, which were used to level the device.

- Loading platen, which was used to provide a proper contact surface between the glued circular foam and the tacked surface.

- Moveable loading cells to provide sufficient resistance against the tensile forces.
- Sensor controller device (wireless data acquisition) to wirelessly transfer the collected data (load and time) to the computer and control the device.
- An environmental chamber and exhaust pipe were developed to maintain a constant temperature.

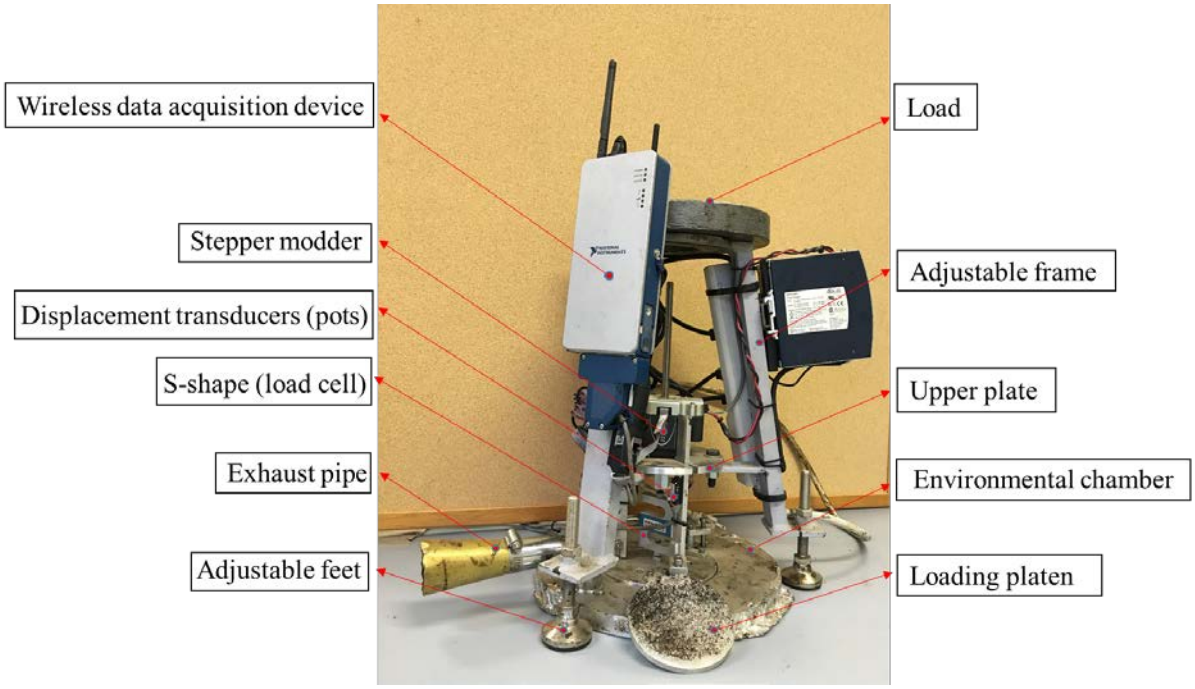

Figure 7.1: OFTCT device

7.4.2.2 Acquisition Software

The developed software was designed to collect data from the OFTCT (Figure 7.2). The software allowed the users to change the displacement rate, control the device, deliver graphical results, and collect data transferred from the data acquisition system.

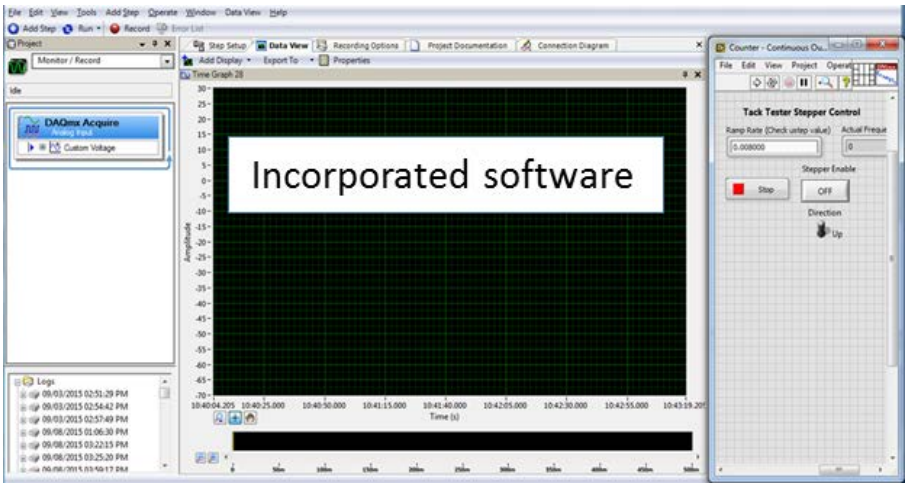

Figure 7.2: Developed software to control the OFTCT and collect data.

7.4.2.3 Prototype Version

The prototype version of the OFTCT device was developed at OSU by using the specifications of the LTQCT (Figure 7.3a). Also, several types of foams for the contact surface were evaluated and a high-density polyethylene foam was found to give the best adhesion among all the assessed materials. The prototype version of the OFTCT device was used to conduct all field experiments during construction. The reliability and repeatability of the test results were controlled using a control system and electronic sensors to ensure that the target displacement rate was applied accurately. The prototype version of OFTCT tester provided accurate displacement rates after being calibrated. A user-friendly software was developed to control the device and collect test data. The prototype OFTCT was connected to a computer using a cable. Difficulty in the movement of the wired OFTCT tester in the field was observed, which resulted in practicality issues such as reduced mobility and increased testing time. Using an infrared reflective heating lamp also resulted in excessive heating of the applied tack coat material and resulted in high test results' variability.

7.4.2.4 Wireless Version

Several modifications were implemented in the new OFTCT device to overcome some technical issues that were observed in the prototype version of the OFTCT device (Figure 7-3b). The mobility and practicality issues were solved by installing a wireless acquisition and control system to facilitate the movement and the operation of the OFTCT device. Development of a user-friendly software also reduced the testing time and provided accurate results. Furthermore, the variability of the test results was reduced by developing an environmental chamber with an adjustable mobile heat gun to control the temperature of the tacked surface during testing. A procedure was then developed to determine the optimum curing time for the specified emulsion and determine the reasonable contact time between the loading platen and the tacked surface. Figure. 3b illustrates the new version of the OFTCT device.

(a) **(b)**

Figure 7.3: system improvements (a) OFTCT prototype version (b) OFTCT wireless version.

7.4.3 OFTCT Test Procedure

Several types of emulsions and residual application rates were applied over milled and overlay surfaces. The selected site work was divided into three locations and each location was separated into three sections (see section 3.3.1). A specified emulsion type and a predetermined application rate were applied to all sections. Table 3.1 shows the application rates, pavement surface types, and tack coat types for all sections. After applying the tack coats, the OFTCT device was used to conduct replicate experiments on the milled and overlay surfaces. In addition, several experiments at Oregon State University's (OSU) laboratory and parking lot were performed to develop a test procedure for the OFTCT device. The procedure for operating the OFTCT device is given as follows (Figure 7.4):

- Circular pieces of high-density thick foam were cut to approximately four inches in diameter.
- The circular foam was then glued to the loading platen using a fast setting high bond strength glue.
- A proper amount of time was allowed for the glue to cure, to be able to attach the loading platen to the load frame (Figure 7.4a).
- After the tack coat application, random locations were selected within the section to conduct the experiments.
- The emulsion was heated for eight minutes at the specified temperature to evaporate water component in the tack coat (Figure 7.4b).
- 80 lb weight was placed on top of the frame to provide enough resistance against the tensile force (Figure 7.4c).

- The loading platen was lowered down, and a compressive load of 60 lbs was applied for three minutes using the developed software (Figure 7.4d).

- A constant displacement rate of 0.008 in/sec was applied to pull the loading platen up, and the maximum tensile stress (tensile strength) applied to break the bond was recorded. Figure 7.4e shows the pavement surface after a field experiment. Figure 7.4f shows a typical test result from a field experiment.

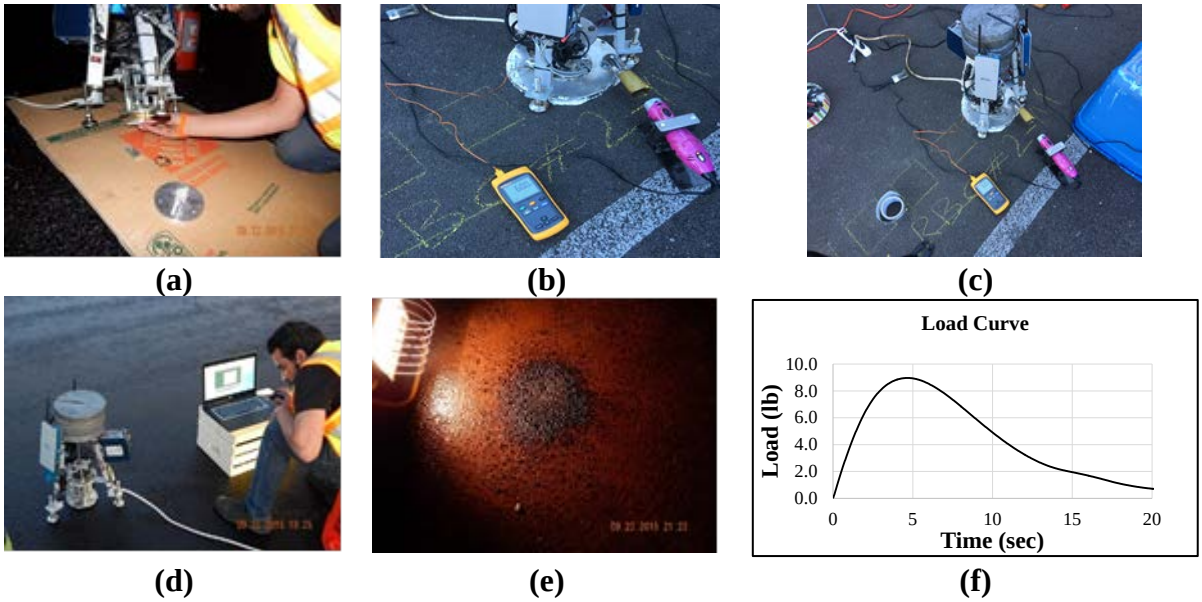

Figure 7.4: General procedure followed for OFTCT field experiments

7.4.4 OFTCT Cleanliness Experiments

Proof-of-concept testing was conducted at the OSU parking lot to determine the possibility of using OFTCT as a quality control (QC) and quality assurance (QA) test during construction to evaluate the degree of cleanliness of pavement surfaces before tack coat application. To determine the impact of cleanliness on measured tensile strength, three control experiments were conducted on the pavement surface cleaned by sweeping and washing. CO1_CSS 1H_b emulsion at a medium application rate (0.07 gal/yd^2) was used for testing. Six-inch by six-inch squares were drawn on the pavement (Figure 7.5a) and calculated application rate was applied using a paintbrush (Figure 7.5b). To be able to determine the effect of cleanliness on the bond strength, again CO1_CSS 1H_b emulsion was applied at a medium application rate after applying the dust. A 0.07 lb/ft^2 of dust was applied using a paintbrush on a six by six- inch square (Figure 7.5d) before applying the specified emulsion. Average tensile strength from the locations with and without dust was compared to evaluate the impact of cleanliness on bond strength.

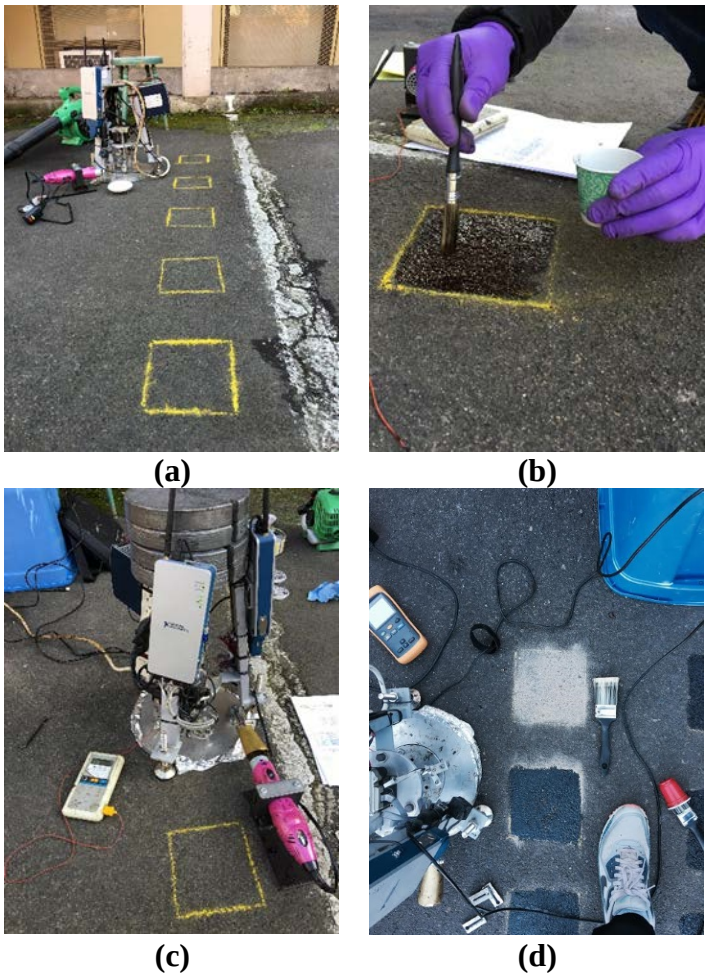

Figure 7.5: Step-by-step procedure to determine the effect of dust on tensile bond strength

7.4.5 Temperature Control System to Reduce Test Results' Variability

A new temperature control system was developed to reduce measurement variability. Several replicate tests with CO1_CSS 1H_b emulsion at a medium rate were conducted. Six-inch by six-inch squares were drawn on a steel plate surface, and a medium application rate (0.07 gal/yd^2) of CO1_CSS 1H_b emulsion was applied on the squares using a paint brush. The new temperature system was used to break the emulsion and control temperature during testing. To determine the contribution of using the new temperature control system to reduce test results' variability, results of the tests conducted with an adjustable heat gun with the aluminum chamber (new heating system) was examined and compared with the standard infrared reflective lamp. After spraying the emulsion, both the infrared reflective lamp and the adjustable heat gun were used to break the emulsion and control the temperature on six-inch by six-inch test squares for eight minutes. After eight minutes, the loading platen was lowered down to come into contact with the tacked surface for three minutes to create an adequate contact surface between the loading platen and the tacked surface. Then, the loading platen was raised upward and the tensile strength of the tack coat was measured. Using an adjustable heat gun heating system (Figure 7.6) allowed for

accurate temperature control and provided an adequate means to prevent the tacked surface from the excessive heating.

Figure 7.6: A new temperature control system for OFTCT to reduce measurement variability

7.4.6 Laboratory Shear Testing

The laboratory shear tests were conducted in accordance with the AASHTO TP114 (2015) specification. Laboratory shear test results were considered as the reference data (ground truth) to evaluate the effectiveness of OFTT results. Details of the laboratory shear test procedure are described in Section 3.3.3.

Ten six inch diameter cores from each section were drilled and taken to the OSU pavement laboratory for shear testing.

7.5 RESULTS

7.5.1 Comparison of Test Results' Variability for the Standard and New Heating Systems

Figure 7.7 shows the results of the tests conducted by using an adjustable heat gun with the aluminum chamber (new system) and infrared reflective heating lamp (standard system). It can be observed that using the new temperature system provided a reduction of approximately 12% in total measurement variability when compared with the infrared reflective heating lamp. However, using the new system resulted in lower strength values. The reduction in the measurement variability helps to provide a more reliable evaluation of the tack coat performance. In addition, results revealed that using the new heating system provided a more accurate control of the test temperature. This contribution is expected to enhance the reliability of the test results.

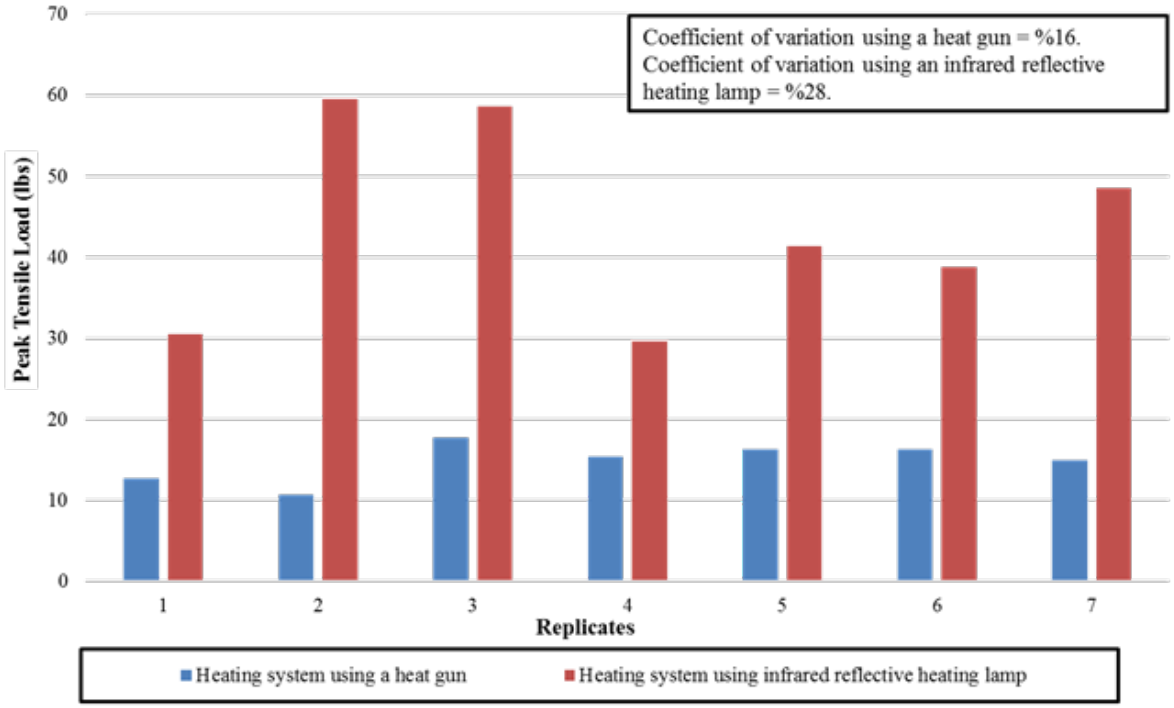

Figure 7.7: Heat gun vs. infrared reflective heating lamp

7.5.2 Cleanliness Experiments

Results of the cleanliness experiments showed that having dust on the pavement surface before tack coat application created a significant reduction (about 10 to 20 %) in the measured tensile strength of the tested tack coat (CO1_CSS 1H_b) (Figure 7.8). The applied dust breaks the bond between the pavement surface and the applied tack coat and creates a lower bond strength. The same experiment can be conducted in the field during construction to evaluate the cleanliness of the pavement surface before tack coat application. After milling and sweeping the pavement surface during construction, one side of the pavement can be cleaned by washing to conduct control experiments. Test results from the actual pavement surface (without further cleaning) can be compared with the results from the cleaned surface to evaluate the cleanliness of the pavement surface. An allowable percentage reduction in tensile strength (should be less than 10%) can be set to use this experiment as a QC/QA tool during construction to evaluate cleanliness. If the measured percent reduction in strength is higher than the allowable value, further sweeping and cleaning can be done to increase the bond strength.

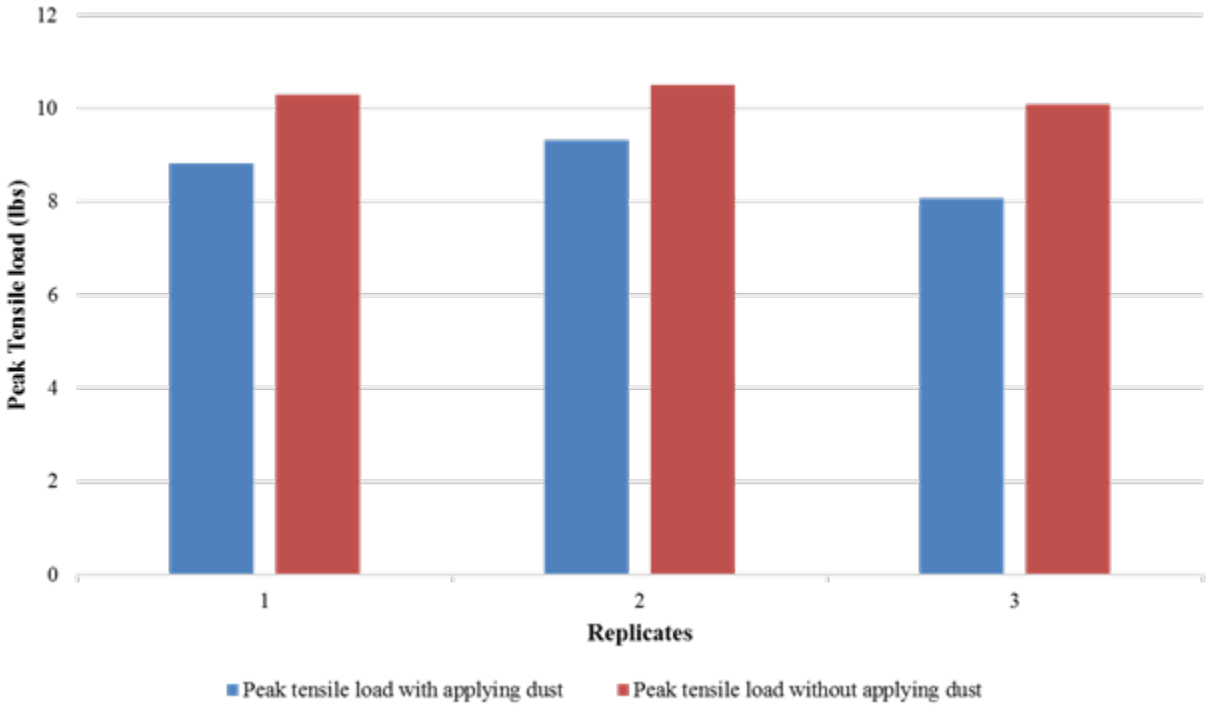

Figure 7.8: The effect of dust on peak tensile load at a medium application rate

7.5.3 Correlation Between the OFTCT and Laboratory Shear Test Results

The correlation between OFTCT and laboratory shear test results for the milled surface tests was observed to be weak due to the impact of milled surface texture on laboratory shear test results. Since OFTCT measures the tensile strength of the tack coat, the impact of texture on bond strength is not captured. However, it should be noted that several studies in the literature (See section 2.0) suggested that shear mode is the major factor controlling bond failures in the field.

Average measured OFTCT strengths and average shear strengths measured from field cores from all 9 test sections are shown in Figure 7.9. It can be observed that the correlation between OFTCT and laboratory shear test results is not statistically significant with a coefficient of determination of 0.1427. However, when the results from the section sprayed with the contractor's distributor truck, Location 3-Overlay, were excluded from the comparisons, the correlation between OFTCT and laboratory shear test results becomes statistically significant with a coefficient of determination of 0.5189 (See Figure 7.10). Since the contractor's distributor truck was not able to apply tack coat uniformly (See Figure 3.12), OFTCT results from this section had a very high variability, which resulted in low correlations. It should be noted that OFTCT was able to identify the tack coat type with the highest ISS. The lower correlation for OFTCT (R^2 = 0.5189) when compared to OFTT correlations (R^2 = 0.972) can be related to the following two factors:

- Different loading mechanisms: Tensile loading mechanism for the OFTCT is entirely different from the shear loading mechanism. In addition, tensile loads for the OFTCT are applied directly on the tacked surface while the shear loads are applied between

the two layers of pavement after construction. Thus, the impact of surface texture on ISS cannot be directly measured by OFTCT.

- The use of the old heating system for the field tests might have increased the variability in the OFTCT results since it was not possible to accurately control the temperature during the experiments. In addition, the excessive heating of the tacked surface might have created unreliable test results. The new temperature control system developed in this study is expected to minimize these problems.

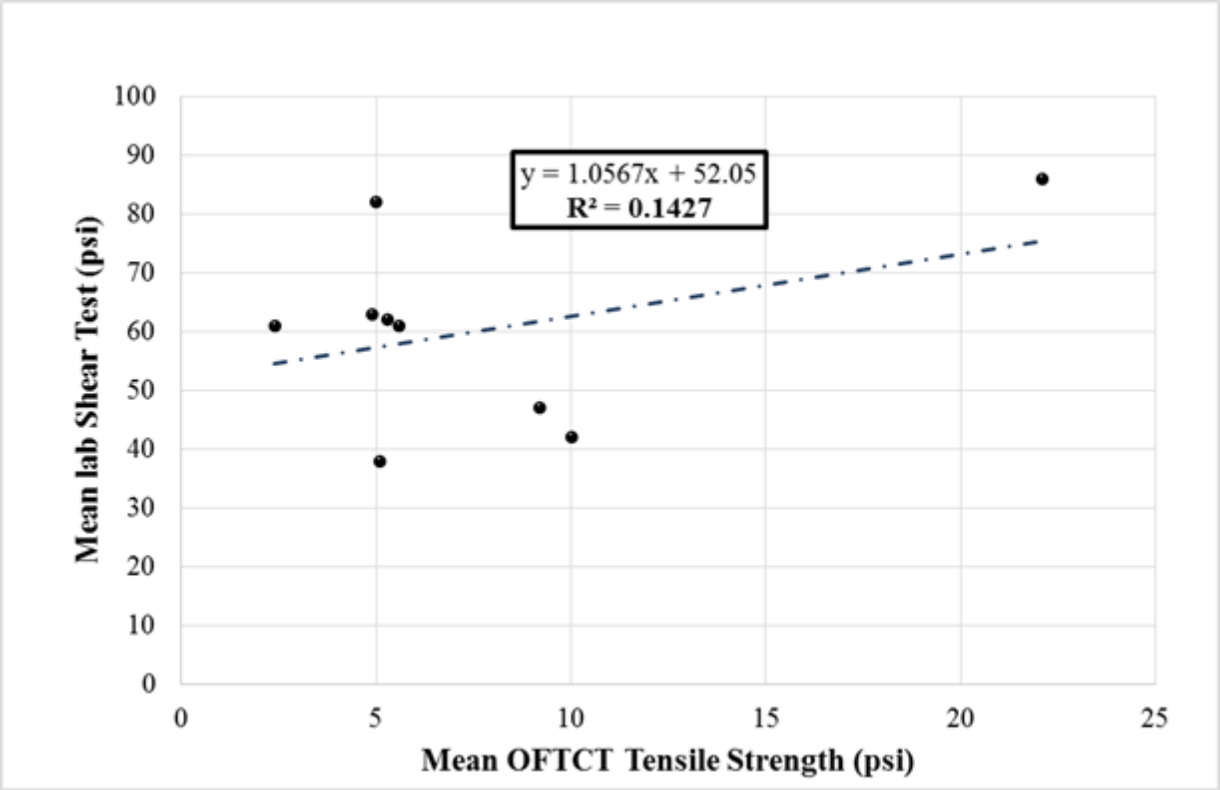

Figure 7.9: Comparison of mean OFTCT tensile strength and mean laboratory shear strength measured on overlay surfaces

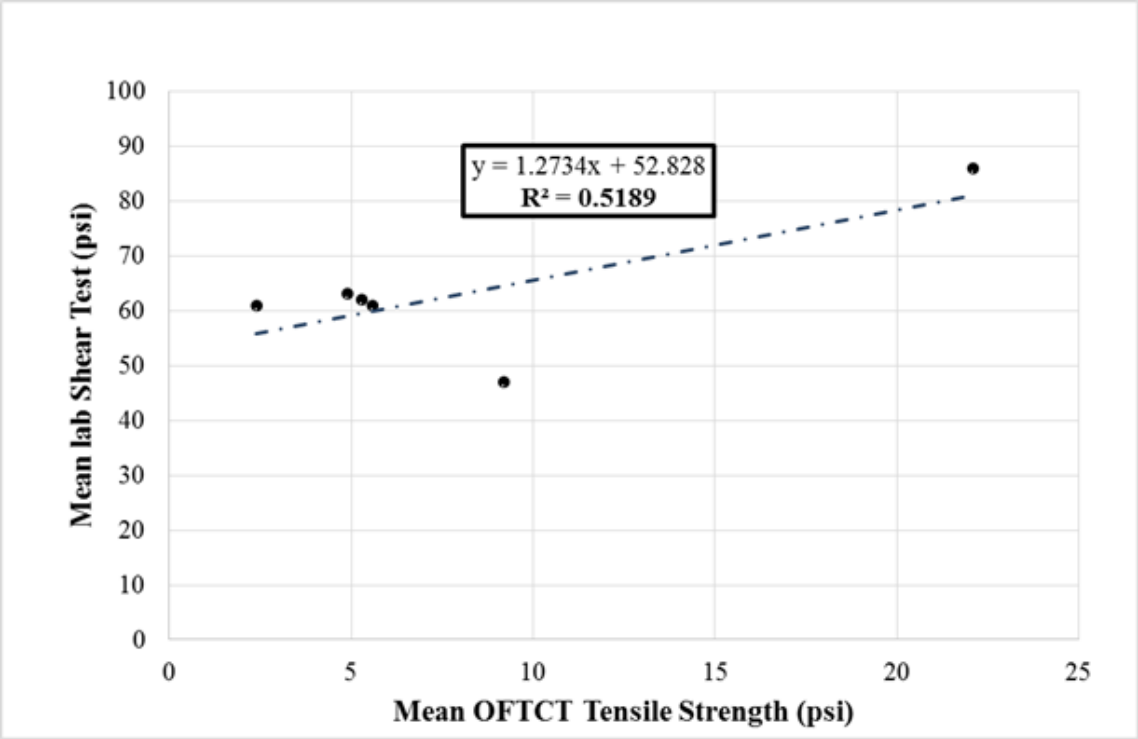

Figure 7.10: Comparison of mean OFTCT tensile strength and mean laboratory shear strength measured on overlay surfaces after excluding the results for Location 3-Overlay (the section with non-uniform tack coat application)

7.6 SUMMARY AND CONCLUSIONS

In this part of the study, Oregon Field Tack Coat Tester (OFTCT) was developed by using the Louisiana Tack Coat Quality Tester (LTCQT) device as a reference in order to create a practical method and test system to evaluate and improve the long-term tack coat performance. The OFTCT system was developed to predict the long-term performance of tack coat bonds based on the results of tests conducted during construction. In addition, the OFTCT device was used to evaluate the impact of pavement surface cleanliness before tack coat application on bond strength. Wireless sensors installed on the OFTCT significantly improved the mobility and practicality of the device in the field. In order to reduce the tack coat's curing time in the field and control temperature during testing, an adjustable heat gun and environmental chamber were developed. The results indicated that the new temperature control system resulted in a 12% reduction in measurement variability. The results further revealed that using the new heating system provided consistent and reliable temperature control, and prevented excessive heating of the tacked surface. It was also determined that the OFTCT can be successfully utilized in the field as a test to quantify the cleanliness of the pavement surfaces before tack coat application. The correlation between OFTCT and laboratory shear test results is determined to be statistically significant ($R^2 = 0.5189$). However, more field experiments need to be conducted to implement it as a test to predict in-situ interlayer shear strength (ISS). It should be noted that OFTCT was able to identify the tack coat type with the highest ISS.

7.7 FUTURE WORK

The following future work is required to improve the OFTCT and start using it for long-term tack coat performance monitoring and cleanliness evaluation:

- Conduct more experiments with the new wireless version of the OFTCT and the new temperature control system on milled and overlay surfaces to evaluate the impact of system improvements on test results.

- Cleanliness experiments should be conducted in the field during construction to determine the effectiveness of this test as QC/QA tool to increase bond strength.

- After conducting several field experiments with the OFTCT and using the test results from this study, a minimum acceptable tensile strength limit should be specified to determine the quality of the tack coat used during construction.

- The OFTCT device should be evaluated by conducting tests with several different tack coat types to create a better understanding of the effectiveness of OFTCT as a QC/QA tool to assess long-term tack coat performance.

•

8.0 SUMMARY AND CONCLUSIONS

This research study presents a comprehensive field investigation consisting of field and laboratory testing, 3D finite element modeling, field coring, and construction sampling of tack coats used in Oregon. Within the study, two new tack coat materials from two companies were, for the first time, evaluated for their performance. Field coring was completed at two different time increments, as well as two travel lines (wheel path and center of the lane), to capture the effect of traffic loading and environmental factors on interlayer shear strength. Recommendations for the most efficient application rate along with interlayer shear strength (ISS) prediction equations based on rheological properties were developed.

In this study, tools and methods to reduce tracking were also developed. Weight evaporation experiments were conducted by varying the application rate, air temperature, wind speed, and tack coat type to determine the curing time and the factors that influence it. Tracking was also evaluated by developing a wheel-tracking device that can be used in the field as a visual tool or by collecting weight data via the removable rubber "tires". Data from weight evaporation tests were used to create a linear regression model to predict in-situ curing times and develop a smartphone app (for Android and IOS) using the created model. Prediction of in-situ curing times and not allowing construction vehicles before curing will reduce tracking and improve tack coat bond performance.

In this study, the Oregon Field Torque Tester (OFTT) and the wireless Oregon Field Tack Coat Tester (OFTCT) were also developed to evaluate the long-term post-construction tack coat performance of pavement sections. Correlations between the results of these two field tests and the results of lab shear tests conducted with cores taken from the field were investigated to determine the effectiveness of these new technologies. Conclusions based on the experimental and analytical findings, products developed, recommendations, and additional research are discussed in the following sections.

8.1 CONCLUSIONS

The major conclusions drawn from the results of this study are:

Tack Coat Rheology and Performance

1. A significant positive correlation between pavement surface texture and interlayer shear strength exists. The influence of surface texture on measured ISS limited results to be confined to overlay pavement surfaces only when comparisons of tack coat materials were to be made regarding performance.

2. The results of statistical analysis of the ISS of cores taken from different travel lines (wheel-path and center of travel lane) show that there is no difference in interlayer shear strength between the two transverse locations for an initial set of cores taken three months after construction. On the other hand, the difference in interlayer shear

strength for the milled and overlay (top and bottom) interfaces is statistically significant.

3. Tack coat materials with higher viscosities exhibit higher softening point temperatures and lower penetration values. For overlay pavement surfaces in this study, positive correlations between rheological test results and interlayer shear strength of field cores taken three months after construction are presented.

4. Traffic loading and environmental factors can create significant reduction in interlayer shear strength.

5. Large consistency issues are present in tack coat application rates via distributor trucks, and there is a need for QC/QA to control tack coat application rates and methods during construction.

Tracking

6. From the laboratory curing time experiments, CO1_New exhibited the longest curing time on all texture types;

7. Regression analysis revealed that mean texture depth (MTD) did not have a significant effect on curing time;

8. Decreasing application rates and increasing wind speeds and temperature will result in reduced curing time;

9. Tack coat tracking, the amount picked up, decreases with curing;

10. Milled surfaces exhibit more tracking, due to tack coat accumulating in grooves of texture, when compared to overlay surfaces;

11. Wheel tracking device can be effectively used to determine tack coat curing time during construction.

Effects of Structural Characteristics on Tack Coat Performance

12. Temperature is the most significant factor that affects critical tack coat shear strain while overlay thickness also had a significant effect. On the other hand, the effects of existing layer thickness, AB layer thickness, and subgrade stiffness are insignificant when compared to the effects of overlay thickness and temperature. This result suggests that tack coat quality and spraying rates must be modified depending on the climate and overlay design thickness.

13. Increasing overlay thickness shifts the critical shear strain location from the tack coat area (OL and AC interface) to mid-overlay area. This phenomenon creates a significant reduction in critical tack coat shear strain with increasing overlay thickness. For this reason, tack coat resistance and strength become more critical for thin overlays.

14. Increasing temperature from 86^{o}F to 113^{o}F results in a significant increase in shear strain. This result suggested that at high summer temperatures tack coat bond failures are likely to occur.

Oregon Field Torque Tester (OFTT)

15. A low cost, practical, and less destructive field test device, the Oregon Field Torque Tester (OFTT), is developed to evaluate the long-term post-construction tack coat performance of pavement sections. Results of field and lab experiments showed that OFTT is an effective test to characterize in-situ bond strength and evaluate long-term bond performance.

Oregon Field Tack Coat Tester (OFTCT)

16. The Oregon Field Tack Coat Tester (OFTCT) is developed to predict the long-term tack coat performance during construction and quantify the cleanliness of the pavement surfaces before tack coat application. The correlation between OFTCT and lab shear test results is determined to be statistically significant. It was also determined that the OFTCT can be successfully utilized in the field as a test to quantify the cleanliness of the pavement surfaces before tack coat application.

8.2 MAJOR RESEARCH PRODUCTS DEVELOPED IN THIS STUDY

The major research products developed in this study are given as follows:

1. Recommended application rates for different tack coat products;

2. A smart phone app for Android and IOS to predict tack coat curing time to be used to reduce tracking;

3. A wheel tracking device to evaluate tracking during construction;

4. The Oregon Field Torque Tester (OFTT) to evaluate and monitor the long-term tack coat performance of pavement sections after construction;

5. The Oregon Field Tack Coat Tester (OFTCT), to predict the long-term tack coat performance during construction and quantify the cleanliness of the pavement surfaces before tack coat application; and

6. A 3D finite element model to determine the impact of structural properties on tack coat performance.

8.3 RECOMMENDATIONS AND FUTURE WORK

8.3.1 Tack Coat Rheology and Performance

The recommended application rates (Table 3.5) should be applied during construction to maximize interlayer shear strength of pavement layers for selected Oregon tack coat materials.

The accuracy and precision of application rates should be measured in the field. Based on the measured application rates, distributor truck should be calibrated to achieve the target application rate. Uniformity of applied tack coat should also be checked during construction. Non-uniform tack coat application can create localized distresses and premature failures.

Results of tack coat rheology and performance investigations in this study provide new insight, but further investigation is required to extend the analysis. In this study, of the six tack coat materials used, only three were used on overlay surface and three on milled surface. For a complete analysis, all tack coat materials should be utilized on both milled and overlay surfaces to be able to make direct comparisons.

It is recommended to take field cores from other sites with similar characteristics and measure the interlayer shear strength (ISS) using the *Asphalt Tack Bond Shear Strength Apparatus.* These results should then be compared with the ISS predicted from measured rheological properties by using the equations developed in this study. This will complement the conclusions from this study and help improve the predictability of the equations.

8.3.2 Tracking

Future studies should conduct testing by comparing the smartphone app predictions with field and laboratory curing times. These comparisons should be used to validate or calibrate the regression model used for app development. In addition, the smartphone app should be utilized alongside the wheel-tracking device in the field and the parking lot to determine whether calculated curing times from the app are close to the wheel-tracking device results.

8.3.3 Effects of Structural Characteristics on Tack Coat Performance

3D viscoelastic finite element model developed in this study should be modified to simulate cases with different bonding levels. In this study, stresses and strains are calculated by assuming that the two asphalt layers are completely bonded (100% bonding level). The change in stresses and strains around tack coats for different percentages of bonding should also be simulated. The impact of bond strength and bonding levels on long-term pavement performance for different climates and traffic levels in Oregon should also be simulated using the software AASHTOWare (also known as MEPDG). Based on the AASHTOWare performance outputs, analysis should be performed to monetize the impact of bond strength on life-cycle costs.

8.3.4 Oregon Field Torque Tester (OFTT)

The following future work is required to improve the OFTT and start using it for long-term tack coat performance monitoring:

- Conduct additional experiments and identify practicality issues to improve the OFTT;
- Develop a wireless system to allow more practical testing. The wireless system could be developed by creating a tablet application that permits for the control of the OFTT device wirelessly;

- Conduct more experiments on thin asphalt layers to investigate the effectiveness of the OFTT device on thin overlay sections; and

- Conduct tests at different temperatures to determine the effect of temperature on bond strength and test results' variability.

8.3.5 Oregon Field Tack Coat Tester (OFTCT)

The following future work is required to improve the OFTCT and start using it for long-term tack coat performance monitoring and cleanliness evaluation:

- Conduct more experiments with the new wireless version of the OFTCT and the new temperature control system on milled and overlay surfaces to evaluate the impact of system improvements on test results;

- Cleanliness experiments should be conducted in the field during construction to determine the effectiveness of this test as a QC/QA tool to increase bond strength;

- After conducting several field experiments with the OFTCT and using the test results from this study, a minimum acceptable tensile strength limit should be specified to determine the acceptability of the tack coat used during construction; and

- The OFTCT device should be evaluated by conducting tests with several different tack coat types to create a better understanding of the effectiveness of OFTCT as a QC/QA tool to assess long-term tack coat performance.

9.0 REFERENCES

AASHTO TP114. *Standard Method of Test for Determining the Interlayer Shear Strength (ISS) of Asphalt Pavement Layers*. American Association of State Highway and Transportation Officials (AASHTO), Washington, D.C., 2015.

ASTM Standard D140. *Standard Practice for Sampling Bituminous Materials*. ASTM International, West Conshohocken, PA, 2015. http://doi.org/10.1520/D0140

ASTM Standard D2995. Standard Practice for Estimating Application Rate of Bituminous Distributors and Residual Application Rate of Bituminous Distributors. ASTM International, West Conshohocken, PA, 2014. http://doi.org/10.1520/D2995-99R09.Copyright

ASTM Standard D36. Standard Test Method for Softening Point of Bitumen (Ring-and-Ball Apparatus). ASTM International, West Conshohocken, PA, 2014. http://doi.org/10.1520/D0036

ASTM Standard D4402. Standard Test Method for Viscosity Determination of Asphalt at Elevated Temperatures Using a Rotational Viscometer. ASTM International, West Conshohocken, PA, 2015. http://doi.org/10.1520/D4402

ASTM Standard D5. Standard Test Method for Penetration of Bituminous Materials. ASTM International, West Conshohocken, PA, 2013. http://doi.org/10.1520/D0005-13.2

ASTM Standard D6997. Standard Test Method for Distillation of Emulsified Asphalt. ASTM International, West Conshohocken, PA, 2012. http://doi.org/10.1520/D0020-03R09.2

ASTM Standard D711. Standard Test Method for No-Pick-Up Time of Traffic Paint. ASTM International, West Conshohocken, PA, 2010. http://doi.org/10.1520/D1849-95R08

ASTM Standard D7175. Standard Test Method for Determining the Rheological Properties of Asphalt Binder Using a Dynamic Shear Rheometer. ASTM International,West Conshohocken, PA, 2015. http://doi.org/10.1520/D7175-15.2

ASTM Standard E965. Standard Test Method for Measuring Pavement Macrotexture Depth Using a Volumetric Technique. ASTM International,West Conshohocken, PA, 2015. http://doi.org/10.1520/E0965-96R06.2

Baumgaertel, M., and H.H. Winter. Determination of Discrete Relaxation and Retardation Time Spectra from Dynamic Mechanical Data. In Rheologica Acta, Vol. 28, 1989, pp. 511–519. http://doi.org/10.1007/BF01332922

Buchanan, S., and M. Woods. Field Tack Coat Evaluator (ATACKer). Publication FHWA/MS-DOT-RD-04-168. Construction Materials Research Center. Starkville: Mississippi State University. 2004.

CalTrans. Paint binder (Tack Coat) Guidelines. Publication CPB 03-1. California Department of Transportation. 2003.

Clark, T.M., T.M. Rorrer, and K.K. McGhee. Trackless Tack Coat Materials: A Laboratory Evaluation for Performance Acceptance. Publication VCTIR 12-R14. Charlottesville, VA, 2012.

Coleri, E., J.T. Harvey, K. Yang, and J.M. Boone. Development of a Micromechanical Finite Element Model from Computed Tomography Images for Shear Modulus Simulation of Asphalt Mixtures. Construction and Building Materials, Vol. 30, 2012, pp. 783–793. http://doi.org/10.1016/j.conbuildmat.2011.12.071

Cortina, A.S. Optimization of In-Situ Tack Coat Application Rate and Installation. Illinois at Urbana-Champaign. 2012.

De Jong, D.L. Computer Program BISAR Layered System Under Normal and Tangential Loads. External Report AMSR 6. Konin Klijke Shell-Laboratorium, Amsterdam, 1973.

Deysarkar, I. Test Set-Up to Determine Quality of Tack Coat. Univeristy of Texas at El Paso. 2004. Retrieved from http://search.proquest.com/docview/305103314

Ferry, J.D. Viscoelastic Properties of Polymers. John Wiley and Sons, 1980.

FPO. Technical Bulletin: Proper Tack Coat Application. Dublin, OH. 2001.

Hachiya, Y., and K. Sato. Effect of Tack Coat on Bonding Characteristics at Interface between Asphalt Concrete Layers. In 8th International Conference on Asphalt Pavements, 1997, pp. 349–362. Retrieved from https://trid.trb.org/view.aspx?id=501638

Hanson, D.I., and B.D. Prowell. Evaluation of Circular Texture Meter for Measuring Surface Texture of Pavements. NCAT Report 04-05. 2004. http://doi.org/10.3141/1929-11

King, G., and R. May. New Approaches to Tack Application. In 83rd Annual Meeting of the Transportation Research Board. Washington, D.C., 2003.

Krebs, R.D., and R.D. Walker. Highway Materials. New York, New York: McGrawHill Inc. 1971.

Lavin, P.G. Asphalt Pavements: A Practical Guide to Design, Production, and Maintenance for Engineers and Architects. New York, New York: Spon Press. 2003.

Leng, Z., I.L. Al-Qadi, S.H. Carpenter, and H. Ozer. Interface Bonding Between Hot-Mix Asphalt and Various Portland Cement Concrete Surfaces. Transportation Research Record: Journal of the Transportation Research Board, No. 2014.Transportation Research Board of the National Academy of Sciences, Washington, D.C., 2008, pp. 46–53. http://doi.org/10.3141/2127-03

Mohammad, L.N., and J. Button. Optimization of Tack Coat for HMA Placement. In National Cooperative Highway Research Program, No. NCHRP 9-40. National Cooperative Highway

Research Program (NHCRP), Transportation Research Board, National Research Council, Washington, D.C. 2005.

Mohammad, L.N., M.A. Elseifi, A. Bae, N. Patel, J. Button, and J.A. Scherocman. Optimization of Tack Coat for HMA Placement. In National Cooperative Highway Research Program, No. NCHRP 712. National Cooperative Highway Research Program (NHCRP), Transportation Research Board, National Research Council, Washington, D.C., 2012.

Muslich, S. Assessment of Bond Between Asphalt Layers. The Univeristy of Nottingham, 2009.

Raab, C., and M.N. Partl. Effect of Tack Coats on Interlayer Shear Bond of Pavements. In 8th Conference On Asphalt Pavements For Southern Africa, 2004, p. 9.

Roffe, J.C., and F. Chaignon. Characterization tests on bond coats: worldwide study, impact, test, and recommendations. In 3rd International Conference of Bituminous Mixtures and Pavements. Thessaloniki. 2002. Retrieved from https://trid.trb.org/view.aspx?id=681964

Sholar, G., G. Page, J. Musselman, P.B. Upshaw, and H.L. Moseley. Preliminary Investigation of a Test Method to Evaluate Bond Strength of Bituminous Tack Coats (with discussion). Association of Asphalt Paving Technologies, Vol. 73, 2004, pp. 771–806. Retrieved from https://trid.trb.org/view.aspx?id=750009

Tashman, L., K. Nam,, and T. Papagiannakis. Evaluation of the Influence of Tack Coat Construction Factors on the Bond Strength Between Pavement Layers. Report No.WCAT 06-002. Report prepared for Washington State Department of Transportation, 2006.

Tayebali, A.A., M.S. Rahman, M.B. Kulkarni, and Q. Xu. A Mechanistic Approach to Evaluate Contribution of Prime and Tack Coat in Composite Asphalt Pavements. No. FHWA/NC/2004-05. North Carolina Department of Transportation Research and Analysis, Raleigh, NC, 2004.

Tran, N.H., R. Willis, and G. Julian. (2012). Refinement of the Bond Strength Procedure and Investigation of a Specification, Report No. NCAT 12-04, Auburn University, 2012.

Tsai, B.-W., V. Kannekanti, and J. Harvey. Application of Genetic Algorithm in Asphalt Pavement Design. In Transportation Research Record: Journal of the Transportation Research Board, No. 1891, Transportation Research Board of the National Academy of Sciences, Washington, D.C., 1891, 2004, pp. 112–120. http://doi.org/10.3141/1891-14

TxDOT. Proper Use of Tack Coat. Texas Department of Transportation, 2001.

USACE. Hot-mix Asphalt Paving Handbook. Washington, D.C.: U.S. Army Corps of Engineers, AASHTO, FAA, FHA, NAPA, APWA, NACE. 2000.

USACE. Bituminous Tack and Prime Coats. In Unified Facilities Guide Specifications U.S. Army Corps of Engineers. 2008, pp. 1-17. http://doi.org/10.1017/CBO9781107415324.004

Walsh, I.D., and J.T. Williams. HAPAS Certificates for Procurement of Thin Surfacing. Highways and Transportation, Vol. 48, Nos. 7-8, 2001, pp. 12–14. Retrieved from https://trid.trb.org/view.aspx?id=715783

West, R.C., J. Zhang, and J. Moore. Evaluation of Bond Strength Between Pavement Layers. In NCAT Report 05-08. National Center for Asphalt Technology. Auburn University, 2005.

Willis, J.R., and D.H. Timm. (2007). Forensic Investigation of Debonding in Rich Bottom Pavement. In Transportation Research Record: Journal of the Transportation Research Board, No. 2040, Transportation Research Board of the National Academy of Sciences, Washington, D.C., 2007, pp. 107–114. http://doi.org/10.3141/2040-12

Wilson, B.T., M.S. Sakhaeifar, M. Yelpale, A. Seo, and S. Shah. Development of Test Procedures to Measure Tracking Resistance of Non-Tracking Tack Coat. Conference of Airfield and Highway Pavements, 2015, pp. 203–214.

Yoo, P.J., I.L. Al-Qadi, M.A. Elseifi, and I. Janajreh. Flexible Pavement Responses to Different Loading Amplitudes Considering Layer Interface Condition and Lateral Shear Forces. International Journal of Pavement Engineering, Vol. 7, No. 1, 2006, pp. 73–86.

APPENDIX A: COMPLETE TESTS RESULTS AND ALL REGRESSION MODELS FOR THE CURING TIME EXPERIMENTS

A .1 TEST RESULTS

Data for each experiment were collected at every ten seconds via a connection from the scale to a computer. Each test was run until the weight of the applied emulsion appeared to be constant. Emulsion set time varies with emulsion type, application rate, and test temperature. It should be noted that tests were conducted in an environmental chamber without simulating the effect of the wind on evaporation. For this reason, measured emulsion set times can be considered to be conservative values. Due to the effect of wind, emulsion set times are expected to be lower at the construction site.

A .1.1 Steel Plates

The results of all 48 steel plate tests are shown in Figure A-1. Figure A-1a, Figure A-1c, and Figure A-1e show the results of the low-temperature tests. Figure A-1b, Figure A-1d, and Figure A-1f show the high-temperature test results. From the plots, it can be observed that emulsion EBS.RBC has a significantly higher water content and longer set time than all other emulsions regardless of the conditions. The emulsion type with the shortest set time cannot be easily observed from Figure A-1but further statistical analysis (Section 4.0) revealed that emulsion EE has the shortest set time when compared to other three emulsion types.

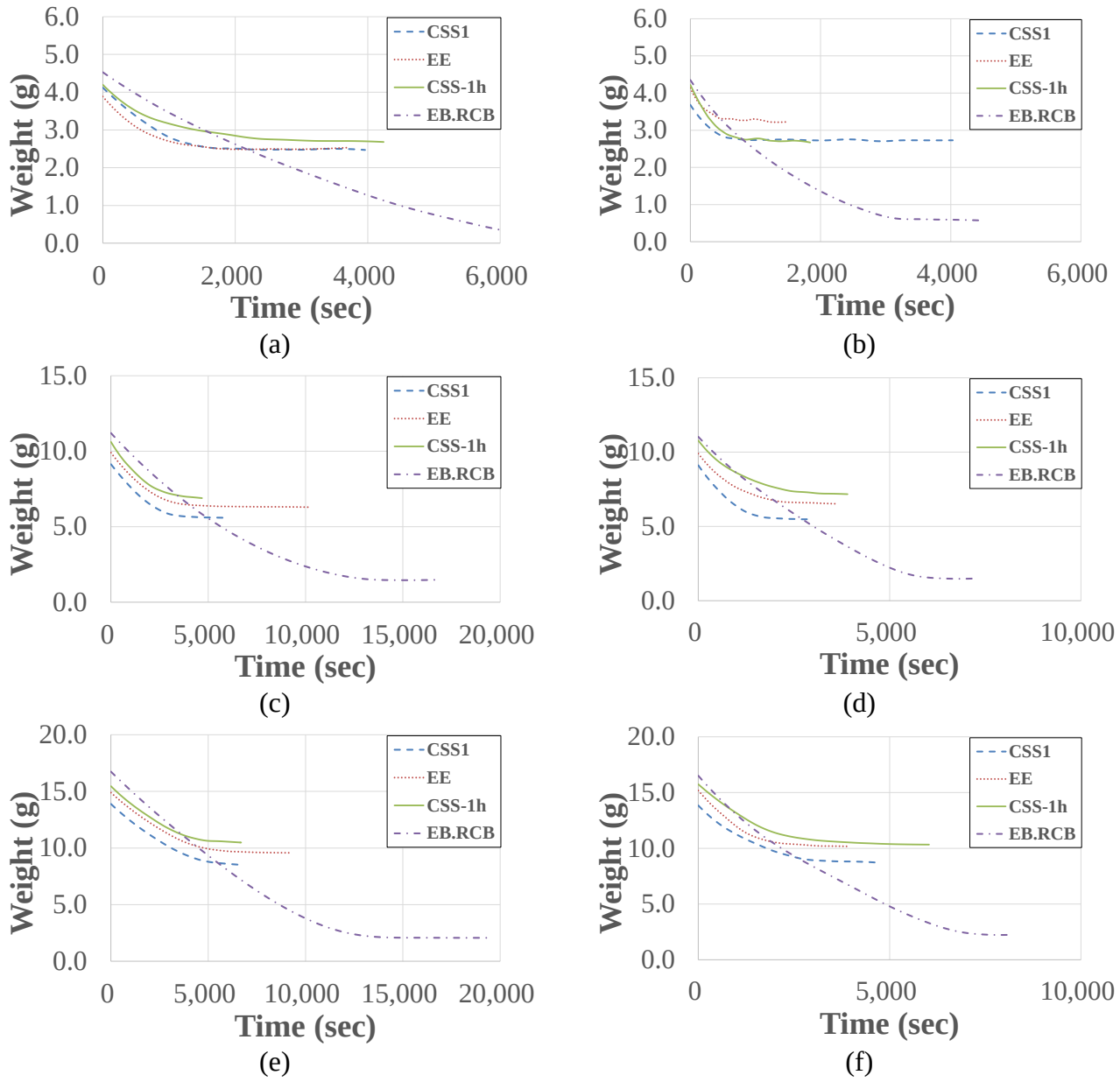

Figure A-1: Steel plate emulsion evaporation curves, (a) 59 °F, low rate (0.045 gal/yd2) (b) 95 °F, low rate (c) 59 °F, medium rate (0.105 gal/yd2) (d) 95 °F, medium rate (e) 59 °F, high rate (0.164 gal/yd2) (f) 95 °F, high rate.

A .1.2 AC Cores

The results of all 48 AC tests are shown in Figure A- 2 and Figure A- 3. Figure A- 2 presents the test results for the DG specimens while Figure A- 3 presents the test results for the OG specimens. From the plots, it can be observed that emulsion EBS.RBC has a significantly longer set time than all other emulsions regardless of the conditions. The emulsion type with the shortest set time cannot be easily observed from Figure A- 2 or Figure A- 3 but further statistical

analysis revealed that emulsion EE has the shortest set time when compared to other three emulsion types.

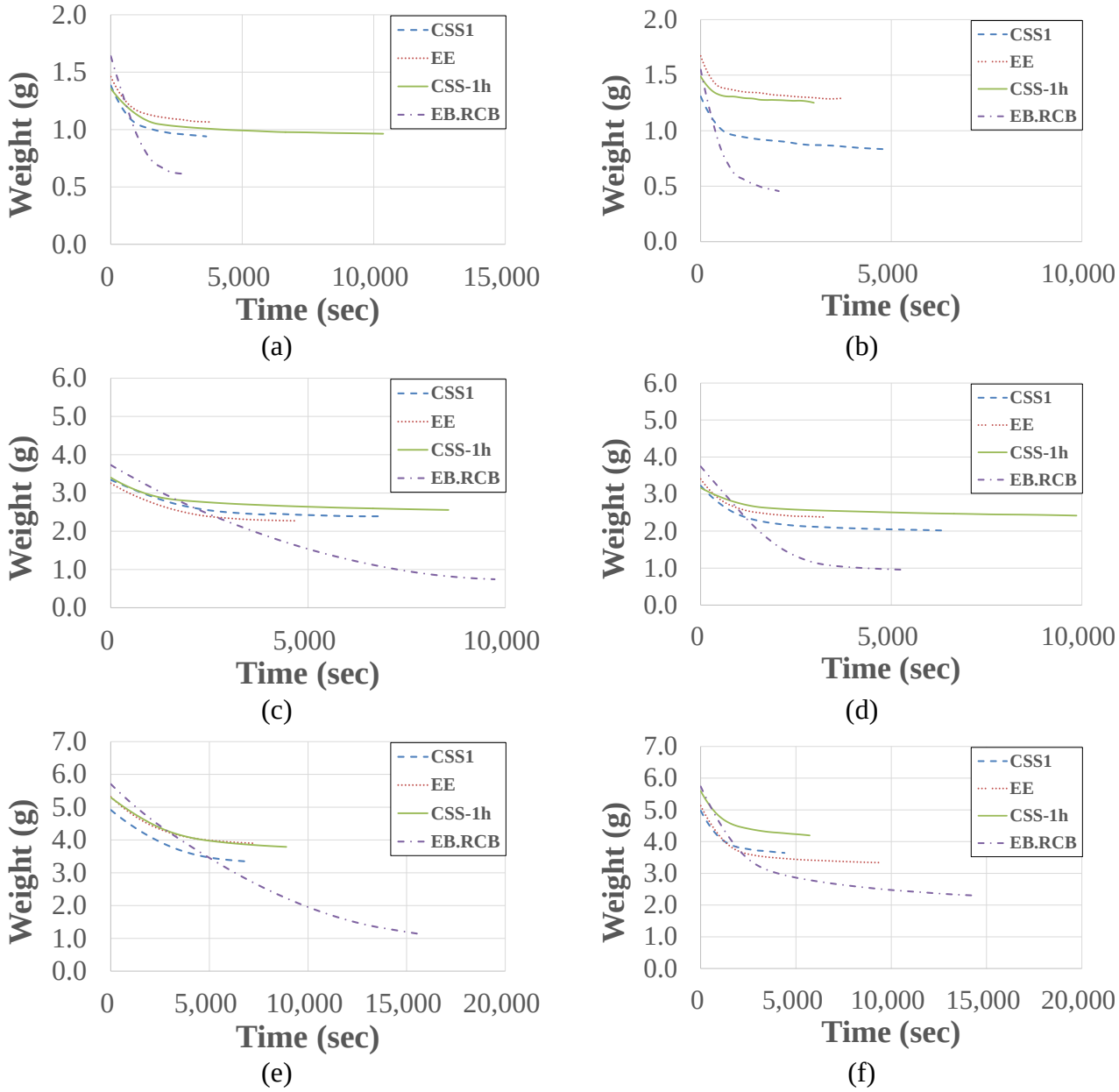

Figure A- 2: DG emulsion evaporation curves, (a) 59 °F, low rate (0.045 gal/yd2) (b) 95 °F, low rate (c) 59 °F, medium rate (0.105 gal/yd2) (d) 95 °F, medium rate (e) 59 °F, high rate (0.164 gal/yd2) (f) 95 °F, high rate.

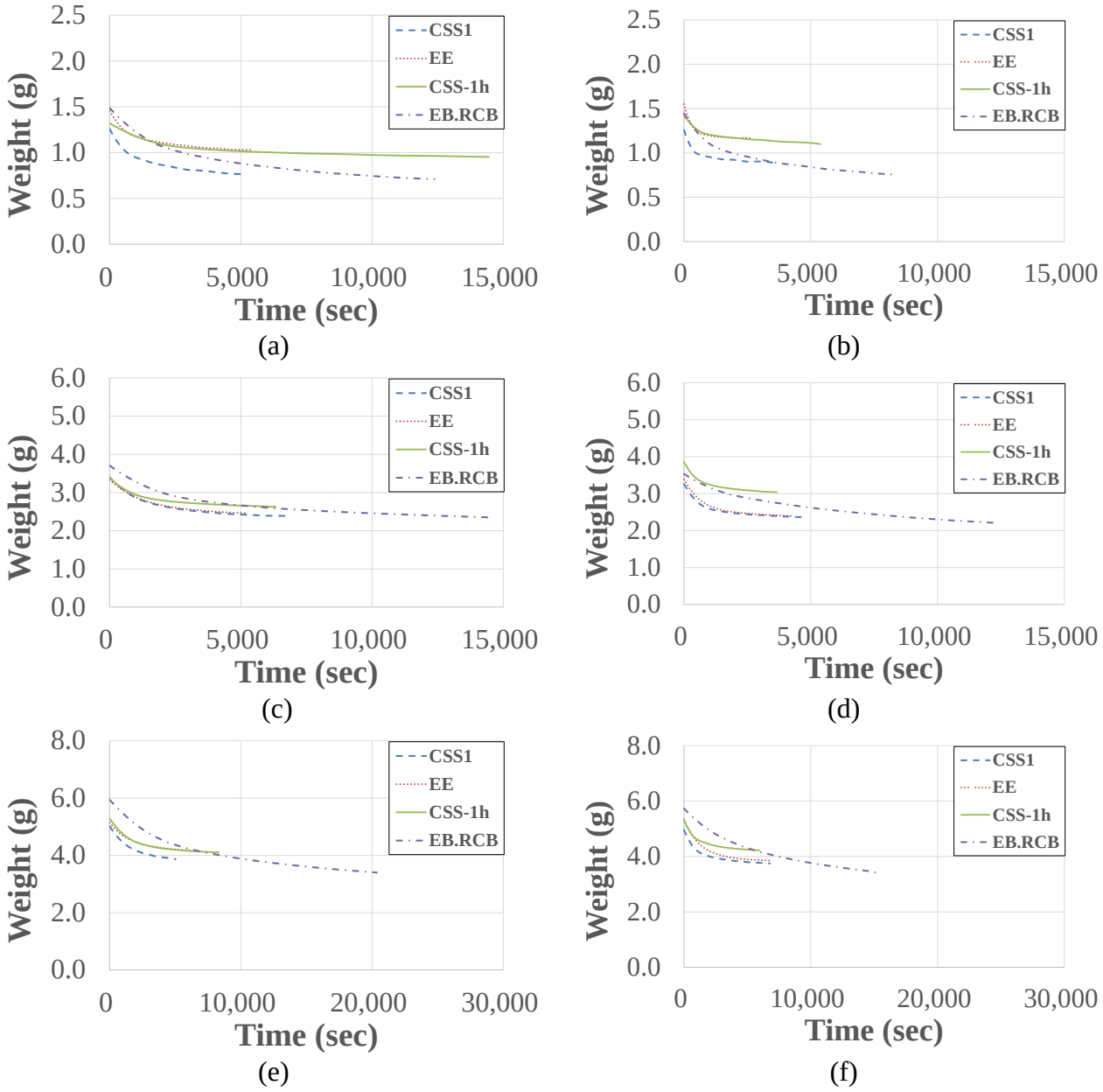

Figure A- 3: OG emulsion evaporation curves, (a) 59 °F, low rate (0.045 gal/yd2) (b) 95 °F, low rate (c) 59 °F, medium rate (0.105 gal/yd2) (d) 95 °F, medium rate (e) 59 °F, high rate (0.164 gal/yd2) (f) 95 °F, high rate.

A .2 DEVELOPMENT OF LINEAR REGRESSION MODELS TO PREDICT IN-SITU TACK COAT SET TIME

The primary objective of this section is to develop regression equations to predict emulsion set time by considering temperature, emulsion type, application rate, and surface texture. Developed regression equations can be used during construction to determine in-situ tack coat set times. By avoiding construction vehicle traffic before the calculated set time, tracking can be minimized. Developed regression equations will be validated and calibrated using the data from field tests. Regression models were developed for four different scenarios:

- OG and DG cores
- Steel plates:
    - Using two replicates
    - Using a single replicate
- Combined dataset: AC cores and steel plates.

A .2.1 Statistical analysis procedure used for linear model development (Demonstration example – AC core tests results)

In this section, regression analysis procedure followed to construct a linear regression model, correlating material and environmental variables to emulsion set time, is demonstrated. In statistics, regression analysis examines the relation between a dependent variable (response variable) to specified independent variables (predictors or explanatory). The mathematical model of their relationship is called the regression equation. In this study, the dependent variable used for model development is the emulsion set time (measured in seconds) and the independent variables are those that describe the emulsion being used (emulsion type and rate applied), surface texture and surrounding environment (temperature).

For the first scenario, only AC cores were utilized for model development to extract possible relationships between the emulsion set time and the independent variables considered. Table A-1 shows the variables used for the development of the model and their numerical ranges.

Table A- 1: Dependent and independent variables used for AC core model

Variable Type	Variable	Description	Range
Dependent	SET	Set time of applied emulsion in seconds	340-18,880
Independent	TEMPF	Temperature of chamber during test in degrees Fahrenheit	59, 95
	MTD	Mean Texture Depth, a measure of the texture of each tested sample in inches	0.0177-0.1281
	EMUL	Indicator of which emulsion was used for the test	CSS 1, CSS 1H, EBS.RBC, EE
	ACTR	The amount of emulsion applied to the sample during testing, measured in gal/yd^2	0.044-0.175

The model selection procedure includes the following steps:

- Plot a scatter (pairs) plot matrix to inspect possible relationships amongst predictor variables,
- Construct a correlation matrix of all variables to further assess relationships,
- Develop an Analysis of Variance (ANOVA) table to identify significant variables,
- Apply regression analysis to develop linear equation,
- Plot the residuals to determine if regression model is suitable for the data being used.

A .2.1.1 Scatter (pair) plot matrix

Figure A-4 is a matrix of scatter plots which depict the interactions between the dependent and independent variables that were used in model development. Several trends are illustrated in Figure A-4, for example, higher temperatures result in shorter set times, emulsion EBS.RBC has the largest range of setting times on average, and higher application rates yield longer set times. It can also be observed that independent variables are not correlated and can be used for regression model development.

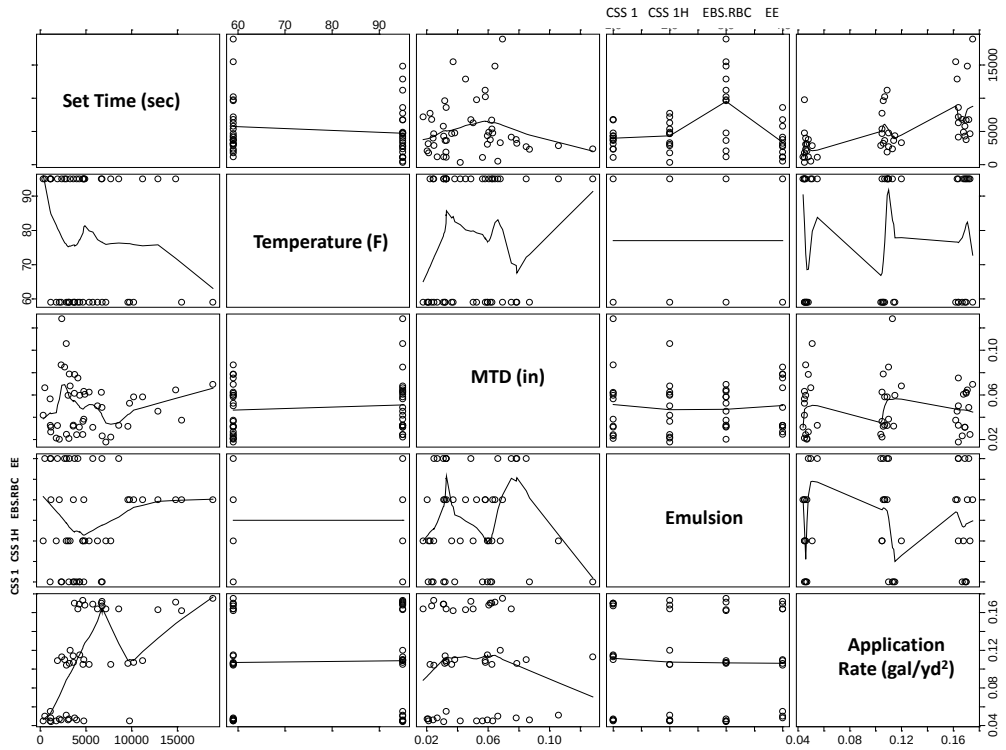

Figure A-4: Scatter plot matrix for AC Cores

A .2.1.2 Correlation matrix

A correlation matrix indicates the strength and direction of the linear relationship between two random variables. Values range from -1 to +1, where a negative sign represents an inverse relationship and a positive sign represents a direct relationship (if one variable increases, so does the other). A strong relationship (high correlation) is shown by those coefficients that have an absolute value closer to one (1.0). Shown in Table A-2 are the correlation coefficients for the variables used for AC core experiments. No combination of independent variables is highly correlated (values are less than 0.5 or -0.5), which indicates the variables are independent of each other. Application rate is shown to be highly correlated with the dependent variable (set time), which is seen by longer set times when higher rates are used.

Table A-2: Correlation matrix results for AC Cores

	Temperature	MTD	Emulsion	Application Rate	Set Time

	(F)	(in)		(gal/yd^2)	(sec)
Temperature (F)	**1.000**	0.123	0.000	0.019	-0.114
MTD (in)	0.123	**1.000**	-0.017	-0.034	-0.011
Emulsion	0.000	-0.017	**1.000**	-0.009	0.112
Application Rate (gal/yd^2)	0.019	-0.034	-0.009	**1.000**	0.552
Set Time (sec)	-0.114	-0.011	0.112	0.552	**1.000**

A .2.1.3 ANOVA table

ANOVA (analysis of variance) technique compares the variance within groups to the variance between groups. The result is an F-value that is a measure of the predictive capability of that variable. Larger F-values represent those variables that are more significant in predicting the emulsion set time. The general statistical terms in an ANOVA table can be expressed as follows (Seber 1977):

Degrees of Freedom (DF): Total number of degrees is one less than the number of observations. Each sum of square value is associated with the degrees of freedom.

Sum of Squares: Represents the total amount of variability in the dataset that can be estimated by calculating the sum of squared differences between each observation and the overall mean.

Mean Square: Determined by dividing the sum of squared error by the corresponding degrees of freedom.

F-value: The most important term in the estimation of the statistical significance of the independent variables. It represents whether the variable has significant predictive capability. F value is the ratio of the model mean square to the error mean square.

Pr(F)-value: Presents the percent error for a single independent variable in the representation of the dependent variable. It ranges from 0 to 1 and values that are closer to 0 indicate strong correlations with the dependent variables.

Table A- 3 shows the ANOVA results for the estimation of emulsion set time using only the test results from the AC cores. For this model, Temperature, Emulsion, and Application Rate are found to be significant and have the most effect on the setting time, while MTD does not have any considerable effect on emulsion set time.

Table A- 3: ANOVA results for AC Cores

	Df	Sum of Sq	Mean Sq	F Value	Pr(F)
Temperature (F)	1	10254554	10254554	1.79	0.1882

MTD (in)	1	7592	7592	0.00	0.9711
Emulsion	3	287883643	95961214	16.76	0.0000
Application Rate (gal/yd^2)	1	250166490	250166490	43.68	0.0000
Residuals	41	234795307	5726715		

A .2.1.4 Regression analysis for model development

The results of the statistical analysis yielded the following linear model relating emulsion set time to the various parameters used:

$$\underset{}{SET = 612.60} \underset{(0.7475)}{- 29.856 \times TEMPF} \underset{(0.1304)}{+ 10{,}877.52 \times MTD} \underset{(0.4622)}{+ 539.11 \times CSS\ 1H}$$

$$\underset{(0.5850)}{+ 5{,}784.47 \times EBS.RBC} \underset{(0.0000)}{- 329.613 \times EE} \underset{(0.7376)}{+ 46{,}226.40 \times ACTR} \underset{(0.0000)}{}$$

$$\mathbf{R^2 = 0.70}$$

Each number inside the parentheses are the p-values associated with the regression coefficients they are under. “p” values range from 0 to 1. Smaller p-values indicate more significance (lower error rates).

Since the variable MTD was found not to be significant according to the ANOVA table, another regression model was developed without it. The equation without the texture variable (MTD) can be considered to be more practical since it may not be possible to conduct sand patch tests during the construction to measure surface MTD. The resulting equation is below:

$$\underset{}{SET = 1{,}063.70} \underset{(0.5533)}{- 28.08 \times TEMPF} \underset{(0.1488)}{+ 489.71 \times CSS\ 1H} \underset{(0.6169)}{}$$

$$\underset{(0.0000)}{+ 5{,}729.40 \times EBS.RBC} \underset{(0.7274)}{- 340.97 \times EE} \underset{(0.0000)}{+ 46{,}026.99 \times ACTR}$$

$$\mathbf{R^2 = 0.70}$$

The R^2 value, which gives an estimate of the strength of the relationship between the independent variables of the linear regression model and the set time, is 70%. Although this value gives an indication of a good fitting model, residual plots must still be assessed to determine any bias, overfitting issues, and outliers.

Developed equation can be used to predict the setting time of all emulsion types used in this study. Table A- 4 shows a set of contrast values, which aid in using the equation for a selected emulsion type. Since each emulsion type has a corresponding coefficient and term within the equation, not all of the terms are used when a specific emulsion type is selected. For example, to

find the setting time of emulsion type CSS 1H, simply insert a one (1) into the equation where CSS 1H appears and zeros (0) for the other emulsion types. Similarly, to find the set time for CSS 1, insert zeros (0) for all the emulsion terms. The contrast values to insert into the equation are found by going to the appropriate row or column in Table A- 4 that corresponds to the selected emulsion type. An example calculation is provided below:

Given Conditions:
Emulsion: CSS 1H
Actual Rate: 0.045 gal/yd^2
Temperature: 75 °F
MTD (measure of texture): 0.02 in

$$SET = 612.60\text{-}29.86\times(\mathbf{75})+10{,}877.52\times\mathbf{(0.02)}+539.11\times\mathbf{(1)}$$

$$+5{,}784.47\times\mathbf{(0)}\text{-}329.61\times\mathbf{(0)}+46{,}226.40\times(\mathbf{0.045)}$$

Set Time= 1,210 seconds=20.2 minutes

Table A- 4: Emulsion type contrast values

	CSS 1H	EBS.RBC	EE
CSS 1	0	0	0
CSS 1H	1	0	0
EBS.RBC	0	1	0
EE	0	0	1

Further details of the regression model can be seen in Figure A- 5. Figure A- 5a illustrates the fitted values versus the residuals. The residual values should be close to zero for a reliable model. In addition, if the residuals present a constant trend (linear, parabolic, hyperbolic etc.), the mathematical function used for model development must be changed. For this regression model, the pattern of the residual plot is acceptable. Figure A- 5b shows the same residual plot where the absolute value of residuals is plotted in order to compare the negative and positive residuals. Figure A- 5c represents the final model fit on a line of equality (predicted vs. measured). Figure A- 5d shows that the distribution of residuals is very close to normal, meaning a majority of the points fall on the dotted line. In Figure A- 5e, the range of the fitted values is higher than the residuals, which also proves the statistical strength of the model. Finally, Figure A- 5f demonstrates the potential outliers encountered during model development. Although distance values for observations 44 and 45 are higher than the rest, they cannot be considered as outliers since they are close to the distance values for other observations.

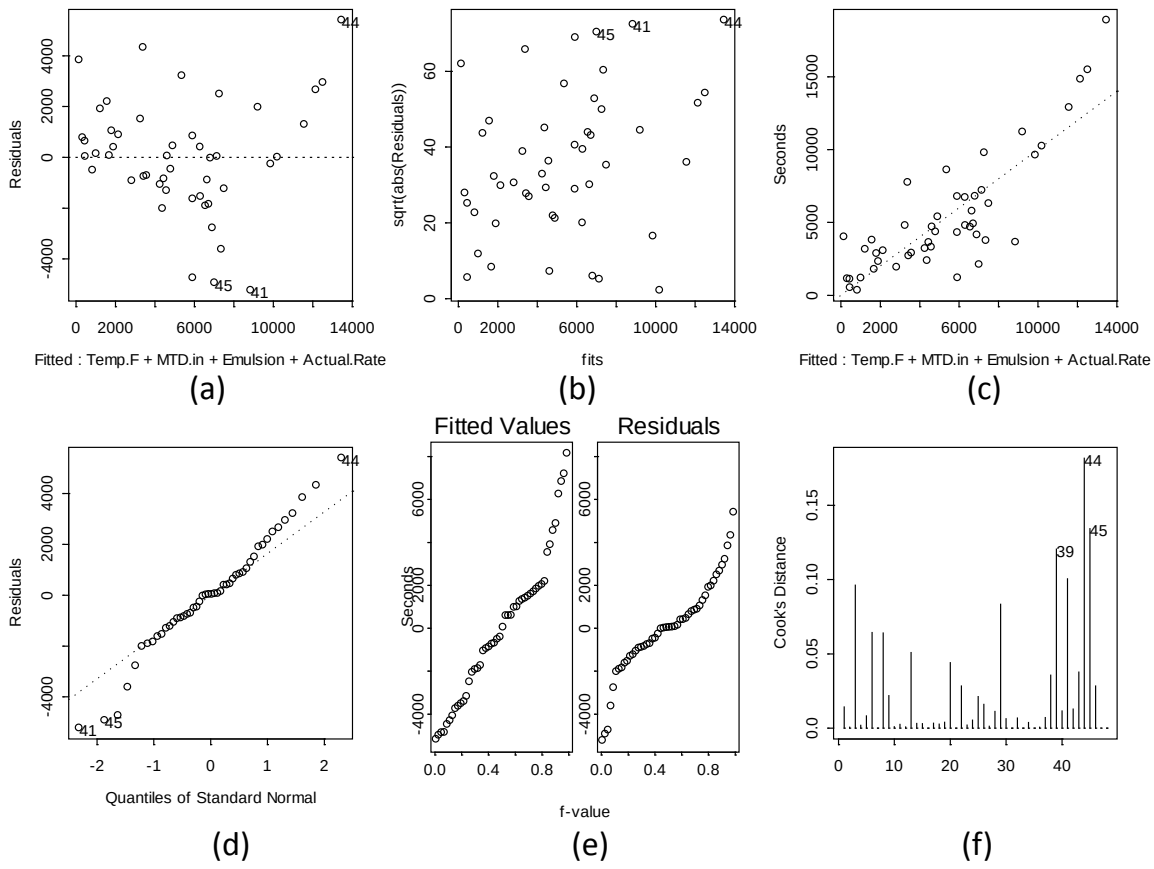

Figure A- 5: Residual plots for AC Cores

A .2.2 Linear models for steel plate tests and combined data

The model development procedure explained in Section A.2.1 is carried out for the estimation of emulsion set times for a dataset with only steel plate experiments and a combined dataset containing the AC core and steel plate experiments. Steel plate experiments were performed in order to determine whether texture has an effect on the setting time. Two steel plate regression models were developed to determine whether replicate experiments are necessary. The ranges of independent variables for the steel plates and combined datasets are given in Table A- 5 and Table A- 6, respectively.

Table A- 5: Variables used for Steel Plate models

Variable Type	Variable	Description	Range
Dependent	SET	Set time of applied emulsion in seconds	870-14,700
Independent	TEMPF	Temperature of chamber during test in degrees Fahrenheit	59, 95
	EMUL	Indicator of which emulsion was used for the test	CSS 1, CSS 1H, EBS.RBC, EE
	ACTR	The amount of emulsion applied to the sample during testing, measured in gal/yd^2	0.043-0.175

Table A- 6: Variables sued for AC Cores & Steel Plates (combined data) model

Variable Type	Variable	Description	Range
Dependent	SET	Set time of applied emulsion in seconds	340-18,880
Independent	TEMPF	Temperature of chamber during test in degrees Fahrenheit	59, 95
	MTD	Mean Texture Depth in inches, a measure of the texture of each sample tested	0.0177-0.1281
	EMUL	Indicator of which emulsion was used for the test	CSS 1, CSS 1H, EBS.RBC, EE
	ACTR	The amount of emulsion applied to the sample during testing, measured in gal/yd^2	0.044-0.175

A .2.2.1 Steel plate – All replicates

Figure A- 6 is a matrix of scatter plots which depict the interactions between the dependent and independent variables that were used in model development. Several trends are illustrated in Figure A- 6, for example, higher temperatures result in shorter set times, emulsion EBS.RBC has the largest range of setting times, and higher application rates yield longer set times. These are similar to the trends also seen in the model developed for AC core test results.

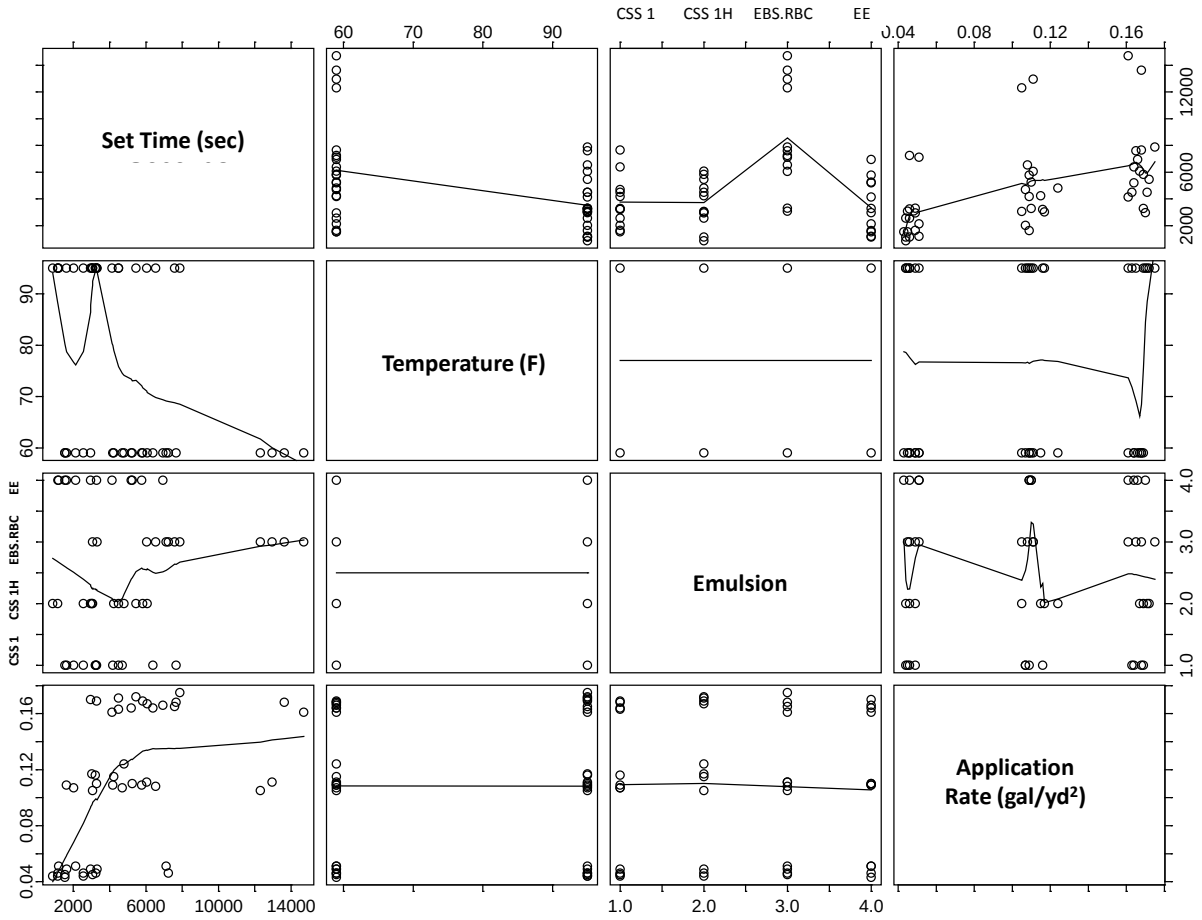

Figure A- 6: Scatter plot matrix for Steel Plate - All replicates

Table A- 7 shows the ANOVA outputs. Similar to the AC cores, temperature, emulsion, and application rate are all statistically significant predictors of set time. This is reflected by the large F-values and small p-values. Steel plates were assigned a texture of zero and MTD was not considered in steel plate analysis since the steel plate texture is negligible when compared to asphalt texture.

Table A- 7: ANOVA for results Steel Plate - All replicates

	Df	Sum of Sq	Mean Sq	F Value	Pr(F)
Temperature (^{o}F)	1	79258800	79258800	40.67	0.0000
Emulsion	3	217139742	72379914	37.14	0.0000
Application Rate (gal/yd^2)	1	123744751	123744751	63.50	0.0000
Residuals	42	81851632	1948848		

Fitting a linear regression model to the steel plate dataset yielded the following equation:

$$\underset{}{SET = 3463.71} \underset{(0.0001)}{- 128.57 \times TEMPF} \underset{(0.0000)}{- 135.28 \times CSS\ 1H}$$

$$+ \underset{(0.0000)}{4{,}764.94 \times EBS.RBC} \underset{(0.5747)}{- 322.32 \times EE} + \underset{(0.0000)}{32{,}591.99 \times ACTR}$$

$$\mathbf{R^2 = 0.84}$$

As seen in the equation, terms with negative signs indicate an increase in this variable will decrease the setting time. For example, higher temperatures and using emulsion EE will decrease the set time. An R^2 value of 84% indicates that this model is a good fit for the data. Figure A- 7 depicts more details of the regression model. Figure A- 7a has an acceptable pattern of residuals, also indicating that the developed model is reliable.

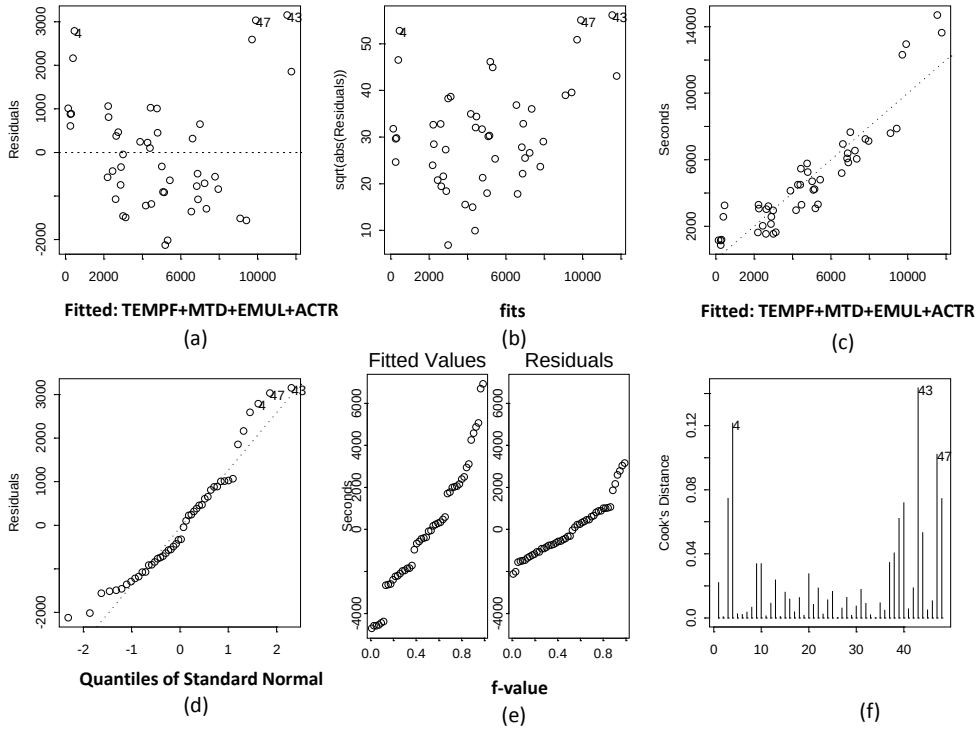

Figure A- 7: Residual plot for Steel Plate - All replicates

A .2.2.2 Steel plate – Replicate 1 only

Figure A- 8 is a matrix of scatter plots which depict the interactions between the dependent and independent variables that were used in model development. Data trends seen in the AC cores and all steel plate replicates can also be observed here. This is an indication that texture has no significant effect on the setting time.

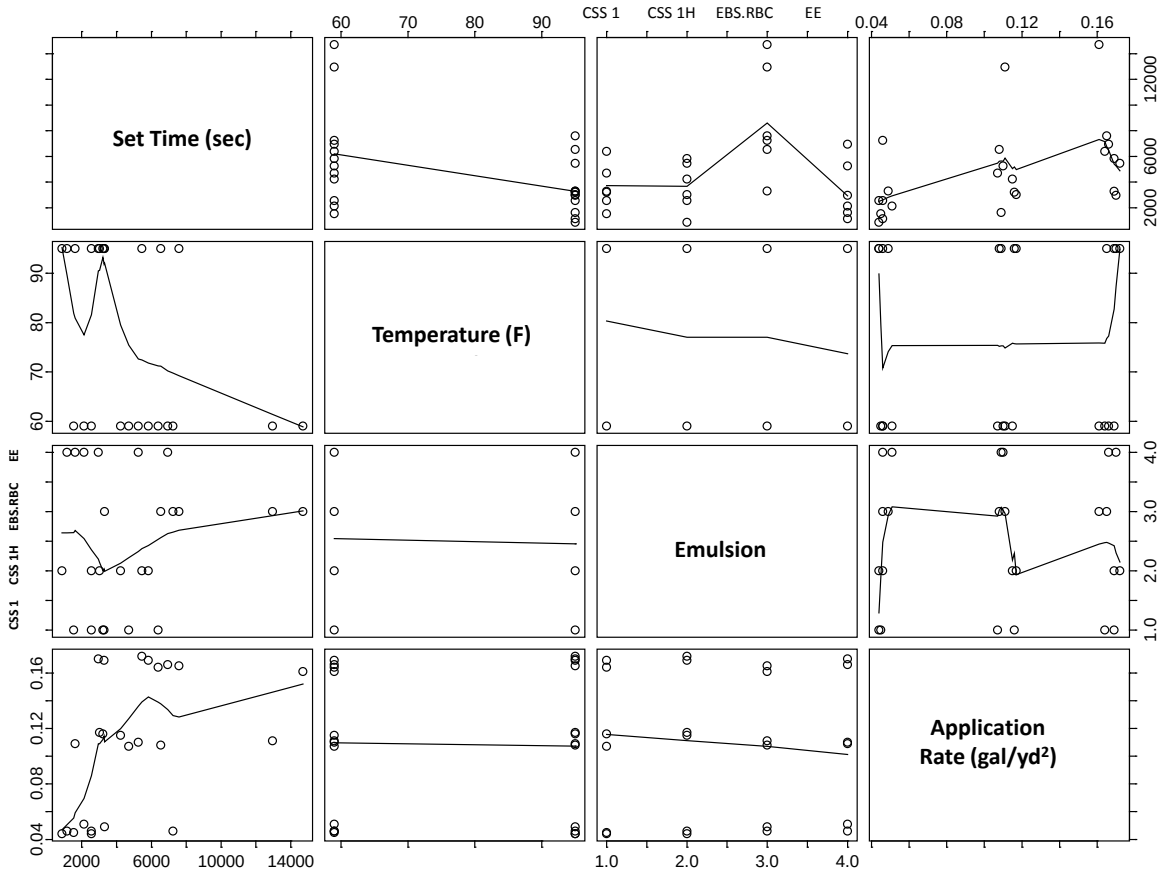

Figure A- 8: Scatter plot matrix for Steel Plate - Replicate 1 only

Table A- 8shows the ANOVA table for the Replicate 1 only model for the steel plates. Similar to the previous model (using all replicates), the same variables are determined to be significant. Obtaining similar results between models is another indication that replicate tests are not needed to improve the predictive capability of the model.

Table A- 8: ANOVA for results for Steel Plate - Replicate 1 only

	Df	Sum of Sq	Mean Sq	F Value	Pr(F)
Temperature (^{o}F)	1	45045600	45045600	19.48	0.0003
Emulsion	3	121208000	40402667	17.47	0.0000
Application Rate (gal/yd^2)	1	62678163	62678163	27.10	0.0000
Residuals	18	41632037	2312891		

Fitting a linear regression model to the Replicate 1 only steel plate dataset yielded the following equation:

$$\underset{}{\text{SET} = 3{,}582.80} \underset{(0.0077)}{- 139.46 \times \text{TEMPF}} \underset{(0.0003)}{- 51.526 \times \text{CSS 1H}} \underset{(0.9539)}{}$$

$$+ \underset{(0.0000)}{5133.94 \times \text{EBS.RBC}} \underset{(0.7269)}{- 311.52 \times \text{EE}} + \underset{(0.0001)}{32{,}730.85 \times \text{ACTR}}$$

$$\mathbf{R^2 = 0.85}$$

An R^2 value of 85% indicated that developed model is a good fit for the data. Figure A- **9** depicts more details of the regression model. Figure A- 9a has an acceptable pattern of residuals, also indicating the model developed is reliable.

The similarities in regression model coefficients of the two models (with and without replicates) point out the similarity in replicate tests. Similar trends can also be observed from the scatter plot matrices (Figure A- 6 and Figure A- 8). Overall, using a replicate test did not improve the regression outputs, therefore replicate experiments were not conducted for testing AC cores.

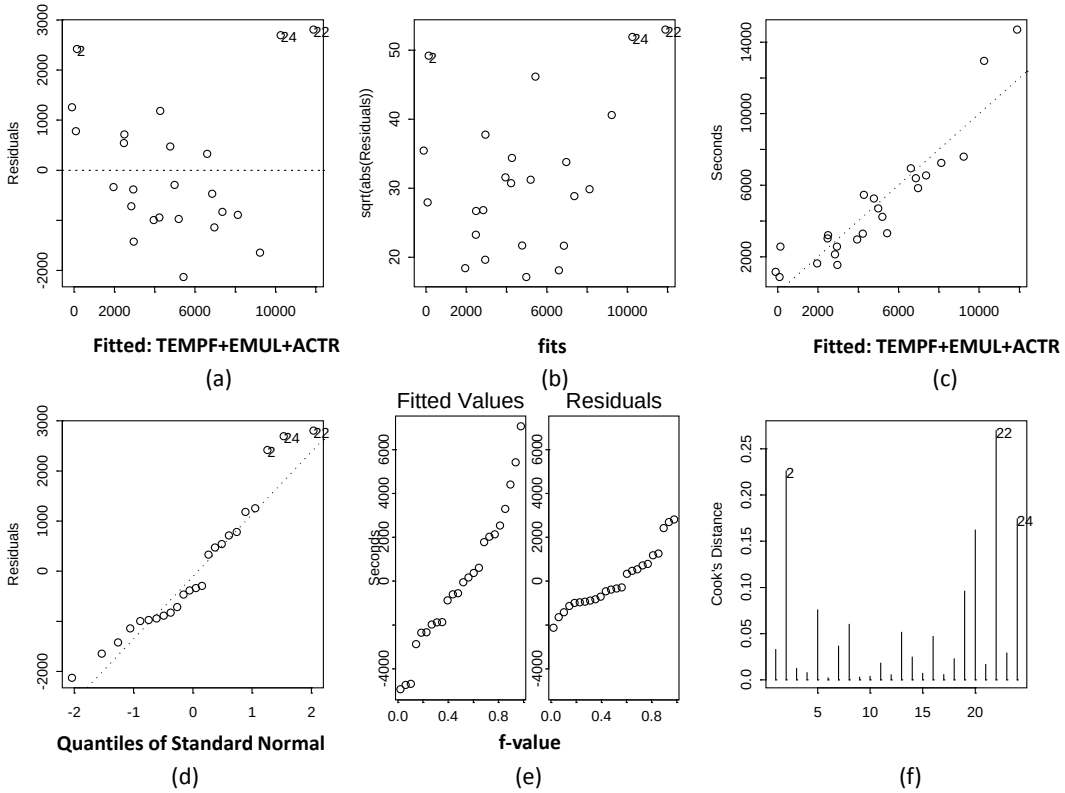

Figure A- 9: Residual plot for Steel Plate - Replicate 1 only

A .2.2.3 AC Core and Steel Plates (combined data)

Figure A- 10 shows the trends amongst variables in the model for the combined data of AC core and steel plate test results. Again, the trends are the same as before, which were observed for AC cores and all the steel plate models.

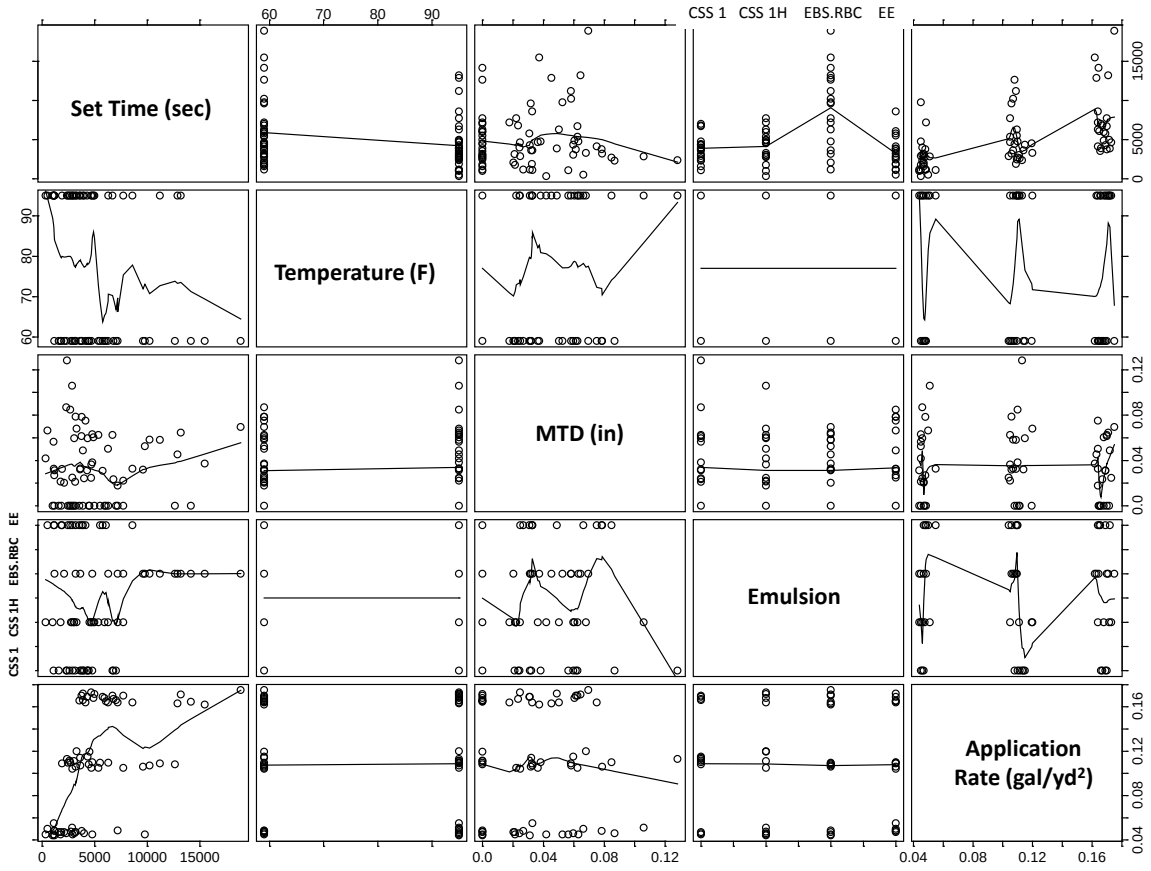

Figure A- 10: Scatter plot matrix for combined data

From the ANOVA table (Table A- 9) all the variables for this model are significant, because of their large F-values and small p-values, with the exception of MTD.

Table A- 9: ANOVA results for combined data

	Df	Sum of Sq	Mean Sq	F Value	Pr(F)
Temp.F	1	45961676	45961676	10.58	0.0018
MTD	1	1858407	1858407	0.43	0.5155
Emulsion	3	392072912	130690971	30.07	0.0000
Actual.Rate	1	281691882	281691882	64.82	0.0000
Residuals	65	282484572	4345916		

Linear regression yields the following equation for the AC core and steel plate model:

$$\underset{}{SET = 2{,}799.99} \underset{(0.0342)}{- 46.79 \times TEMPF} \underset{(0.0011)}{+ 9{,}185.86 \times MTD} \underset{(0.2618)}{+ 294.57 \times CSS\ 1H} \underset{(0.6732)}{}$$

$$\underset{}{+ 5{,}336.73 \times EBS.RBC} \underset{(0.0000)}{- 493.39 \times EE} \underset{(0.4802)}{+ 40{,}088.63 \times ACTR} \underset{(0.0000)}{}$$

$$\mathbf{R^2 = 0.72}$$

Since the variable MTD was found not to be significant from the ANOVA table, another regression model was also developed without it. The equation without the texture variable can be considered to be more practical since texture may be hard to determine during construction. The resulting equation is given below:

$$\underset{}{SET = 3{,}054.59} \underset{(0.0196)}{- 45.79 \times TEMPF} \underset{(0.0014)}{+ 266.94 \times CSS\ 1H} \underset{(0.7027)}{}$$

$$\underset{}{+ 5{,}305.85 \times EBS.RBC} \underset{(0.0000)}{- 499.74 \times EE} \underset{(0.4755)}{+ 39{,}970.96 \times ACTR} \underset{(0.0000)}{}$$

$$\mathbf{R^2 = 0.71}$$

As seen in the equation, terms with negative signs indicate that an increase in this variable will decrease the setting time. For example, higher temperatures and using emulsion EE will decrease the set time. An R^2 value of 72% indicates that this model is a good fit for the data. (Figure A-11) depicts more details of the regression model. Figure A- 11a has an acceptable pattern of residuals, also indicating that the developed model is reliable. A summary of all linear regression models developed and their equations can be seen in Table A- 10**.**

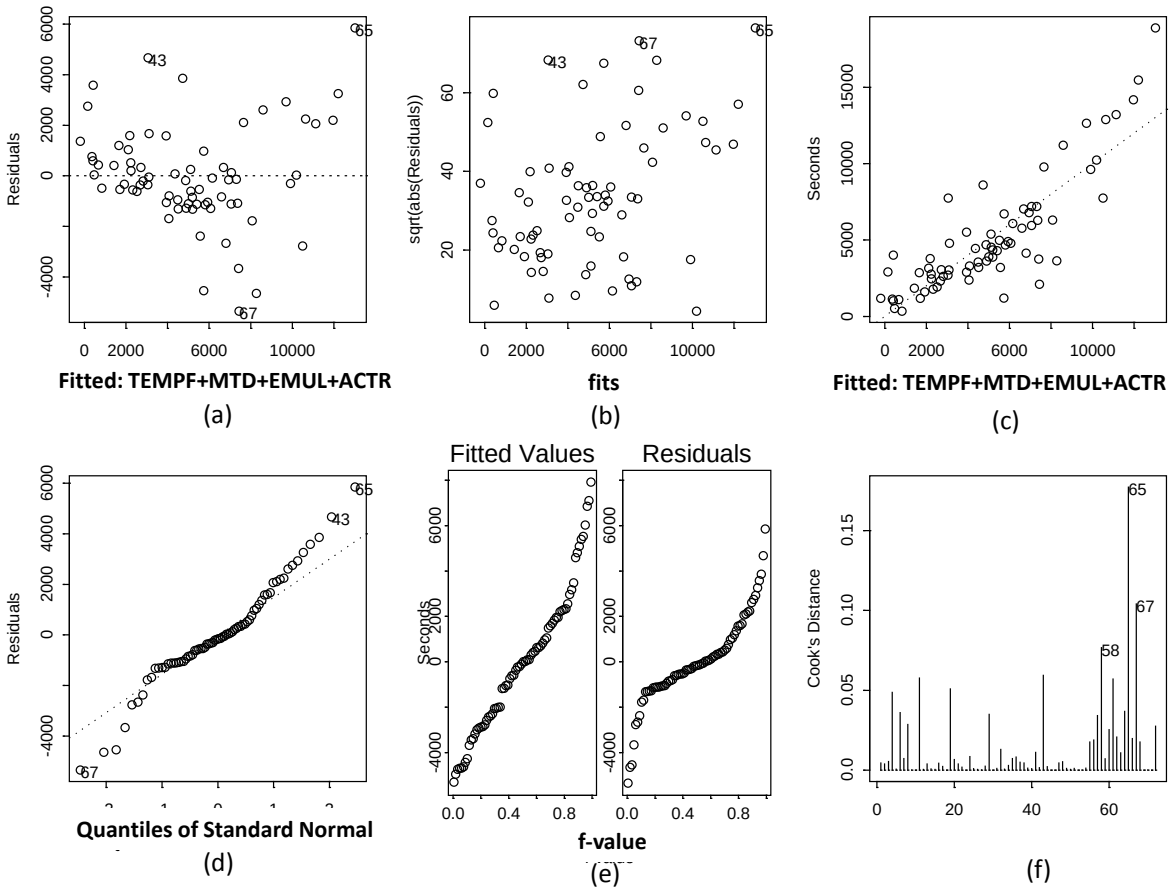

Figure A- 11: Residual plot for combined data

A .3 DEVELOPMENT OF REGRESSION MODELS WITH INTERACTION TERMS (NON-LINEAR) TO PREDICT IN-SITU TACK COAT SET TIME

The possibility of using interaction terms in the regression models is also investigated using the data from AC cores. Developed nonlinear equation for AC cores is given below:

$$\underset{}{SET} = \underset{}{2{,}053.85} \underset{(0.6362)}{- 14.81 \times TEMPF} + \underset{(0.6057)}{28{,}859.99 \times MTD} + \underset{(0.6497)}{1{,}530.91 \times CSS\ 1H} + \underset{(0.9032)}{417.07 \times EBS.RBC}$$

$$\underset{(0.4665)}{- 2{,}575.57 \times EE} + \underset{(0.4819)}{17{,}272.87 \times ACTR} \underset{(0.7848)}{- 162.12 \times TEMPF \times MTD} \underset{(0.3594)}{- 34.97 \times TEMPF \times CSS\ 1H}$$

$$\underset{(0.0072)}{- 106.65 \times TEMPF \times EBS.RBC} \underset{(0.7706)}{- 10.80 \times TEMPF \times EE} + \underset{(0.2850)}{285.72 \times TEMPF \times ACTR}$$

$$\underset{(0.5975)}{+ 13{,}837.44 \times MTD \times CSS\ 1H} + \underset{(0.0001)}{162{,}018.30 \times MTD \times EBS.RBC} + \underset{(0.4848)}{18{,}738.16 \times MTD \times EE}$$

$$\underset{(0.1204)}{- 372{,}157.92 \times MTD \times ACTR} + \underset{(0.6257)}{6{,}634.98 \times CSS\ 1H \times ACTR} + \underset{(0.0004)}{54{,}510.08 \times EBS\ RBC \times ACTR}$$

$$\underset{(0.1776)}{18507.8483 \times EE \times ACTR}$$

$$\mathbf{R^2 = 0.91}$$

It can be observed that coefficient of determination (R^2) for the nonlinear model is 0.91. Since interaction terms added nonlinearity to the model, R^2 for the regression model with interaction terms is significantly higher than the R^2 for the linear regression model developed in section A.2.1 for AC cores (0.70). However, it should be noted that high R^2 for the nonlinear model is a result of the added variables and does not necessarily point out an improved predictive capability. In order to quantify the actual improvement, a cross-validation procedure called "leave-one-out" is used. In this procedure, one of the observations (result from a single test) from the dataset is randomly selected and excluded from the dataset. The regression equation is developed without using this single observation. Then, the developed equation is used to predict emulsion set time for the excluded observation. This process is repeated for all observations (tests) in the dataset and predictions are recorded for every iteration. Using this procedure, the actual R^2 for the regression model with interaction terms is calculated to be 0.74 (Figure A- 12). Although 0.74 is higher than the 0.70 R^2 calculated for the linear regression equation, it does not provide a significant improvement. It should be noted that regression models with interaction terms given in this report should only be used when the input variables are within the ranges given in Table A- 1 and Table A- 6. Extrapolations can result in unrealistic predictions due to the nonlinear nature of the model. On the other hand, linear regression models given in this report can be used for extrapolations.

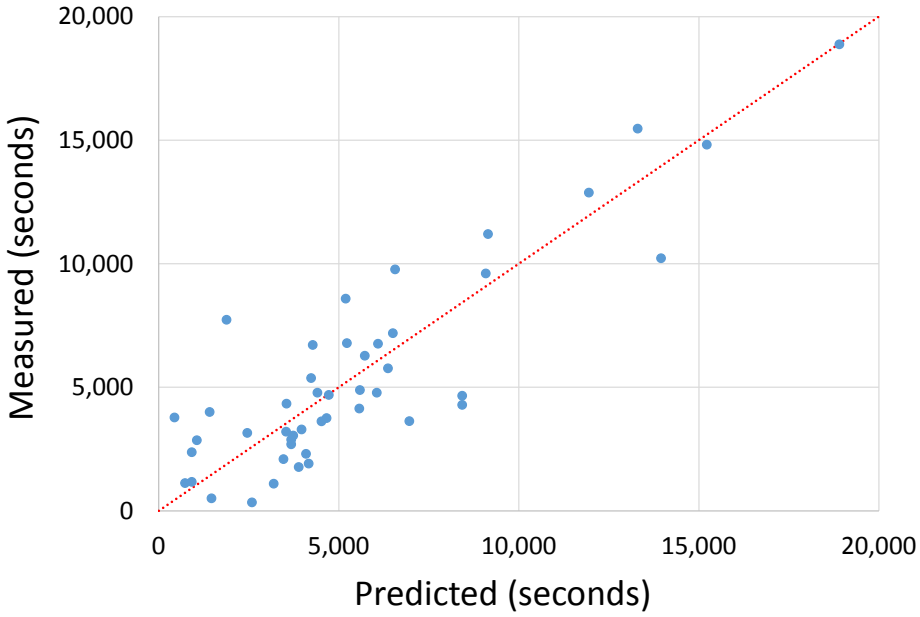

Figure A- 12: Measured and predicted emulsion set times for the "leave-one-out" cross-validation procedure (R2=0.74).

Table A- 10: Summary of linear regression models (Section A.2) for emulsion set time

Model Type	Model Specification	R^2
Eq.#1: AC Core	SET = 612.60-29.856×TEMPF+10,877.52×MTD+539.11×CSS 1H+5,784.47×EBS.RBC-329.61×EE (0.7475) (0.1304) (0.4622) (0.5850) (0.0000) (0.7376) +46,226.40×ACTR (0.0000)	0.70
Eq.#2: AC Core w/ no MTD	SET = 1,063.70-28.076×TEMPF+489.71×CSS 1H+5,729.40×EBS.RBC-340.97×EE+46,026.99×ACTR (0.5533) (0.1488) (0.6169) (0.0000) (0.7274) (0.0000)	0.70
Eq.#3: AC Core + Steel	SET = 2,799.99-46.791×TEMPF+9,185.86×MTD+294.57×CSS 1H+5,336.73×EBS.RBC-493.39×EE (0.0342) (0.0011) (0.2618) (0.6732) (0.0000) (0.4802) +40,088.63×ACTR (0.0000)	0.72
Eq.#4: AC Core + Steel w/ no MTD	SET = 3,054.59-45.79×TEMPF+266.94×CSS 1H+5,305.85×EBS.RBC-499.74×EE+39,970.96×ACTR (0.0196) (0.0014) (0.7027) (0.0000) (0.4755) (0.000)	0.71

Note: Numbers in the parentheses are the p-values of the regression coefficient.